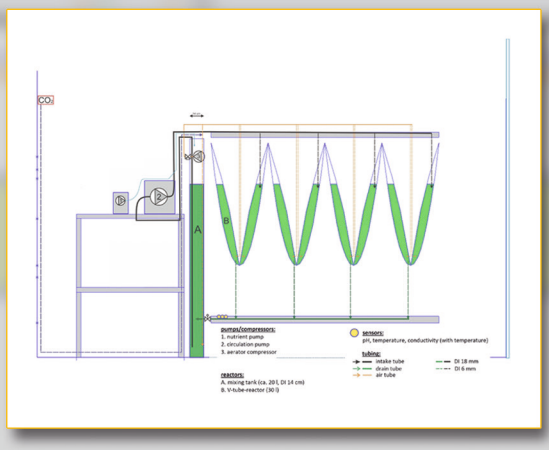

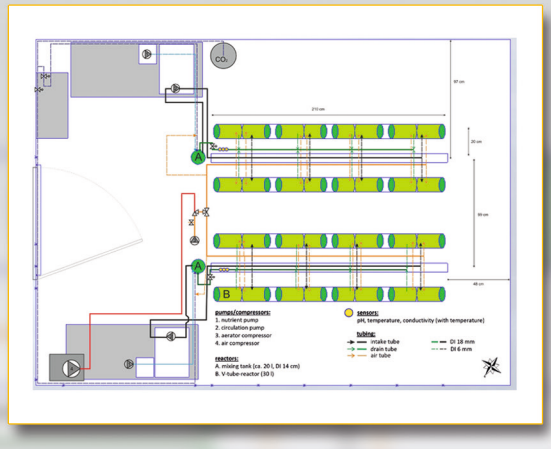

Phenotyping Nannochloropsis gaditana under different conditions in controlled photobioreactors in laboratory and upscaled photobioreactors in greenhouse

Regina Braun

Member of the Helmholtz Association

JÜLICH
FORSCHUNGSZENTRUM

Schriften des Forschungszentrums Jülich
Reihe Energie & Umwelt / Energy & Environment Band / Volume 221

Forschungszentrum Jülich GmbH
Institute of Bio- and Geosciences
Plant Sciences (IBG-2)

Phenotyping Nannochloropsis gaditana under different conditions in controlled photobioreactors in laboratory and upscaled photobioreactors in greenhouse

Regina Braun

Schriften des Forschungszentrums Jülich
Reihe Energie & Umwelt / Energy & Environment Band / Volume 221

ISSN 1866-1793 ISBN 978-3-89336-975-1

Bibliographic information published by the Deutsche Nationalbibliothek.
The Deutsche Nationalbibliothek lists this publication in the Deutsche Nationalbibliografie; detailed bibliographic data are available in the Internet at http://dnb.d-nb.de.

Publisher and Distributor: Forschungszentrum Jülich GmbH
Zentralbibliothek
52425 Jülich
Tel: +49 2461 61-5368
Fax: +49 2461 61-6103
Email: zb-publikation@fz-juelich.de
www.fz-juelich.de/zb

Cover Design: Grafische Medien, Forschungszentrum Jülich GmbH

Printer: Grafische Medien, Forschungszentrum Jülich GmbH

Schriften des Forschungszentrums Jülich
Reihe Energie & Umwelt / Energy & Environment, Band / Volume 221

D 61 (Diss. Düsseldorf, Univ., 2013)

ISSN 1866-1793
ISBN 978-3-89336-975-1

The complete volume is freely available on the Internet on the Jülicher Open Access Server (JUWEL) at www.fz-juelich.de/zb/juwel

Abstract

Since resources of fossil fuels are limited, alternatives for energy production need to be explored. Besides plants as biomass and energy crops, the interest in microalgae has been increasing, as they can synthesize many valuable compounds with a large application range, including transport fuels or fish and animal feed, without competing with agricultural food production for arable land. Moreover, microalgae can utilize flue gas from industrial emissions and municipal wastewater as a nutrient source. For economically viable production of algae, however, it is necessary to explore the maximal potential of algae by optimized cultivation conditions and targeted genetic modifications based on the knowledge about their physiology as well as regulatory mechanisms of growth and metabolic processes, in addition to technical improvement of photobioreactors (PBRs) and downstream processes.

Circadian clocks synchronize certain physiological, metabolic and developmental processes of organisms with specific phases of recurring changes in their environment, e.g. day and night or seasons. In this study it was investigated whether the circadian clock plays a role in regulation of growth and chlorophyll accumulation in *Nannochloropsis gaditana*, an oleaginous marine microalga that is considered as a potential feedstock for biofuels and for which a draft genome sequence has been published. Optical density (OD) of *N. gadinata* culture was monitored at 680 and 735 nm under 12 h/12 h or 18 h/6 h light-dark (LD) cycles and after switching to continuous illumination (LL) in controlled PBRs in the laboratory. In parallel, chlorophyll fluorescence was measured to assess the quantum yield of photosystem (PS) II. Furthermore, to test if red- or blue-light photoreceptors are involved in clock entrainment in *N. gaditana*, some of the experiments were conducted by using only red or blue light. Growth and chlorophyll accumulation were confined to light periods in the LD cycles, increasing more strongly in the first half than in the second half of the light periods. After switching to continuous light, rhythmic oscillations persisted (especially for OD_{680}) at least in the first 24 h, with a 50%

decrease in the capacity to grow and accumulate chlorophyll during the first subjective night. Pronounced free-running oscillations were induced by blue light, but not by red light. In contrast, the PS II quantum yield was determined by light conditions. Continuous blue light also enhanced accumulation of vaucheriaxanthin. The results indicate interactions between circadian and light regulation of growth and chlorophyll accumulation in *N. gaditana*.

Mutants with reduced pigment contents and lower capacities of thermal energy dissipation, allowing better penetration of light into PBRs with a smaller loss of absorbed light energy, are considered as a good strategy to improve the yield of biomass or other high-value products under light-limited conditions. Therefore, two EMS-mutants of *N. gaditana*, *npq3* and *npq21* previously selected for their pale appearance and low capacities for thermal dissipation, were examined for their growth and photosynthetic properties in comparison with the wild type (WT) under different light regimes with fluctuating or constant light in LD cycles or LL as well as temperature cycles of 30°C/23°C and 23°C/15°C under controlled laboratory conditions. The OD_{680} and OD_{735} as well as PS II quantum yield were monitored during cultivation and pigment composition was analyzed after several days of acclimation to the different conditions. In addition, biomass production was measured for LD cycle experiments. The *npq21* showed higher OD_{680} and OD_{735} values compared to WT and *npq3* under LD and LL with fluctuating or constant light. No differences for PS II quantum yield were found between the genotypes or treatments under LD, but lower PS II quantum yields were found for *npq3* under LL. In particular, higher biomass production was found for *npq21* under fluctuating LD. The presence of antheraxanthin, an intermediate xanthophyll of the violaxanthin cycle, was found in both mutants under all conditions tested, whereas WT did not accumulate antheraxanthin under non-stressful conditions, such as constant LD or LD with temperature cycle 23°C/15°C. Higher carotenoid to chlorophyll ratios under fluctuating light conditions found in *npq21* seem to facilitate this mutant to better cope with photooxidative stress than WT, while *npq3* always showed the lowest performance of the three, presumably due to negative effects of the mutations. Cultivation under temperature cycles of 23°C/15°C and 30°C/23°C resulted in similar increase in OD_{680} and OD_{735} but lower carotenoid to chlorophyll ratios under 30°C/23°C for *npq21*. In contrast, WT showed enhanced OD_{680} and OD_{735} increase under 30°C/23°C compared to 23°C/15°C without changes in carotenoid

to chlorophyll ratios but retention of antheraxanthin under 30°C/23°C, indicating stress. The results show improved growth for *npq21* under fluctuating light and varying temperature regimes which resemble the conditions in large-scale cultivation in PBRs in greenhouses.

Four replicate PBR systems designed for industrial-scale production of microalgae were established in greenhouses to monitor growth of *N. gaditana* under more natural and realistic conditions. The comparability of the four systems was confirmed by cultivating *N. gaditana* WT. Based on the results obtained under the laboratory conditions, *npq21* was selected for the scale-up trial to compare with the WT under the greenhouse conditions. The algae were harvested whenever the culture density exceeded a threshold during the experimental periods. The results showed higher biomass and higher chlorophyll a production for *npq21* especially during the initial phase until the cell density reached the threshold value. The addition of water, salt and nutrient solution per produced biomass was nearly the same for both genotypes. Thus, *npq21* outcompeted WT under most of the laboratory and greenhouse conditions tested in this study, even though the originally reported phenotypes of low pigmentation and low capacity for thermal energy dissipation had been lost during cultivation of the stock culture in the growth cabinet, suggesting that mutations in other physiological or metabolic processes may have contributed to the increased stress tolerance and higher biomass production of *npq21*. Whatever the genetic explanation for better performance may be, *npq21* seems to be a promising candidate for further investigations.

Zusammenfassung

Da die Ressourcen fossiler Kraftstoffe limitiert sind, ist es notwendig alternativen für die Energieproduktion zu finden. Abgesehen von Pflanzen als Biomasse- und Energielieferanten, steigt das Interesse an Mikroalgen, da sie wertvolle Stoffe mit hoher Applikationsbandbreite synthetisieren können, z.B. für Transportkraftstoffe, Fisch- und Tierfutter, ohne dabei mit der agrarischen Lebensmittelproduktion um fruchtbares Land zu konkurrieren. Darüber hinaus können Mikroalgen Abgasströme von industriellen Emissionen und kommunales Abwasser als Nährstoffquelle verwenden. Um eine ökonomisch realisierbare Mikroalgenproduktion zu erzielen, ist es notwendig das maximale Potential der Algen durch optimierte Kultivierungsbedingungen und gezielte genetische Modifikationen, basierend auf dem Wissen über ihre Physiologie und regulatorischen Mechanismen von Wachstum und metabolischen Prozessen, zusätzlich zur technischen Verbesserung von Photobioreaktoren (PBRs) und nachgeschalteter Verfahren, auszuschöpfen.

Zirkadiane Uhren synchronisieren bestimmte physiologische, metabolische und Entwicklungsprozesse in Organismen mit spezifischen sich wiederholenden Phasen in ihrer Umgebung, z.B. Tag und Nacht oder Jahreszeiten. In dieser Arbeit wurde untersucht, ob die zirkadiane Uhr eine Rolle in der Regulierung des Wachstums und der Akkumulation von Chlorophyll in *Nannochloropsis gaditana* spielt, einer ölhaltigen marinen Mikroalge, die als potentieller Ausgangsstoff für Biokraftstoffe angesehen wird und für die eine vorläufige Genomsequenz veröffentlicht worden ist. Die optische Dichte (OD) der *N. gaditana* Kultur wurde bei 680 nm und 735 nm unter 12 h/12 h oder 18 h/6 h Licht-Dunkel (LD) Zyklen und anschließendem Umschalten zu kontinuierlichem Licht (LL) in kontrollierten PBRs unter Laborbedingungen aufgezeichnet. Parallel dazu wurde die Chlorophyll-Fluoreszenz gemessen um die Quantenausbeute vom Photosystem (PS) II zu bestimmen. Des Weiteren wurden einige Experimente mit nur blauem oder rotem Licht wiederholt um festzustellen, ob Rot- oder Blaulichtphotorezeptoren an der Einstellung der Uhr in *N. gaditana*

beteiligt sind. Das Wachstum und die Akkumulation von Chlorophyll waren auf die Lichtperioden der LD Zyklen beschränkt, wobei eine höhere Zunahme in der ersten Hälfte im Vergleich zur zweiten Hälfte der Lichtperiode stattfand. Nach dem Umschalten zu kontinuierlichem Licht wurden rhythmische Oszillationen (besonders für OD_{680}) mindestens in den ersten 24 h beibehalten, mit 50%-iger Abnahme von Wachstum und Akkumulation von Chlorophyll während der ersten subjektiven Nacht. In blauem Licht blieben ausgeprägte freilaufende Oszillationen von OD_{680} erhalten, jedoch nicht in rotem Licht. Im Gegensatz dazu, wurde die PS II Quantenausbeute von den Lichtbedingungen bestimmt. Kontinuierliches blaues Licht verstärkte die Akkumulation von Vaucheriaxanthin. Die Ergebnisse deuten auf Interaktionen zwischen zirkadianer Uhr und der Lichtregulierung von Wachstum und Akkumulation von Chlorophyll in *N. gaditana* hin.

Mutanten mit reduziertem Pigmentanteil und geringerer Kapazität von thermischer Energiedissipation, wodurch eine verbesserte Lichtdurchlässigkeit in die PBRs mit geringerem Verlust von absorbierter Lichtenergie ermöglicht wird, werden als gute Herangehensweise zur Verbesserung der Biomasseproduktion oder anderer hochwertiger Produkte unter limitierten Lichtverhältnissen angesehen. Aufgrund dessen wurden zwei EMS-Mutanten, *npq3* und *npq21*, die zuvor wegen ihrer blassen Erscheinung und geringen Kapazitäten von thermischer Energiedissipation selektiert wurden, in Hinblick auf ihr Wachstum und ihrer photosynthetischen Eigenschaften im Vergleich zum Wildtyp (WT) unter verschiedenen Lichtbedingungen mit fluktuierendem oder konstantem Licht in LD Zyklen oder LL, sowie verschiedener Temperaturzyklen von 30°C/23°C und 23°C/15°C unter kontrollierten Laborbedingungen untersucht. Die OD_{680} und OD_{735} sowie PS II Quantenausbeute wurden während der Kultivierung aufgezeichnet und die Pigmentzusammensetzung wurde nach Akklimatisierung an die verschiedenen Bedingungen analysiert. Zusätzlich wurde die Biomasseproduktion für die Experimente mit LD Zyklen bestimmt. Es wurden keine Unterschiede für die PS II Quantenausbeute für die verschiedenen Genotypen oder Behandlungen unter LD gefunden, aber geringere PS II Quantenausbeuten wurden für *npq3* unter LL festgestellt. Insbesondere wurde eine höhere Biomasseproduktion für *npq21* unter fluktuierendem Licht gefunden. Die Anwesenheit von dem Xanthophyll Antheraxanthin, das als Zwischenprodukt im Violaxanthinzyklus gebildet wird, wurde in beiden Mutanten unter allen verwendeten Bedingungen gefunden, wohingegen der WT kein Antheraxanthin unter stress-

freien Bedingungen wie konstantes LD oder LD mit dem Temperaturzyklus von 23°C/15°C aufwies. In *npq21* scheinen höhere Carotinoid zu Chlorophyll Verhältnisse unter fluktuierendem Licht dazu zu führen, dass diese Mutante besser mit photooxidativem Stress umgehen kann als der WT, während *npq3* immer die geringste Leistungsfähigkeit unter den drei Genotypen aufwies, möglicherweise aufgrund von negativen Effekten der Mutationen. Kultivierung unter Temperaturzyklen von 23°C/15°C und 30°C/23°C führte zu ähnlichen Zunahmen von OD_{680} und OD_{735}, jedoch zu einem geringeren Carotinoid zu Chlorophyll Verhältnis für *npq21* unter 30°C/23°C. Im Gegensatz dazu wies der WT verstärkte Zunahmen von OD_{680} und OD_{735} unter 30°C/23°C im Vergleich zu 23°C/15°C auf, ohne eine Veränderung der Carotinoid zu Chlorophyll Verhältnisse, jedoch mit der Akkumulation von Antheraxanthin unter 30°C/23°C, was auf Stress hindeutet. Die Ergebnisse zeigen ein verbessertes Wachs- tum von *npq21* unter fluktuierendem Licht und variierenden Temperaturbeding- ungen, welche die Bedingungen der Kultivierung in größerem Maßstab in PBRs in Gewächshäusern wiederspiegeln.

Vier vergleichbare Kultivierungssysteme, die zur Produktion von Mikroalgen im industriellen Maßstab entwickelt wurden, wurden in Gewächshäusern aufgestellt um das Wachstum von *N. gaditana* unter natürlicheren und realistischeren Bedingungen zu untersuchen. Die Vergleichbarkeit der vier Systeme wurde durch die Kultivierung vom *N. gaditana* WT bestätigt. Basierend auf den Ergebnissen, die unter Laborbedingungen produziert wurden, wurde *npq21* für den Versuch im größeren Maßstab selektiert, um diese Mutante mit dem WT unter Gewächshausbedingungen zu vergleichen. Die Algen wurden geerntet sobald die Kulturdichte in den PBRs einen Grenzwert während der Kultivierungsperiode überschritt. Die Ergebnisse zeigten höhere Produktionen von Biomasse und Chlorophyll *a* für *npq21*, insbesondere während der Initialphase, bis die Zelldichte den Grenzwert erreichte. In Bezug auf die Biomasse war die Zugabe von Wasser, Salz und Nährlösung für beide Genotypen ungefähr gleich. Daher hat *npq21* den WT unter den meisten verwendeten Labor- und Gewächshausbedingungen auskonkurriert, obwohl die ursprünglich beschriebenen Phenotypen mit niedrigem Pigmentgehalt und niedrigerer Kapazität von thermischer Energiedissipation während der Kultivierung der Stammkultur im Klimaschrank verloren gegangen sind. Dies deutet auf Mutationen in anderen physiologischen oder metabolischen Prozessen hin, die zu erhöhter Stresstoleranz und höherer Biomasseproduktion von *npq21* beigetragen haben. Was die genetische

Erklärung für die bessere Leistungsfähigkeit auch sein mag, so scheint *npq21* ein vielversprechender Kandidat für weitere Untersuchungen zu sein.

Contents

1 Introduction

1.1 Biofuels

Ensuring energy supply is an issue of utmost importance as the stock of fossil energy resources is running out while the global energy demand is ever growing. Furthermore, the use of fossil fuels has a negative impact on the environment through greenhouse gas emissions contributing to the global climate change [1]. There is a need of sustainable and more climate neutral energy sources, such as biomass from photosynthetic organisms that can assimilate inorganic carbon from carbon dioxide (CO_2) into organic compounds by using solar energy [2].

The first generation of biofuels is based on the conversion of biomass from food crops containing sugar and starch for ethanol production or oilseeds for biodiesel production [3], leading to a strong competition with the food market as arable land is needed [4, 5]. Increase in population makes agricultural land more valuable and therefore a use of food crops and arable land for biofuel production is ethically not accepted [3, 5]. The second generation of biofuels includes non-food crops such as straw and wood [6] which contain lignocellulose [7] and are often difficult to separate from valuable carbohydrates [8]. The third generation of biofuels is the use of algal biomass [9, 10] which usually contains 20%-50% oil per dry weight, but can also exceed these values [11]. Production of algae does not compete with agricultural processes as there is no need for fertile land [9] since algae can be grown in open ponds or photobioreactors (PBRs).

In Fig. 1.1 [12] a simplified scheme of the production processes of algal biomass to organic compounds for energy, food additives, pharmaceutical and cosmetics is shown. The bottleneck of algae cultivation is the high costs which arise during cultivation and downstream processing [7, 9]. This can be overcome by the use of waste products such as heat from power plants [13] for temperature regulation and

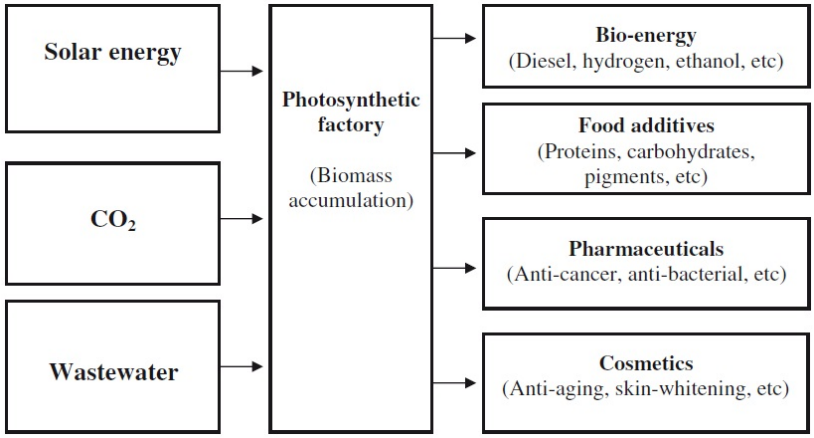

Figure 1.1: Scheme of photosynthetic conversion of solar energy for production of different products obtained from algal biomass, by using CO_2 and nutrients from wastewater (figure from [12]).

waste CO_2 [9, 14] from flue gas with concentrations up to 15% [15]. During production of 100 t algal biomass about 183 t CO_2 are fixed [9]. Wastewater contains many nutrients [13] which can be eliminated by the algae and thus support the wastewater treatment. Solar light conversion is also higher in algae compared with plants, which makes energy-to-biomass conversion more efficient. In order to meet 50% of the U.S. transport fuel needs, as much as 24% of the total cropland would be needed with oil palm as a high-yielding oil crop, whereas only up to 3% would be sufficient when producing algal biomass [11].

The photosynthetic microorganisms are divided into two groups, prokaryotes and eukaryotes. Photosynthesis performed in photosynthetic organisms can either be anoxygenic or oxygenic. Based on the fact, that flue gas, which is of high interest as a CO_2 source, can contain up to 4-5% oxygen, anoxygenic photosynthetic bacteria are excluded from the group of attractive organisms as they need strict anaerobe conditions for CO_2 fixation [2]. Cyanobacteria are single or multicellular prokaryotes with sizes up to 60 µm [16]. They operate oxygenic photosynthesis and have an additional antenna complex, the phycobilisom, which makes it possible to use a larger light spectrum. Also eukaryotic microalgae can be composed of single or multicells. The size varies between 1 µm to over 2 mm (see Table 1.2), so that the

sizes of cyanobacteria and microalgae overlap. Similar to cyanobacteria, microalgae also perform oxygenic photosynthesis.

Genetic engineering of cyanobacteria and microalgae has gained in importance as modification of metabolic pathways can improve production of high-value products [17]. One approach is to construct hydrogenase mutants, such as the *Anabaena* sp. PCC 7120 mutant *hupL*$^-$ which produces H_2 at a four to seven times higher rate compared to the wild type [18]. Another approach is to increase the lipid content in the cells by blocking starch accumulation, which is an energy-rich storage compound, e.g. in *Chlamydomonas reinhardtii* [19]. The starch-deficient mutants *sta6* and *sta7* with disruptions in the ADP-glucose pyrophosphorylase or isoamylase genes [19] have been shown to increase the triacylglyceride (TAG) accumulation under nitrogen deprivation [20]. The advantage of genetic engineering has also been used by the company JOULE® (USA) that developed the platform Helioculture™ [21] where the cells take up CO_2 and convert it to alkane fuel in a SolarConverter®, which is directly secreted into the medium. This method circumvents the cracking process that is usually required for extraction of lipid bodies synthesized by the cells.

1.2 Range of products from algae

The microalgal and cyanobacterial biomass contains many compounds of which different products can be derived (Fig. 1.1, Table 1.1), yet the availability and amount of the compounds within the cells differ amoung the species. Energy-rich compounds are e.g. **hydrocarbons** [2, 8, 22] and **lipids** [22] which are of value for the production of biodiesel [5, 6, 10, 14, 21, 23, 24], **methane** [2, 5, 6, 11, 14, 25–27], **hydrogen** [5, 6, 11, 14, 23, 26], **alkanes** [7], **ethanol** obtained by degradation to smaller sugars and subsequent fermentation [5, 6, 21–24, 26, 27] and **butanol** [7]. The transformation of the biomass into biofuel is processed by liquidification, pyrolysis, gasification [9], extraction, transesterification or anaerobic fermentation [6].

Further interesting products which can be obtained from the biomass are **glycerol** [2, 5] and **carbohydrates** [25] such as polysaccharides [2, 5], which can be used for the production of cosmetics. Polysaccharides can also be a source for ba-

sic chemicals [8] and growth enhancing chemicals for agriculture or ingredients for health food [28–30].

High value products such as **proteins** [2, 5, 25, 31], **amino acids** [25], **phycobiliproteins** in cyanobacteria and a few microalgae [12, 29], **pigments** [2, 5, 23, 31] like **carotenoids** [5, 24, 31], **vitamins** [5, 24, 31] and **fatty acids** [2, 5, 31] such as **eicosapentaenic acid** (EPA) and **docosahexaenic acid** (DHA) are also contained in the biomass. EPA and DHA are especially important for the growth of fish larvae, shrimp, mollusks and fish [28, 32]. These long-chain, unsaturated fatty acids are also important for human health as they reduce the blood pressure and blood viscosity, prevent cardiovascular diseases, cancer, Alzheimer's disease and schizophrenia [32]. As **phospholipids** are surface-active they are utilized as emulsifying agents in foods, cosmetics and pharmaceutical products [8]. In addition, the biomass can also be utilized for the production of nutritional supplement [14, 22], medicine, animal feed [5, 14, 22, 25, 31, 33] and fertilizer [5, 14, 22, 26].

1.3 Nannochloropsis

Nannochloropsis is a member of the Eustigmatophyceae which has spherically shaped cells with a diameter of 2-4 µm [35]. It contains a variety of nutrients and is thus of interest as a nutritional source [36] with protein contents of up to 22% [37]. This marine alga is especially a good candidate for biodiesel production as its lipid content is very high, with up to 68% in dry weight [11]. *Nannochloropsis* has also been found to be a robust alga as it can recover quickly from high irradiance or high pH-values [38] showing the ability to cope with varying environmental conditions. But also pigment content has been found to be a further point of interest, as *Nannochloropsis* contains a wide range of carotenoids, including violaxanthin and vaucheriaxanthin as major ones and further carotenoids such as astaxanthin, canthaxanthin [39] and β-carotene [40]. In comparison to other *Nannochloropsis* sp. as well as other algae, *Nannochloropsis gaditana* (Fig. 1.2 [41]) shows a high lipid yield and is therefore a suitable source for oil for biodiesel production [42]. Further, *N. gaditana* contains high amounts of EPA, which makes it interesting as feed for rotifers [43]. A draft genome sequence of *N. gaditana* [44] as well as the genome of *N. oceanica* [45] have been recently published, so that a better char-

Table 1.1: Products which can be obtained from algal and cyanobacterial biomass.

energy	**hydrocarbons** [*Botryococcus braunii* [34]] **lipids** [*Dunaliella salina* [5]] **biofuel** [*Chlorella* [12]] **biodiesel** [*Nannochloropsis* [12], *Botryococcus braunii* [12], *Chlorella protothecoides* [4]] **methane** [*Chlorella vulgaris* [4]] **hydrogen** [*Cladophora fracta, Chlorella protothecoides* [6]] **alkanes** [7] **ethanol** [*Chlorella vulgaris* [4]] **butanol** [7]
raw material	**glycerol** [*Dunaliella salina* [5]] **carbohydrates** [*Spirogyra sp.* [9], *Porphyridium cruentum* [9]] **polysaccharides** [*Porphyridium sp.* [30]] **cosmetics** [*Chlorella* [12], *Dunaliella salina* [12]]
high value products	**proteins** [*Dunalliela salina* [5]] **amino acids** [25] **phycobiliproteins** (cyanobacteria) [*Arthrospira (Spirulina) platensis* [12]] **pigments** **carotenoids** **astaxanthin and lutein** [*Haematococcus pluvialis* [23]] **β-carotene** [*Dunaliella salina* [23]] **vitamins (biotin)** [*Euglena gracilis* [23]] **ascorbic acid** [*Prototheca moriformis* [23]] **fatty acids** e.g. **eicosapentaenoic acid (EPA)**, [*Nannochloropsis* [12], *Chlorella minutissima* [23]] **docosahexaenoic acid (DHA)** [*Schizochytrium spp.* [23]] **foods** [*Chlorella* [12], *Dunaliella salina* [12], *Arthrospira (Spirulina) platensis* [12], *Haematococcus pluvialis* [12]] **medicine** [*Arthrospira (Spirulina) platensis* [12], *Haematococcus pluvialis* [12]] **animal feed** [*Chlorella* [12]] **fertilizer** [5, 14, 22, 26]

acterization of genotypes and development of genetic engineering techniques can be expected for the genus *Nannochloropsis* in the near future. With the arrival of efficient transformation protocols, *N. gaditana* is supposed to become a biofuel production platform [46]. Indeed, first approaches by using endogenous promoters to enhance biomass and/or lipid biosynthesis have already been patented [47].

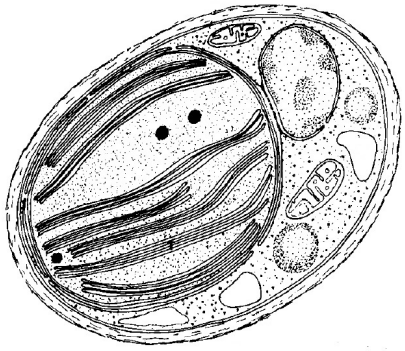

Figure 1.2: *Nannochloropsis gaditana* (modified figure from [41])

1.4 Endogenous rhythms

Good knowledge and understanding of metabolic pathways and their regulation within organisms are essential to design cultivation methods or explore genetic manipulation to improve the production of target products for industrial applications.

In many organisms certain physiological, developmental or behavioral events are synchronized with specific phases of recurring changes in their environment, such as day and night or seasons, to avoid unfavorable conditions for these events. Endogenous biological oscillators that maintain rhythms of approximately 24 h under constant conditions, the so-called circadian clocks, allow anticipation of recurring environmental changes needed for such temporal coordination [48–51]. In photosynthetic organisms the circadian clocks regulate, for instance, day-night changes in gene transcription [52], starch degradation [53, 54] and cell division [55–57]. The clocks can be entrained by light and temperature [58, 59] that serve as "Zeitgeber" ("time-giver" [60]). The components and physiological roles of circadian

clocks have been investigated in different photosynthetic organisms, from prokaryotic cyanobacteria [61] to eukaryotic green microalgae as *C. reinhardtii* [62, 63] and higher plants as *Arabidopsis thaliana* [49]. In microalgae circadian regulation has been found for gene expressions and for the timing of cell division [50]. For example, the expression of the chloroplast encoded gene *tufA* of *C. rheinhardtii* [64] or the photosystem (PS) II gene *psbA* of the cyanobacterium *Synechococcus* [65] are under circadian control. According to the genom of *N. oceanica* CCMP1779 no obvious genes encoding proteins similar to plant, animal or bacterial clock proteins were found; only two genes encoding bHLH-PAS proteins, which are important in the circadian regulation in animals, were identified [45]. Further, three genes encoding CCT (CONSTANS, CO-like, and TOC1) domain-containing proteins were found. The CCT-proteins are present in plants and green algae and function in light regulation, circadian and photoperiodic responses. These findings led to the assumption, that the circadian clock of *Nannochloropsis* is probably different from those of plants or animals [45].

1.5 Photosynthesis

Oxygenic photosynthesis, requiring light, water and CO_2 [66], is found in cyanobacteria, algae and vascular plants [67]. There are two main steps in photosynthesis, the light-dependent reactions and the dark reactions. The light reactions generate energy (stored in adenosine triphosphate, ATP) and reducing power in the form of nicotinamide adenine dinucleotide phosphate (NADPH), whereas in the dark reactions (Calvin cycle) glucose is produced by reduction of the carbon atom of CO_2 [66]. The main components for absorption and conversion of light energy are two photosystems, PS I and PS II which are multisubunit transmembrane pigment-protein complexes catalyzing electron transport within the thylakoid membrane [68, 69]. Electrons are transported from the donors (H_2O) in the thylakoid lumen to the acceptor (NADPH) outside the thylakoid. Each photosystem contains a core complex with the reaction center where the primary charge separation occurs [67]. Peripheral of the reaction centers are the antennae which have the function of light harvesting and transfer of excitation energy to the reaction center. Cyanobacteria contain phycobilisomes as peripheral antenna systems, which are soluble proteins attached to the surface of the photosynthetic membranes [70]. During evolution, the phycobilisomes were replaced by the light-harvesting complexes (LHC), consisting

of proteins localized in the thylakoid membranes with chlorophyll and carotenoid ligands. LHC has functions in light harvesting as well as in photoprotection [67].

N. gaditana has a LHC containing a relatively high proportion of xanthophylls and nine chlorophyll *a* molecules per apoprotein, whereas in higher plants, 14 chlorophyll molecules with four xanthophyll molecules are in the LHC II [71, 72]. The primary structure of the apoprotein of the LHC in *N. gaditana* is different compared to analogous proteins from non-green algae, green algae or higher plants, as for *N. gaditana* no cross-reactivity with antibodies was found [73]. In *N. salina* less than 10% of the chlorophyll *a* is closely associated with PS I, whereas in higher plants the value lies at about 35% leading to almost four times fewer PS I reaction centers per chlorophyll in this alga. Similar properties of the PS II complex were found for *N. salina* and spinach, yet again, a lower proportion of PS II core complex relative to LHC was reported for the alga. Most of the chlorophyll *a* and xanthophylls in *N. gaditana* are associated with the LHC complex [74]. In cyanobacteria the major antenna complex consists of phycobiliproteins [75]. The major light-harvesting chlorophyll *a*/*b*-binding protein in plants (LHC II) is similar to the chlorophyll-protein in *C. reinhardtii* [76]. Each pigment-protein subunit contains eight chlorophyll *a*, six chlorophyll *b*, two luteins, one neoxanthin and one violaxanthin [77]. Unlike in vascular plants, green algae and diatoms, the major LHC in *Nannochloropsis* is a violaxanthin-chlorophyll *a* complex [78].

Pigments are compounds absorbing specific wavelengths and thus exhibit typical colors. The physico-chemical nature of the pigments in photosynthetic organisms influences light energy absorption. In microalgae major pigment groups are chlorophylls (green), phycobilins (blue and red) and carotenoids (yellow and orange). Chlorophylls have a magnesium atom in the center of a polyconjugated tetrapyrrole ring; this magnesium atom is involved in the primary charge separation that initiates photosynthetic electron transport and is therefore the most important group. The main task of carotenoids is the protection of chlorophyll by dissipating excess light [66] and scavenging reactive oxygen species (ROS) [79] generated by excitation energy transfer to O_2 molecules continuously produced in the light by the PS II activity.

The genus *Nannochloropsis* contains chlorophyll *a* as higher plants, green algae and cyanobacteria do [80], whereas chlorophyll *b* which is found in green algae [81], e.g. *C. reinhardtii* [82], *c* in certain brown algae, yellow algae and diatomes [83] and *d* in red algae [80] are absent. Besides violaxanthin, vaucheriaxanthin and β-carotene, further minor carotenoids such as astaxanthin and canthaxanthin are present [39, 40]. The xanthophyll lutein, which is present in higher plants [74], the green alga *C. reinhardtii* [84] and other algae such as *Phaeophyta* or *Chrysophyta* [85], is absent in *N. gaditana* [74, 86]. During light phases the chlorophyll *a* and carotenoid contents increase [87]. Under high light conditions the conversion of violaxanthin to zeaxanthin has been found [40]. Ageing cultures show an increase in accumulation of canthaxanthin and astaxanthin in *N. gaditana* [39, 88].

1.6 Photoprotection

1.6.1 Excited chlorophyll

Light is essential for photosynthetic processes, yet too much light can cause damages. Absorption of light energy leads to the formation of excited singlet chlorophylls (^{1}Chl*), whereafter the absorbed energy can be re-emitted as fluorescence with no further impact on the cell, dissipated as heat or transferred to reaction centers to drive photochemical processes [89]. The second pathway, namely the protective processes of dissipating excess energy non-photochemically in form of heat, brings excited singlet chlorophyll back to the ground state [89]. If excess light energy is transferred to excited singlet chlorophylls, they can be converted to excited triplet chlorophylls (^{3}Chl*) which have a much longer lifetime (ms instead of ns) in the light harvesting antenna and can thus react with oxygen (O_2). This can lead to the formation of singlet oxygen ($^1O_2$*), a ROS [89–91] which can damage proteins, lipids and pigments in and around the photosystems [91].

1.6.2 Non-photochemical quenching

Non-photochemical quenching (NPQ) can be divided in three major components showing different relaxation kinetics: energy dependent quenching (qE), state-transition quenching (qT) and photoinhibitory quenching (qI) [89, 92]. The energy dependent component qE can change within seconds and is therefore important

for plants and algae that are exposed to fluctuating light. Excessive light leads to a decrease in pH in the thylakoid lumen triggering the protective reactions of qE [89, 91]. Besides zeaxanthin and/or antheraxanthin as components of qE [93], in land plants including mosses and green macroalgae, the LHC-like protein PsbS contributes to photoprotective energy dissipation in qE [94–96], whereas in green and brown algae and some mosses the LHC protein LHCSR activates qE [97]. In *N. oceanica* CCMP1779 the genes for LHCSR were found, whereas genes encoding PsbS were absent [45]. qT depends on phosphorylation of LHCs accociated with PS II [98] and leads to dissociation of LHCs from PS II with a slower relaxation time ranging in minutes [89]. The third component, qI which is associated with photoinhibition of photosynthesis, has the slowest relaxation kinetics taking up to several hours [89, 91].

1.6.3 Xanthophyll cycle

Carotenoids are isoprenoids having a polyene chain with conjugated double bonds. They can be divided into two groups, carotenes and xanthophylls [40]. Some of the xanthophylls are involved in a photoprotective mechanism, the xanthophyll cycle, which is also known as the **violaxanthin cycle** [99], found in vascular plants and green and brown algae [100]. Its presence has also been found in *N. gaditana* [40] and a gene encoding the violaxanthin de-epoxidase (VDE) like in plants has been found in *N. oceanica* CCMP1779 [45]. The violaxanthin cycle consists of two opposite reactions [91] as shown in Fig. 1.3 [101]. The water soluble enzyme VDE, which is located in the thylakoid lumen, is activated by low luminal pH (maximum activity at pH $<$ 5.8 [102]) under excess light, leading to conversion of violaxanthin to zeaxanthin via the intermediate antheraxanthin in two-step reactions (violaxanthin $\rightarrow$ antheraxanthin, antheraxanthin $\rightarrow$ zeaxanthin) with ascorbate as a cosubstrate [40, 99]. When excess light energy disappears, the pH gradient across the thylakoid membrane decreases, VDE is inactivated and the activity of zeaxanthin epoxidase (ZEP) located outside the thylakoid (optimal activity at pH 7-7.5 [102]) becomes detectable, converting zeaxanthin back into antheraxanthin and in a second step into violaxanthin by using oxygen and NADPH [40, 102]. It is assumed, that energy is transferred from chlorophyll to antheraxanthin and zeaxanthin, or structural changes induced by protonation of LHC or PsbS protein lead to the formation of heat dissipating centers in antenna complexes [102]. In this respect the marine

parasinophycean alga *Mantoniella squamata* is unique because its xanthophyll cycle undergoes only one de-epoxidation step from violaxanthin to antheraxanthin. This alga accumulates high amounts of antheraxanthin under high light and therefore, energy dissipation is independent of zeaxanthin and lutein, which are rarely accumulated or absent [103]. The violaxanthin cycle pigments are mostly located in the thylakoid membranes. Most of the xanthophylls from pigment-protein complexes are located in light-harvesting complexes as LHC II (in case of higher plants and green algae) and additionally, violaxanthin de-epoxidation has also been found in the PS I supracomplex [79]. Yet, operation of violaxanthin de-epoxidation has been shown to be independent of the presence of pigment-protein complexes [79].

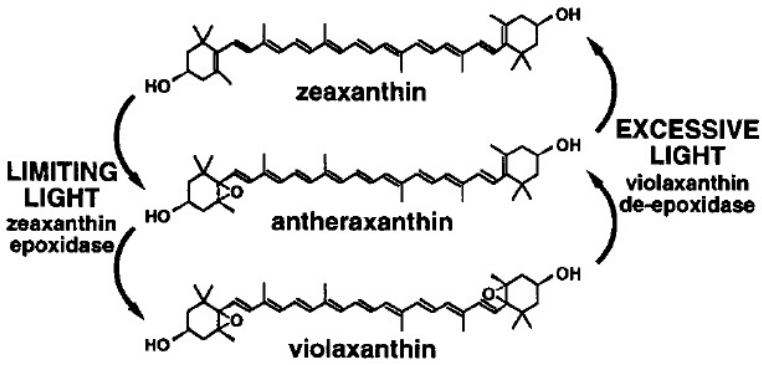

Figure 1.3: The violaxanthin cycle (figure from [101])

Two NPQ mutants have been found in higher plants and *C. reinhardtii* to be defective in the xanthophyll cycle, *npq1* and *npq2*. Mutants which presumably have a defect in VDE are referred to as *npq1*. Deficiency in VDE activities blocks the conversion of violaxanthin to antheraxanthin and zeaxanthin under high light. Vice versa, *npq2* mutants are defective in ZEP, resulting in the lack of all xanthophylls downstream of zeaxanthin epoxidation (e.g. antheraxanthin, violaxanthin and neoxanthin) and constitutive hyper-accumulation of zeaxanthin [93, 101]. The *npq1* mutant is characterized by an impaired induction of NPQ in high light, yet retains a small amount of reversible NPQ which is induced quickly when exposed to high light, possibly due to low levels of antheraxanthin and zeaxanthin produced during biosynthesis of violaxanthin, involvement of lutein or even a xanthophyll independent mechanism. The impairment of reversible NPQ in *Arabidopsis* was

found to be stronger compared with *Chlamydomonas*, therefore reliance on the xanthophyll cycle can differ in different organisms. High levels of zeaxanthin in *npq2* lead to a slower reversibility of NPQ and more energy is dissipated under moderate light conditions. Accordingly, photosynthetic efficiency has been found to be lower [93].

A simpler xanthophyll cycle, the **diadinoxanthin cycle**, is displayed in diatoms and other chromophytes [104], in which diadinoxanthin is converted into diatoxanthin by diadinoxanthin de-epoxidase (DDE) under high light and back to diadinoxanthin with diatoxanthin epoxidase (DEP) under low light. DDE can already operate at a high pH of 7.2, whereas DEP, which is most likely positioned at the stromal side of the thylakoid membrane, is active around pH 7.5, similar to ZEP [100].

Some algae have been shown to possess both xanthophyll cycles, possibly for better adaptation to changing light conditions underwater [105]. In cyanobacteria the violaxanthin cycle and diadinoxanthin cycle are absent, yet can convert β-carotene to zeaxanthin in the xanthophyll biosynthesis pathway at high light [102]. The mechanism of NPQ in cyanobacteria is regulated by the orange carotenoid protein (OCP), which operates in the phycobilisomes [106, 107].

1.7 Potential of photosynthetic microorganisms for industrial production of valuable products and as waste recyclers: A literature survey

The purpose of the following chapter is to give an overview of the current state and limitations of algal biomass production and its potential for industrial applications. Biomass data are generally given in dry weight.

Table 1.2: List of species used in literature

species	size	classification
Aphanothece microscopica Nägeli family: Cyanobacteriaceae	3-30 µm	cyanobacterium
Arthrospira (Spirulina) platensis family: Phormidiaceae	0.3-1 mm	cyanobacterium
Arthrospira (Spirulina) maxima family: Phormidiaceae	0.3-1 mm	cyanobacterium
Botryococcus braunii family: Trebouxiophyceae incertae sedis	$\geq$ 1 mm	microalga
Chaetoceros calcitrans family: Chaetocerotaceae	2.5-6 µm	microalga
Chlorella protothecoides family: Chlorellaceae	5-7 µm	microalga
***Chlorella* sp.** family: Chlorellaceae	2-10 µm	microalga
Chlorella vulgaris family: Chlorellaceae	4-10 µm	microalga
Cladophora fracta family: Cladophoraceae	$\geq$ 85 µm	microalga
Dunaliella salina family: Dunaliellaceae	17-23 µm	microalga

species	size	classification
Dunaliella tertiolecta family: Dunaliellaceae	10-12 µm	microalga
Euglena gracilis family: Euglenaceae	30-70 µm	microalga
Haematococcus pluvialis family: Haematococcaceae	20 µm	microalga
***Isochrysis* sp.** family: Isochrysidaceae	5 µm	microalga
Nannochloropsis oculata family: Monodopsidaceae	1-2 µm	microalga
***Nannochloropsis* sp.** family: Monodopsidaceae	2 µm	microalga
Phaeodactylum tricornutum family: Phaeodactylaceae	15-30 µm	microalga
Porphyridium cruentum family: Porphyridiaceae	10 µm	microalga
***Porphyridium* sp.** family: Porphyridiaceae	5-8 µm	microalga
Prototheca moriformis family: Chlorellaceae	13-15 µm	microalga
***Rhodomonas* sp.** family: Pyrenomonadaceae	9.2-9.9 µm	microalga
***Scenedesmus* sp.** family: Scenedesmaceae	3-78 µm	microalga
***Schizochytrium* spp.** family: Thraustochytriaceae	4-14 µm	microalga
***Spirogyra* sp.** family: Zygnemataceae	up to several centimeters long	microalga
Synechocystis aquatilis family: Merismopediaceae	2 µm	cyanobacterium
***Tetraselmis* sp.** family: Chlorodendraceae	14 µm	microalga

1.7.1 Reactor design

There are two different large scale cultivation systems for microalgae and cyanobacteria: open ponds and closed photobioreactors [5, 9, 21, 25, 108].

1.7.1.1 Open ponds

An aerial image of an open pond is shown in Fig. 1.4. Open ponds are usually build of concrete or are sheaves covered with plastic [4, 6] with a depth of 0.1-0.3 m [25]. With the help of a paddle wheel [22] the culture is circulated, while nutrients are added downstream of the paddle wheel to ensure a good distribution and harvest of biomass is operated upstream of the paddle wheel [4, 6, 9]. Open ponds have a large surface with direct contact to the air so that CO_2 can be taken up from the atmosphere. To improve the production, additional CO_2 can be added at the bottom of the pond [109]. Installation of sensors can be advantageous to control the cultivation conditions as shown in Fig. 1.5.

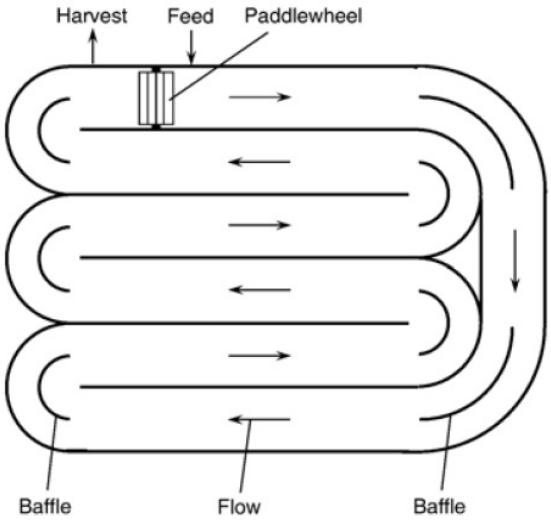

Figure 1.4: Aerial image of an open pond (figure from [11])

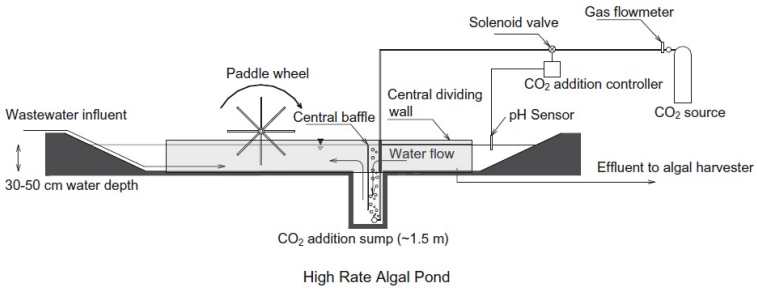

Figure 1.5: Vertical profile of an open pond system (figure from [109])

Advantages:

An important advantage of the open pond system is low costs [5, 23, 110] due to the simple construction. CO_2 can be utilized directly from the atmosphere [7, 12], which makes an additional CO_2 source optional. Further, the system is easy to clean up [5] as there are no inaccessible parts.

Disadvantages:

The main disadvantage of the system is the low production performance [10], since the conditions are difficult to regulate and the microorganisms are directly exposed to UV light [10]. In an open system the risk of contamination [5, 22, 27] is rather high. The culture density is limited by the availability of solar radiation and the circulation can be rather poor, as mixing is only provided by a paddle wheel, which can lead to an uneven distribution [4, 10] of microorganisms and nutrients. The day-night cycles [10] as well as the seasonal climatic differences [4, 11] have a direct impact on the organisms. As the ponds are limited in depth, a larger surface area is needed, which also leads to a higher evaporation loss of water [22].

1.7.1.2 Photobioreactors

Closed PBRs commonly consist of transparent material such as glass or plastic [6, 111] and the turbulent flow inside allows good mixing [11]. The reactors can either be set up vertically or horizontally (Figs. 1.6 and 1.7). Tubular photobioreactors should not exceed a length of 80 m to prevent accumulation of oxygen which

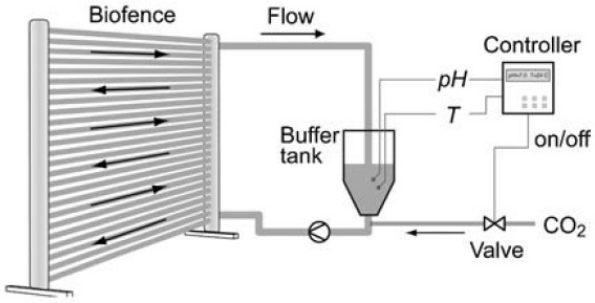

Figure 1.6: Fence photobioreactor (figure from [33])

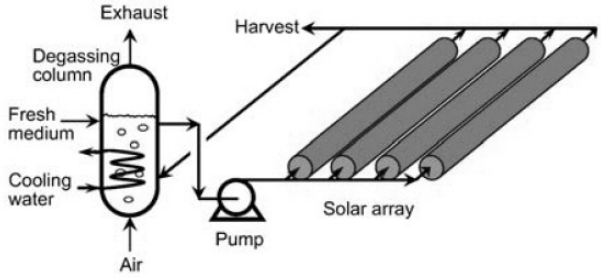

Figure 1.7: Tubular photobioreactor (figure from [11])

damages the cells. To prevent extreme light limitation a diameter of less than 0.1 m is recommended [11]. Due to these dimensions a maximum volume of 315 m^3 can be achieved. Larger flat panel PBRs can have a volume of 200 l; with systems e.g. consisting of five flat panels, a total volume of 1,461,000 l corresponding to 900 m^3 per hectare can be achieved. With column reactors a volume of up to 972 m^3 per hectare is possible [7].

Advantages:

The advantage of closed PBRs is the possibility to cultivate a single species [4, 22] as a nearly pure culture, as the risk of contamination is smaller than in open ponds [5, 108, 112]. Due to a higher achievable cell density [5], greater amounts of biomass [22, 108, 112] can be produced per volume and per area. Photobioreactors have a greater surface-to-volume ratio [9, 24, 108, 110] ensuring a higher amount of available light for the organisms. A further benefit of the closed system is the extremely

low evaporation rate as well as a low loss of CO_2 [7] when CO_2 gas is supplied to the culture. The cultivation conditions can be controlled rather well [5, 23, 112] and a good mixing [5] can be achieved.

Disadvantages:

The major disadvantages to overcome are the high investment costs concerning the construction, operation and maintenance of the system [5, 22]. In the closed system the possibility of overheating is high as well as the decay of biomass. If the system is not equipped with enough degassing points, the risk of oxygen accumulation is high, leading to cell damage. The higher complexity of the system makes upscaling of closed PBRs more difficult than for open pond systems [5].

1.7.1.3 Hybrid-system

It is further possible to combine the two systems, closed PBRs and open ponds, to a hybrid-system [9]. With this system the algae are first cultivated in the closed system. After reaching a high density, the open pond system is inoculated with this culture. The cell density is of importance to prevent contamination with other organisms. An additional way to prevent contamination is the regular cleaning of the ponds, so this system is especially suitable for batch cultures [6].

1.7.1.4 Light transfer

Biomass production with algae is particularly dependent on the availability of light. To increase the biomass production, the availibility of light can be improved by using an additional light source. Light can be transferred from the outside to the inside of the reactor with optical fibers. This leads to a more homogenous distribution inside the reactor. LED have the advantage of less heat production in comparison to other light sources, so that installation around the reactor can supply additional light. Higher costs due to the need of more current can be prevented by installing photovoltaic or wind energy on site [10] (Fig. 1.8). In chapter 1.7.2.2 the impact of light availability is further discussed.

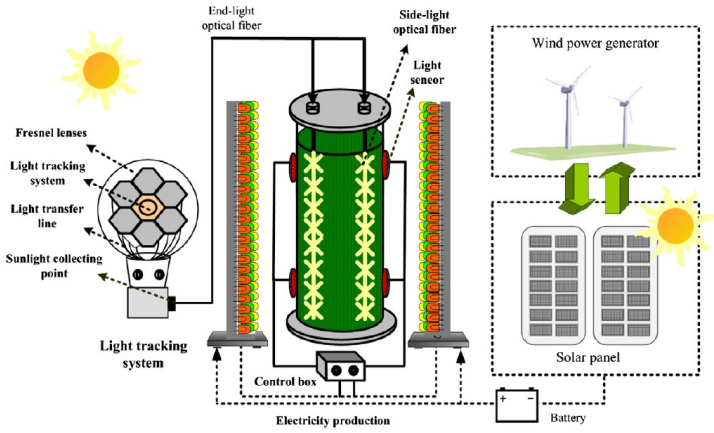

Figure 1.8: Scheme of a possible setup for illumination of a PBR with simultaneous current production by solar panel and wind power generators for operation (figure from [10]).

1.7.1.5 Comparison of the productivity of open pond systems with closed photobioreactors

In Table 1.3 the differences of several cultivation parameters for the production of 100 t biomass in open ponds and closed PBRs are shown. The data are a summary of biomass productivity and concentration of different species cultivated in large-scale ponds and PBRs [11] in different countries. The volumetric productivity is more than 10-times higher in closed PBRs than in open ponds and thus closed PBRs can achieve an areal productivity twice as high as that of open ponds. This is due to a much higher biomass concentration which can be produced within the closed system. Further, the oil production is higher in the PBRs and less area is needed for the same biomass production. In both systems an equal amount of CO_2 (183,333 kg) is fixed for the same amount of biomass production.

Further parameters of different cultivation systems are shown in Table 1.4 for the production of 1 kg of *Spirulina* dry biomass per day in an open pond, tubular reactor, one free-standing flat plate PBR and several flat plate PBRs with a space of 20 cm in between based on estimated capacity [110]. The lowest volume for the production is needed for the free-standing flat plate reactor and the largest for the pond system. The largest surface area for light absorption is achieved on the least land area with the lined-up flat plate PBRs. In a free-standing flat plate

Table 1.3: Comparison of different parameters for the cultivation of microalgae in an open pond system and in closed PBRs (values taken from [11]).

parameters of algal cultivation	**closed PBR**	**open pond**
annual biomass production (kg)	100,000	100,000
volumetric productivity (kg m^{-3} d^{-1})	1.535	0.117
areal productivity (kg m^{-2} d^{-1})	0.072 (based on area of PBRs)	0.035 (based on area of pond)
biomass concentration in medium (kg m^{-3})	4.00	0.14
oil production (m^3 ha^{-1})	136.9 (70% oil content) 58.7 (30% oil content)	99.4 (70% oil content) 42.6 (30% oil content)
required land area (m^2)	5,681	7,828
annual CO_2 consumption (kg)	183,333	183,333
system geometry	132 parallel tubes per unite, 80 m long tubs, 0.06 m diameter; 6 units	978 m^2 per pond, 12 m wide, 83 m long; 8 units

bioreactor the light exposure is particulary high, which makes it possible to reach the highest culture density and with that the highest volumetric productivity. The highest areal productivity is attributed to lined-up bioreactors and the best reactor efficiency is obtained by the free-standing reactor. These data show the importance of light availability for algal biomass production, which is strongly influenced by the design of the cultivation system.

1.7.2 Productivity

1.7.2.1 Limiting factors

The productivity of cultivation systems is limited by different factors, especially **light**, **temperature** and **nutrient availability**. Availability of light [24, 33] limits the biomass production, as it is necessary for photosynthetic processes. Good locations for production are for example in arid states of the USA (California, Arizona and New Mexico) where up to 90% of days are sunny and bright [25]. The amount of solar energy available depends on the location. In Phoenix, Arizona, USA yearly solar radiation lies at 7,300 MJ m^{-2} a^{-1}, while further east in Cambridge, Massachusetts, USA there are 4,800 MJ m^{-2} a^{-1} [21], whereas the recorded values in Zara, Jordan were 7,297.5 MJ m^{-2} a^{-1} [113] and at the most sunny location of Germany in Friedrichshafen 4,523 MJ m^{-2} a^{-1} [114].

Light:

Figure 1.9 [115] shows the mean global solar radiation. In the northern half of Europe as well as in Canada, Greenland, Russia and most southern land parts of the southern hemisphere the lowest solar energy amounts of up to 175 W m^{-2} (1 W=1 J s^{-1}) are available. Especially high energy amounts were recorded in most parts of Africa, as well as in Australia, Mexico, Arabian countries and China. It is important to point out that only 50% of the light spectrum within photosynthetically active radiation (400-700 nm) can actually be utilized for photosynthesis by algae and cyanobacteria [21, 111, 116] and only 3% of solar energy can be converted into biomass [117]. Due to these solar energy limitation and rather poor light-to-biomass energy conversion rates, it is necessary to make sure that the density of

Table 1.4: Comparison of different parameters for the production of 1 kg dry *Spirulina* biomass per day in a open pond system and in different closed PBRs (values taken from [110]).

parameters for the production of 1 kg of dry *Spirulina* biomass per day	**open pond (15 cm deep)**	**horizontal tubular reactor (diameter$_{outside}$ 2.9 cm, diameter$_{inner}$ 2.5 cm)**	**vertical flat plate PBR, fully exposed (2.5 cm light path)**	**vertical flat plate PBRs (20 cm apart, 2.5 cm light path)**
volume (l)	5,550 (150 l m^{-2})	629 (171 l m^{-2})	416 (25 l m^{-2})	1,138 (125 l m^{-2})
area (m^2)	37.0	37.0	17.0	9.1
illuminated reactor surface (km^2)	37.0	37.0	34.0	91.0
optimal culture density (g l^{-1})	0.4	4.8	6.0	2.2
volumetric production rate (g l^{-1} d^{-1})	0.18	1.60	2.4	0.90
areal production rate (g m^{-2} d^{-1})	27.0	27.0	60.0	110.0
reactor efficiency (volumetric production rate/illuminated surface) x 10^2	0.5	4.3	7.0	1.0

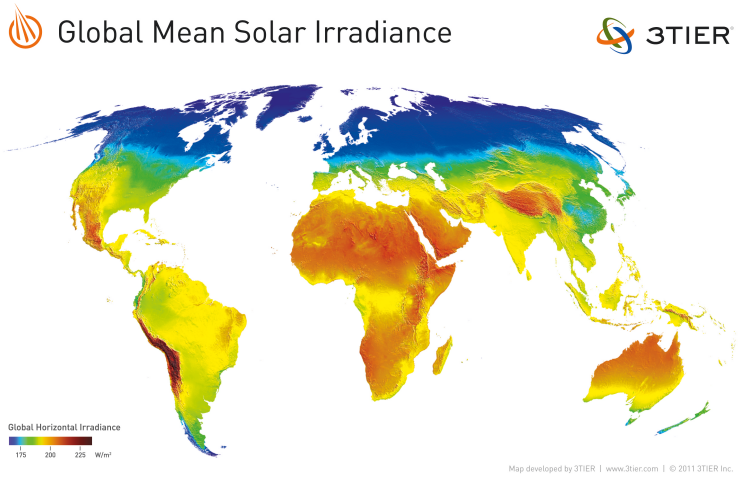

Figure 1.9: Global average solar irradiance (figure from [115])

the algal culture is not too high so that light can penetrate deep into the culture. Further, the depth of the ponds should not exceed 0.3 m [25] or the choice of diameter of the reactors should be made to ensure a good light supply inside the reactor [110]. In order to achieve these requirements, a high surface-to-volume ratio [14] should be chosen, as well as means assuring good mixing of the culture [24, 110]. Yet, too strong light intensities can lead to photoinhibition, which would result in reduced photosynthetic efficiency and growth [11]. This problem can especially occur during noon time [25], when light intensity is usually the highest.

Temperature:

Temperature is another factor which influences the production of photosynthetic microorganisms. Shallow ponds have the disadvantage of extreme temperature fluctuations [25], as they can heat up quickly but also cool down very fast, which leads to growth inhibition [33]. In Fig. 1.10 [118] the global average temperature is shown. Countries with optimal temperatures between 20-30°C are located from southern Mexico till southern Brazil as well as almost the entire African continent, the Arabian countries, India and from Thailand to central Australia, whereas in central Europe lower average temperatures of 5.5-10°C are reached. It is important

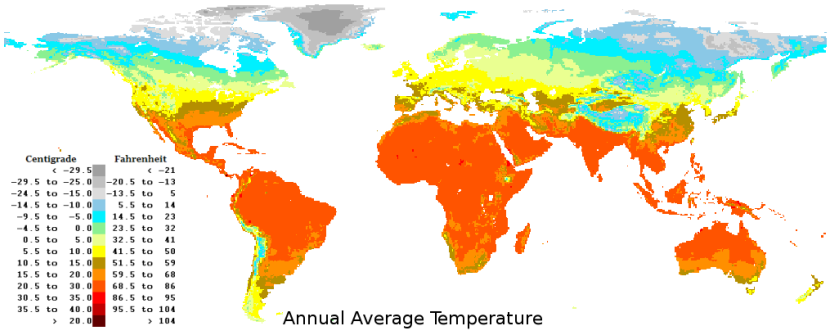

Figure 1.10: Global annual average temperature (figure from [118])

to take into account that at locations with high average temperatures, temperatures during the hottest season or the hottest time of the day are often too high for optimal cultivation, so that cooling systems are of need. In contrast, heating might be necessary in cooler regions, especially in the winter months. Use of industrial waste heat, such as heat from the cooling water of a power plant, can be utilized.

Nutrients:

The third main limiting factor is the availability of nutrients, as nutrients are essential for growth. Hereby especially the concentration [119] as well as the ratios [120] of the elements are of importance. The most important nutrients needed for cultivation are macronutrients such as nitrogen and phosphorus and micronutrients e.g. iron, magnesium and trace elements [108]. More information on nutrients is given in section 1.7.4.

1.7.2.2 Impact of cultivation conditions

The influence of different environmental parameters on growth and production of compounds within the cells are discussed below based on:

- nutrient availability
- temperature
- light duration

- light path
- light availability

Cultivation under different conditions leads to a change in physiological processes and by that also a change in production of different organic compounds. For example, *Nannochloropsis* sp. cultivated in Schott glass bottles containing 9 l medium in a laboratory achieved the highest biomass production at medium nitrogen (600 µM NaH_2NO_3) and phosphorus concentrations (25 µM NaH_2PO_4) [121]. Lower **nutrient availability** led to higher lipid and carbohydrate contents. The protein content increased with increasing nitrogen concentrations. During cultivation of *Nannochloropsis* sp. under nitrogen deprivation and natural light in Italy, slightly lower biomass productivity (-17% of the biomass under normal conditions) with up to 60% lipid content and a higher lipid productivity (74%) [27] was observed. When the **temperature** was not the optimum, an increase in both lipid and protein content was detected [121]. At lower temperatures higher carbohydrate contents were measured and at higher salt concentrations higher lipid contents. Yet it should be kept in mind that sub-optimal temperatures were also accompanied by reduced cell growth and thus a lower biomass production (here: -4 to -21%).

In order to determine the influence of **light duration** the cyanobacterium *Aphanothece microscopica* Nägeli was cultivated under different light-dark (LD) cycles in a bubble column PBR containing 3 l. Maximal growth as well as maximal CO_2-utilization were found at 22-24 hours illumination per day (Table 1.5). Further, cell concentration and CO_2 uptake decreased in proportion to decreasing duration of illumination. However, growth is not only dependent on light duration but also on light intensity [122].

Light energy available for algae depends also on the **light intensity** as well as the **light path** and the optimum differs between organisms. *Nannochloropsis* sp. showed an optimum of 10 cm in a flat panel PBR under environmental conditions in Sde Boker, Israel, in which an areal productivity of 12.1 g m^{-2} d^{-1} and a productivity per volume of 0.3 g l^{-1} d^{-1} were found, whereas for *Porphyridium* sp. the optimal light path lied at 20 cm and for *Spirulina* it was only 1.3 cm [123].

Table 1.5: Maximal cell density of *Aphanothece microscopica* Nägeli in batch mode under different light-cycles for 160 h (35°C, 150 µmol photons m^{-2} s^{-1}, 15% CO_2 enriched air) (values from [122]).

light-dark-cycle (h)	**cell density$_{max}$ (g l^{-1})**
24:0	5.10
22:2	5.08
20:4	3.4
18:6	2.69
16:8	1.64
14:10	1.3
12:12	2.06
10:14	0.94
8:16	0.34
6:18	0.26
4:20	0.2
2:22	0.15
0:24	0.11

To study the influence of **light availability** on biomass production *Nannochloropsis* sp. was cultivated in a 20 l flat panel PBR [27]. The reactor was illuminated from one side and the intensity was increased from 115 µmol photons m^{-2} s^{-2} to 230 µmol photons m^{-2} s^{-2}. During this experiment the biomass production rose from 0.61 g l^{-1} d^{-1} to 0.85 g l^{-1} d^{-1} with an increasing lipid content from 14.7% to 19.6%. When the reactor was illuminated from both sides with the same increase in light intensity, an increase in biomass production from 0.97 g l^{-1} d^{-1} to 1.45 g l^{-1} d^{-1} as well as a rise in lipids from 24% to 32.5% were measured. By cultivating 110 l *Nannochloropsis* sp. in a Green Wall Panel PBR under natural illumination in Livorno, Italy, a biomass productivity of 0.36±0.10 g l^{-1} d^{-1} with a lipid content of 32.3±1.0% was recorded, corresponding to the lipid production of 117.28 mg l^{-1} d^{-1} [27]. These experiments show that the biomass production as well as the lipid content increase at higher light availability. Further, higher biomass and lipid production are possible under controlled laboratory conditions compared to natural conditions.

1.7.2.3 Production in laboratory conditions

Values reported for productivity in laboratory scale strongly depend on the cultivation conditions. The biomass and lipid productivity of different organisms grown

Table 1.6: Biomass and lipid productivity of different microalgae and of a cyanobacterium cultivated in laboratory scale.

species	**biomass productivity in g l^{-1} d^{-1} (g m^{-2} d^{-1})**	**lipid productivity in mg l^{-1} d^{-1} (g m^{-2} d^{-1})**
microalga		
Nannochloropsis sp.	ca. 0.4 [10] (4.4-13.4) [28]	4.6-20.0 [28] (1.0-4.2) [28]
Isochrysis sp.	0.1-0.2 [10] (6.1-18.8) [28]	6.4-21.1 [28] (1.4-4.4) [28]
Tetraselmis sp.	0.3 [10] (33.1-45.0) [28]	18.6-22.7 [28] (3.9-4.8) [28]
Rhodomonas sp.	(3.8-13.4) [28]	2.1-9.7 [28] (0.4-2.0) [28]
cyanobacterium		
Spirulina maxima	0.2 [10]	8.6 [10]

under varying conditions are shown in Table 1.6. The biomass productivity ranged from 0.1-0.4 g l^{-1} d^{-1}, whereas the areal productivity reached up to 45 g m^{-2} d^{-1} with *Tetraselmis* sp. The lipid productivity depends on the lipid content of the organisms. Lipid production was up to ca. 23 mg l^{-1} d^{-1} or 5 g m^{-2} d^{-1} [10, 28]. As these values were achieved under laboratory conditions it is very likely that they are higher than values achievable by a large-scale production under natural conditions.

1.7.2.4 Production in a large scale

The production data of different microorganisms cultivated in larger outdoor installations are listed in Table 1.7. Because the productivity depends on the species and cultivation conditions, especially the reactor design and location, it is difficult to compare data of different studies obtained from different organisms cultivated in different systems in different places. The productivity of the cyanobacterium *Arthrospira platensis* lied at 2.7 g l^{-1} d^{-1} [124] and *Synechocystis aquatilis* reached 35 g m^{-2} d^{-1} [125]. The microalga *Chaetoceros calcitrans* reached 37.3 g m^{-2} d^{-1} and *Chlorella* sp. 4.3 g l^{-1} d^{-1} and 38.2 g m^{-2} d^{-1} [126]. In contrast, the produc-

tivity of *Nannochloropsis* sp. was 0.7 g l^{-1} d^{-1} [127]. A 300 l *N. oculata* batch culture, which was illuminated during the night, achieved a maximal biomass concentration of 200 mg l^{-1} after 48 h cultivation [32]. Production of 1.4 g l^{-1} d^{-1} of the microalga *Phaeodactylum tricornutum* was reported for a helical tubular PBR [128] whereas a batch culture achieved a maximal biomass concentration of 25 g l^{-1} after 28 d cultivation [24].

Table 1.7: Cultivation of microorganisms in a large-scale.

species	**productivity**	**cultivation conditions**
Arthrospira platensis [124]	2.7 g l^{-1} d^{-1}	0.01 m tube diameter, setup wave-like in rows, continuous operation, natural light, facing north-south, summer time, near Florence, Italy
Synechocystis aquatilis [125]	35 g m^{-2} d^{-1}	reactor consisting of two parallel tubes, tube length 4 m, inner diameter 12.5 cm, static mixer, continuous operation, natural light, summer time, Tsukuba, Japan
Chaetoceros calcitrans [129]	37.3 g m^{-2} d^{-1}	dome-shaped reactor, November-December, Iwata, Japan
Chlorella sp. [126]	4.3 g l^{-1} d^{-1}/ 38.2 g m^{-2} d^{-1}	thin-film reactor, fed-batch, ca. 12 h light per day, July, Czech Republic
Nannochloropsis sp. [127]	0.7 g l^{-1} d^{-1}	horizontal tube reactors, September, Florence, Italy
Nannochloropsis oculata [32]	after ca. 48 h: 200 mg l^{-1}	air-lift reactor in greenhouse, constant temperature of 28°C, illumination during night
Phaeodatykum tricornutum [128]	1.4 g l^{-1} d^{-1}	helical reactor, 106 m long plastic tubes with a diameter of 0.03 m, continuous operation, Spain
Phaeodatykum tricornutum [24]	after 20 d: 25 g l^{-1}	vertical flat panel airlift reactors, temperature control 20°C, 24 h artificial light with 1/3 of the maximal sunlight intensity

1.7.2.5 Lipid production

The amount of oil which can be produced with photosynthetic microorganisms is about 200 times higher than the yield of the highest oil-producing plant oil palm [9, 11]. According to [10] the highest lipid production was achieved with *Chlorella* sp. at 179 mg l^{-1} d^{-1} in a cylindrical glass reactor (30 cm length, 7 cm diameter) at 26°C and continuous illumination with 300 µmol photons m^{-2} s^{-1}. One liter of biodiesel production requires 0.9 kg (900,000 mg) of crude oil [25]. An annual oil production of up to 58,700 l per hectare are possible with microalgae containing 30% oil by wt. in biomass [11]. Possible oil production of up to 143-443 t per hectare [7] based on extrapolated data of *Tetraselmis suecica* or 20,000-80,000 l per acre (1 acre=0.405 hectare) per year [6] have been described for high oil species of microalgae. Comparing the production with and without additional illumination, an oil yield of 100-130 m^3 ha^{-1} can be reached under natural illumination and 172 m^3 ha^{-1} under artificial illumination [10].

Haematococcus pluvialis was cultured in a pilot facility in Hawaii for production of biodiesel with 25,000 l PBRs coupled with 50,000 l open ponds [130] on an area of two hectares [108]. With this facility biomass production of 1.9 kg d^{-1} [108, 130] and productivity of 0.076 g l^{-1} d^{-1} was reached. The oil production was equivalent to 420 GJ ha^{-1} a^{-1} and a maximal production rate of 1,014 GJ ha^{-1} a^{-1}. It is assumed that up to 3,200 GJ ha^{-1} a^{-1} can be achieved with *Chlorella* under favorable conditions in the existing production system [23, 108, 130].

1.7.2.6 Production of polysaccharides

In order to investigate the production of polysaccharides such as xylose, galactose and glucose by *Porphyridium* sp., a study was carried out in a flat panel reactor under natural conditions [30]. The maximal cell density was achieved faster in summer, with longer periods of optimal temperature, than in winter. A reactor with 1.3 cm path brought higher productivity per volume while a reactor with 30 cm path allowed higher areal productivity. With 1.3 cm path a production of 0.110 g l^{-1} d^{-1} was reached in summer and 0.073 g l^{-1} d^{-1} in winter. At a daily harvest of 75%, 3.4 g m^{-2} d^{-1} of soluble polysaccharides could be produced [30].

1.7.3 Wastewater treatment

Another important cost factor during cultivation of microalgae and cyanobacteria are nutrients needed for growth. Even though they can produce 20 times more biodiesel than rapeseed, they also need more nitrogen of up to 8-16 t ha^{-1} a^{-1} [6]. In order to reduce these costs for nutrients, cultivation in wastewater was studied. In the following some examples are given.

Spirulina platensis was cultivated in 20% anaerobic sludge blanket in a continuous process reaching a productivity of 20 g m^{-2} d^{-1} in a 6 l reactor outdoors in Thailand at ambient temperatures [31]. About 12 g m^{-2} d^{-1} were produced in a 100 l reactor achieving a total nitrogen elimination of 34 mg l^{-1} d^{-1} and a total phosphorus elimination of 4 mg l^{-1} d^{-1} [31]. *Botryococcus braunii* cultivated in secondary-teated wastewater of a pigs farm was able to take up 80% of the nitrate at a starting concentration of 788 mg l^{-1} [34].

Centrate is the liquid which remains after concentration of activated sludge. It has an unfavorable N/P-ratio, contains little carbon but high amounts of toxins and bacteria. Due to its turbidity, translucency is rather low. Despite all these, *Chlorella* sp. was able to grow directly in centrate without needing any adaptation phase [131]. Further, no negative impact of bacteria could be observed on growth or productivity. Yet a post-treatment of the centrate was necessary as the nutrient elimination was not sufficient after cultivation. In an experiment with 25 l a decrease of biomass production was observed at a certain time point in comparison with the 100 ml scale. In order to investigate the influence of the bacteria in the centrate, row centrate (after removal of solid matter) was compared to autoclaved centrate [131]. As shown in Table 1.8, there was no difference between these two media concerning nutrient elimination by *Chlorella*.

A further type of wastewater is domestic wastewater, which contains low nitrogen and phosphorus concentrations. This is limiting for cell growth; the higher the initial concentrations of these nutrients are, the higher the maximal cell density that can be achieved. *Scenedesmus* sp. was cultivated in 100 ml media with different nitrogen and phosphorus concentrations, as this alga can also grow well under low nutrient concentrations and is therefore suitable for treatment of secondary wastewater [120]. Phosphorus elimination of almost 100% was achieved at differ-

Table 1.8: Removal of different nutrients from centrate by *Chlorella* sp. grown under 25°C and illumination at light intensity of 50 µmol photons m^{-2} s^{-1} (values taken from [131]).

nutrient	**removal from row centrate**	**removal from autoclaved centrate**
total-phosphate	80.9%	79.0%
NH_4-N	93.9%	93.0%
total-nitrogen	89.1%	89.9%

ent N/P-ratios. Elimination of nitrogen is in contrast dependent on N/P-ratios; decrease in nitrogen elimination was observed at N/P > 8:1 and an initial concentration of total nitrogen > 10 mg l^{-1} or at N/P > 20:1 and an initial concentration of total phosphorus < 0.5 mg l^{-1}. Absolute nitrogen elimination was achieved at N/P-ratios of 2:1-8:1 and at 5:1-8:1 both nitrogen and phosphorus were completely removed [120].

Another example for wastewater treatment is given by cultivation of different microalgae in untreated wastewater from a carpet factory in the USA, with biomass production of 16.1-28.1 t ha^{-1} a^{-1} and a lipid production of 3,260-3,830 l ha^{-1} a^{-1} [26]. Cultivation of *Chlorella vulgaris* in 0.25 dm^3 sterile wastewater free of solid matter from a steel factory in Korea, with 15% (v/v) CO_2 led to a fixation of 26.0 g CO_2 m^{-3} h^{-1} (0.624 g CO_2 l^{-1} d^{-1}) with an uptake of 0.9 g m^{-3} h^{-1} of ammonia [132].

1.7.4 Nutrient balance

The amount and speed of nutrient uptake depends on the microorganisms as well as the cultivation conditions. In Table 1.9 [133] nutrient uptake rates and productivity of different organisms are given. The highest nitrogen uptake rate of 61.8 mg $g_{biomass}^{-1}$ was achieved by *S. platensis* LEB-52 while the highest phosphorus uptake rate of 314.4 mg $g_{biomass}^{-1}$ was found for *C. vulgaris* LEB-104.

To reduce costs for nutrients, there is the possibility of recycling water which is separated from the solid matter during harvesting and fed back to the culture, as it still contains nutrients. The requirement of different nutrients (nitrogen, phos-

Table 1.9: Nutrient uptake and productivity of microalgae and a cyanobacterium (values taken from [133]).

	***Chlorella vulgaris* LEB-104**	***Botryococcus braunii* SAG-13.81**	***Dunaliella tertiolecta* SAG-13.86**	***Spirulina platensis* LEB-52**
nitrogen uptake rate (mg $g_{biomass}^{-1}$)	49.4	40.7	26.1	61.8
magnesium uptake rate (mg $g_{biomass}^{-1}$)	2.9	2.6	58.5	4.2
potassium uptake rate (mg $g_{biomass}^{-1}$)	32.2	15.0	59.7	24.1
phosphorus uptake rate (mg $g_{biomass}^{-1}$)	314.4	175.9	-	247.4
calcium uptake rate (mg $g_{biomass}^{-1}$)	-	-	375.5	-
lipid productivity (mg l^{-1} d^{-1})	11.5	61.4	15.3	14.3
CO_2 fixation per ton biomass (kg)	144.6	178.1	136.2	182.8
max. productivity (g l^{-1} d^{-1})	0.3	0.6	0.4	0.7

phorus, potassium, magnesium and sulfur) for microalgae is described in [134] for cultivation under various conditions. If water is recycled, the need for nutrients can be reduced by up to 55%. By using sea or wastewater instead of fresh water, an addition of only phosphorus and nitrogen is needed and the demand for nitrogen supply can be reduced by up to 94% .

1.7.5 Water footprint

1.7.5.1 Recycling

Water loss during cultivation of microalgae or cyanobacteria is attributable to process operation and evaporation [25]. In open pond systems 140-200 l are needed to bind 1 kg carbon [2]. A typical American consumes 317 GJ per year. In order to produce this much of energy in form of biomass, about 120,000 m^3 of water will be lost at locations such as California, Iowa or Virginia in the USA [135]. To produce 1 kg of biodiesel in a pond system, 3,726 kg of water are needed, of which 84.1% will be lost through harvesting, evaporation and drying process. If sea or wastewater is utilized, then the requirement of fresh water can be reduced by up to 90% [134].

Recycling of water can reduce costs for nutrients, yet it can also lead to concentration of toxic substances such as metals or metabolic products as well as an increase in salinity of the water. Partial recycling of water can reduce the water use from 3,024,067 to 324,149 $m^3\ d^{-1}$ in a 50,000,000 m^3 (5,000 ha) pond. This leads to a water utilization of 278 m^3 per m^3 biodiesel [25]. If water can be used by 100%, 1 m^3 water is needed for production of 0.03 m^3 of biodiesel [25].

Water utilization between pond systems and a tube-shaped airlift PBR was compared by using similar operational processes for biodiesel production [22]. Cultivation of *C. vulgaris* in a pond system in Great Britain had water requirement of 3.8 $m^3\ ton_{biodiesel}^{-1}$ while cultivation in the tube reactor used 13.7 $m^3\ t_{biodiesel}^{-1}$. The lower water usage in the pond system was explained by the partial replacement of water loss with rain water. In comparison, pond cultivation in the Mediterranean area would increase water usage up to 101 $m^3\ t_{biodiesel}^{-1}$. If closed PBRs were used at the same location, they would need to be cooled, e.g. by spraying water onto the reactor surface [5, 22], which would result in water requirement of 362 $m^3\ t_{biodiesel}^{-1}$.

These reports make it clear that the water footprint depends on the reactor as well as climatic conditions of the location.

Further, the need of fresh water is also influenced by cultivation, harvest, drying and extraction as well as transesterification [134]. Especially during harvest, which can cause the largest loss of water, the demand for fresh water can be reduced by recycling water. In sum, whatever the source of water (fresh water, sea and wastewater) is or which cultivation system is used (open or closed) with or without water recycling, addition of fresh water is always essential for cultivation of algae in all climatic conditions.

1.7.5.2 Comparison of water footprint for biodiesel production

Table 1.10 summarizes the water footprint for biodiesel production with different crops in comparison to microalgae [134]. Crops such as corn, potatoes, sugarcane, sugar beet, sorghum and switchgrass are utilized for ethanol production. The water footprint values of these plants show how much water is used to produce ethanol to gain the energy amount equivalent to 1 kg biodiesel. The total water footprint of the microalgae depends on the water recycling rate as well as lipid contents of the cells. For agricultural production, the blue water footprint refers to evaporated surface and ground water for irrigation, green water footprint refers to evaporated rainwater during production and the volume of water becoming pollutant during production is referred to as the grey water footprint [136]. From the data in Table 1.10 it is clear that biodiesel produced from microalgae is competitive to other crops in terms of blue and green water footprint, referring to the evaporated water during process operation, and total water footprint [134]. In addition, the data shows that microalgae are more productive than plants even when the water consumption is taken into account.

Table 1.10: Comparison of the water footprint of biodiesel production from microalgae with other crops (values taken from [134]).

	blue and green water footprint ($\mathbf{kg_{water}/kg_{biodiesel}}$)	**total water footprint ($\mathbf{kg_{water}/kg_{biodiesel}}$)**
corn	1,583-1,972	4,015
potatoes	1,214-1,684	3,748
sugarcane	1,978-2,131	3,931
sugar beet	1,268-1,284	2,168
sorghum	3,153-6,647	15,331
soybean	6,539-7,521	13,676
switchgrass	2,189	N/A
wheat	263-956	N/A
microalgae	399	591-3,650

2 Motivation

The decreasing availability of fossil resources for energy production has led to a renewed focus on bio-based fuels as a sustainable energy source. Besides crops, algae can supply biomass as a non-competing source [7]. Yet, algae production is not yet economically viable, as costs for production are relatively high, especially in regions with limited light availability and lower temperatures. Thus substantial improvements are needed, from reactor design and machines consuming less energy to selection of high biomass and lipid producing algal strains [27]. The first objective of this thesis was to make a literature survey of the current state of the art in algal biomass production and additional benefits.

N. gaditana is a lipid rich microalga suitable for biodiesel production [11]. As biotechnological techniques are becoming available, it is therefore of much interest to understand the regulatory mechanism of growth and metabolism in this alga in order to develop strategies for genetic engineering and improve productivity. The second aim of the study was to examine possible effects of circadian rhythms on growth and photosynthesis to better understand endogenous regulation of these processes in *N. gaditana*.

Light is a major limiting factor during algal cultivation, as cell density and biomass concentration are limited by light penetration into PBRs due to self-shading of the culture. In the last part, two NPQ mutants, *npq3* and *npq21*, which had been previously selected as promising candidates based on their low NPQ capacities and low pigmentation ([137], EMS mutagenesis and isolation originally done by [138]), were evaluated for growth and biomass production under different variable conditions in small controlled PBRs in the laboratory, and for *npq21* also in larger PBRs in greenhouses which are closer to the conditions found in industrial scale production. The aim of this part was to examine if higher production could be achieved by these mutants compared to the wild type, assuming that less energy

dissipation (i.e. less loss of the absorbed light energy) in form of NPQ - as long as such a decrease in the NPQ capacity does not cause photoinhibition and damage under stress conditions - should lead to an increase in solar-to-biomass energy conversion [95].

3 Materials and Methods

3.1 Organisms

N. gaditana Lubián SAG 2.99 was purchased from the Culture Collection of Algae, University of Göttingen (Germany). *N. gaditana* wild type (WT) CCAP849/5 and EMS-performed mutants *npq3* and *npq21* were kindly provided by Roberto Bassi, Dipartimento di Biotecnologie, Università degli Studi di Verona (Italy).

3.2 Chemicals

Utilized chemicals were purchased from the companies VWR International GmbH (Germany), Sigma-Aldrich (Germany), Merck KGaA (Germany), AppliChem GmbH (Germany) and LGC Standards GmbH (Germany).

3.3 Cultivation of stock cultures

In a climate cabinet, *N. gaditana* Lubián SAG 2.99 as well as *N. gaditana* WT (CCAP849/5) and its EMS-performed mutants *npq3* and *npq21* were cultivated in 5-liter flasks in autoclaved f/2-medium [139] with 2% Tropic Marin® sea salt (Tropic Marin, Dr. Biener GmbH, Germany) buffered with 10 mM HEPES (pH 7.2) [40]. The cultures were continuously aerated with ambient air and the temperature in the climate chamber was kept constant at 23°C. LD cycles in the climate cabinet were programmed according to the LD cycle applied at the beginning of the experiment, so that the microalgae were acclimated to this condition for at least one week. The intensity of photosynthetically active radiation (PAR) during the light period was 100 µmol photons m^{-2} s^{-1} (OSRAM L 36W/77 Flura, Germany).

Prior to the experiments the microalgae were centrifuged (Sorvall RC 6 Plus Centrifuge, Thermo Scientific, Germany) at 23°C and 1,580 x g for 30 min and cells were washed with distilled water to remove salt and nutrients.

3.4 Cultivation in photobioreactors in the laboratory

The cells were transferred in fresh medium at an optical density (OD) value of 0.2 measured at 680 nm (OD_{680}) (UVKON®XL, Goebel Instrumentelle Anakytik, Germany). Then the algae were filled into 1-liter PBRs (Photobioreactor FMT-150, Photon Systems Instruments, Czech Republic). The PBRs were equipped with a red (centered at 627 nm) and blue (centered at 455 nm) light LED panel. The culture was continuously stirred with a magnetic stirrer and aerated with 1% CO_2 in air with a flow rate of 400 ml min^{-1}.

3.5 Measurements of OD

The OD was measured in the PBRs at OD_{680} and OD_{735}.

For the samples from greenhouse PBRs, OD was measured with a spectral photometer (UVKON®XL, Goebel Instrumentelle Anakytik, Germany) at 540 nm, 680 nm and 735 nm and ultrapure water (Milli-Q Synthesis, Q-Gard® 2 Merck Millipore, Germany) was used as the blank value. According to [35] OD_{540} is a suitable wavelength for representing cell numbers and biomass, while OD_{680} is the absorbtion maximum of chlorophyll. Light scattering measured at 735 nm was used as a proxy for cell density [140]. If the OD exceeded 1.0, the culture was diluted to an OD value between 0.1-1.0.

3.6 Chlorophyll a fluorescence measurements

Measurements of PS II quantum yield were performed in the PBRs. The quantum yield was estimated by measuring chlorophyll *a* fluorescence within the wavelength range of 665-750 nm and by applying saturation pulses (455 nm and/or 627 nm,

ca. 800 µmol photons m^{-2} s^{-1}). The PS II quantum efficiency was defined as (Fm-Fo)/Fm for dark adapted measurements and (Fm'-Fs)/Fm' for light adapted measurements, where Fm and Fo are the maximal and minimal chlorophyll fluorescence intensity in the dark and Fm' and Fs are the maximal and actual intensity in the light.

NPQ was determined by running a light induction program with a Plant Efficiency Analyzer (Handy PEA, Hansatech Instruments, Germany) equipped with red LEDs optically filtered to a peak wavelength of 650 nm. Three ml algae culture were dark adapted for 15 min and then exposed to the light induction program starting with 30 s light-off, then 5 min at 1000 µmol m^{-2} s^{-1} and 3 min of light-off. Saturation light pulses of 0.8 s (3500 µmol m^{-2} s^{-1}) were applied every 30 s to measure Fm or Fm'. Values of NPQ were defined as (Fm-Fm')/Fm'.

3.7 Biomass dry weight

From each PBR 150 ml algae culture were taken and centrifuged (Allegra 25R, Beckman Coulter GmbH, Germany) in 50 ml tubes at 4°C and 3,007 x g for 30 min. The cells were washed with ultrapure water to remove salt and nutrients, then the biomass was transferred into dried and pre-weighed 1.5 ml tubes and centrifuged (Eppendorf Centrifuge 5417 R, Eppendorf AG, Germany) at 4°C and 20,817 x g for 20 min, after which the supernatant was discarded. The tubes containing biomass were dried in an oven at 105°C for 48 h until constant weight was reached. Subsequently, the tubes containing the biomass were put in an exsiccator and cooled down to room temperature. The dry weight was determined with a fine scale (Explorer®R, OHAUS®, Switzerland) to obtain the biomass.

For a larger volume of sampling, one liter algae culture from each PBR system was centrifuged (Sorvall RC 6 Plus Centrifuge, Thermo Scientific, Germany) at 4°C and 2,820 x g for 30 min in pre-weighed tubes. The cells were washed with ultrapure water to remove salt and nutrients, centrifuged again (4°C, 2,820 x g, 30 min) and the supernatant was discarded. The procedures for drying and weighing of biomass were as described above.

3.8 Cell number

The number of cells was counted with a hemocytometer (Neubarer-improved, Paul Marienfeld GmbH & Co. KG, Germany). Cell counting was performed with images taken under a light microscope (Laborlux S, Leitz, Germany) at the magnification of 40x.

3.9 Total-nitrogen

Three ml algae culture were centrifuged (Eppendorf Centrifuge 5417 R, Eppendorf AG, Germany) at 4°C and 20,817 x g for 20 min and the pellet was washed with ultrapure water. Then the pellet was suspended in 1.5 ml ultrapure water and the nitrogen content was determined with a cuvette test according to the manufacturer's instructions (LATON® total nitrogen, LCK 138, HACH LANGE GmbH, Germany).

3.10 Nitrate

For the experiments in greenhouse PBRs (see 3.14), nitrate concentration in the medium was determined to calculate the amount of nitrate and f/2 nutrient solution, respectively, to be added to the culture. A sample (1.5 ml) was taken from the algal culture, centrifuged (Eppendorf Centrifuge 5417 R, Eppendorf AG, Germany) at 4°C and 20,817 x g for 20 min. The nitrate concentration was measured in the supernatant with a kit (Nitrate-Test in Seawater 0.2-17.0 mg l^{-1} NO_3-N; 0.9-75.3 mg l^{-1} NO_3, Merck KGaA, Germany) following the manual of the kit.

3.11 Pigment analysis

For pigment analysis microalgal biomass was collected by centrifugation (Eppendorf Centrifuge 5417 R, Eppendorf AG, Germany) of 3 ml culture at 4°C and 20,817 x g for 20 min, frozen in liquid nitrogen and grounded in methanol until the pellet was white. The methanol containing extracted pigments was separated

from the cell fragments by centrifugation at 4°C and 20,817 x g for 20 min. The supernatant was taken and the volume was adjusted to 1.5 ml. The extracts were filtered through a syringe filter (Chromafil®, 0.45 µm, Macherey-Nagel, Germany) prior to the HPLC analysis.

Separation of pigments was performed with an Allsphere ODS-1 column (5 µm particle size, 250 mm x 4.6 mm; Alltech Associates Inc., USA). The solvents and protocols were modified from [141], whereby solvent A (acetonitrile:methanol:Tris HCl (0.1 M, pH 8) (80:12:8.5)) and solvent B (hexane:methanol (1:4)) were used for the mobile phase. The HPLC program started with 100% solvent A within the first 24 min followed by a linear gradient to 90% solvent B within 2 min, whereafter 90% solvent B was run from 26 to 30 min followed by a linear gradient to 100% solvent B at 36 min. Subsequently, a linear gradient back to 100% solvent A was conducted in 4 min and the system was equilibrated with 100% solvent A for 3 min before the next sample was injected. The flow rate was constant at 1 ml min^{-1} and the sample injection volume was 20 µl.

The identification of the pigments was carried out by determination of the retention times and the absorption spectra observed with a photodiode array detector (Waters 996 PAD, Waters Corporation, USA). Integration of the peaks was done in the chromatograms detected at 440 nm and data analysis was performed with Waters Empower software. Pure standards of carotenoids and chlorophylls (DHI LAB Products, Denmark) were utilized for calibration of the HPLC system.

Figure 3.1 shows a typical chromatogram of a pigment extract from *N. gaditana* with peaks of vaucheriaxanthin (putative), violaxanthin, antheraxanthin, chlorophyll *a* and β-carotene. Two additional peaks were often detected, but could not be clearly identified (probably vaucheriaxanthin ester) and therefore were not included in the analysis. The HPLC system was not calibrated for vaucheriaxanthin, thus as an approximation of vaucheriaxanthin was calculated by using the same conversion factor as for violaxanthin.

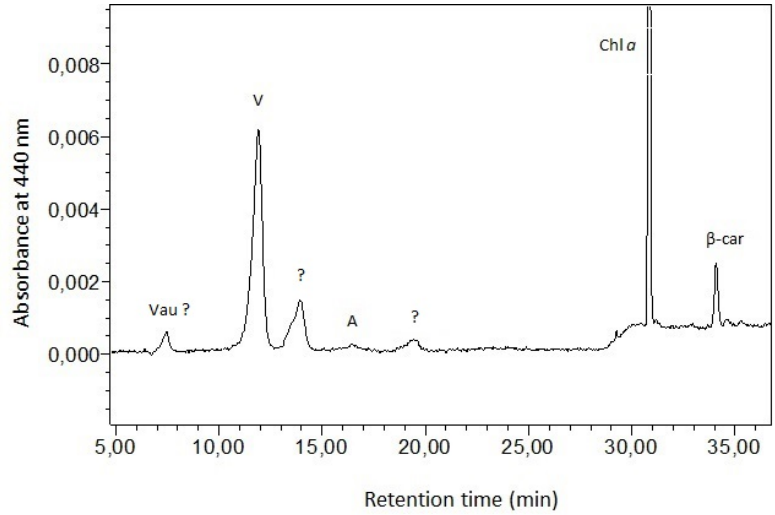

Figure 3.1: Typical chromatogram of algae pigment extract. Vau (vaucheriaxanthin), V (violaxanthin), A (antheraxanthin), Chl *a* (chlorophyll *a*), β-car (β-carotene).

3.12 Chlorophyll a content

Algal biomass in 3 ml culture was collected by centrifugation (Eppendorf Centrifuge 5417 R, Eppendorf AG, Germany) for 20 min at 20,817 x g, 4°C. The pellet was frozen in liquid nitrogen and ground in methanol. Then the sample was heated for 5 min at 50°C under gentle agitation (1,200 rpm), and centrifuged at 4°C and 20,817 x g for 20 min. The absorbance (A) was measured in the supernatant at 750 nm, 665.2 nm and 652 nm and the chlorophyll *a* content was calculated with equation 3.1 and 3.2 [142].

$$\text{Chl}\,a\,(\text{g}\,\text{ml}^{-1}) = 16,29 * A_{(665.2-750)} - 8.54 * A_{(652-750)} * \text{ml}^{-1}_{\text{MeOH}} \tag{3.1}$$

$$\text{Chl}\,a\,(\text{nmol}\,\text{ml}^{-1}) = 18,22 * A_{(665.2-750)} - 9.55 * A_{(652-750)} * \text{ml}^{-1}_{\text{MeOH}} \tag{3.2}$$

3.13 Treatments in photobioreactors in the laboratory

3.13.1 Experiments with N. gaditana SAG 2.99

Experiments to study the effects of circadian clock and red/blue light treatments were performed with *N. gaditana* Lubián SAG 2.99. In the climate cabinet *N. gaditana* was cultivated under 12 h/12 h or 18 h/6 h LD cycles. The maximal light intensity in the PBRs was 100 µmol photons m^{-2} s^{-1} given by either equal amounts of red and blue LED or by red or blue LED alone. For aeration 1% CO_2 in synthetic air (80% nitrogen, 20% oxygen) was applied and the temperature was kept constant at 23°C.

The experiments started after one day of cultivation in the PBRs under conditions described above. Then, the LD regime was either kept unchanged at 12 h/12 h or 18 h/6 h (control) or switched to continuous light (LL) at different time points during the dark period. Figure 3.2 illustrates the light treatments in the experiments starting with 12 h/12 h LD. Because light is a major "Zeitgeber" that synchronizes the endogenous clock with external LD cycles [58], Zeitgeber time (ZT), which starts with light-on (ZT0), was used in all experiments. The different treatments are abbreviated according to the time of the LD-LL stitching: after 12 h (ZT0), 3 h (ZT15), 6 h (ZT18) or 9 h (ZT21) of darkness.

3.13.2 Experiments with N. gaditana CCAP849/5

N. gaditana WT (CCAP849/5) and EMS-performed mutants *npq3* and *npq21* were cultivated under 12 h/12 h LD cycles or continuous light in the climate cabinet at 23°C, depending on the conditions of the following experiment. In the first experiment with LD cycles (Fig. 3.3A), the maximal light intensity in the PBRs was 200 µmol photons m^{-2} s^{-1} given by equal amounts of red and blue LED (≈8 mol m^{-2} d^{-1}). For the treatment with fluctuating light (Fig. 3.3B), PAR was varied between 10 µmol photons m^{-2} s^{-1} and 770 µmol photons m^{-2} s^{-1} in form of sinus curves with a time span of 4 min during the light period of LD cycles (≈17 mol m^{-2} d^{-1}). In the second experiment with LL (Fig. 3.4), constant illumination in the PBRs (200 µmol photons m^{-2} s^{-1}) was given by equal amounts of red and blue

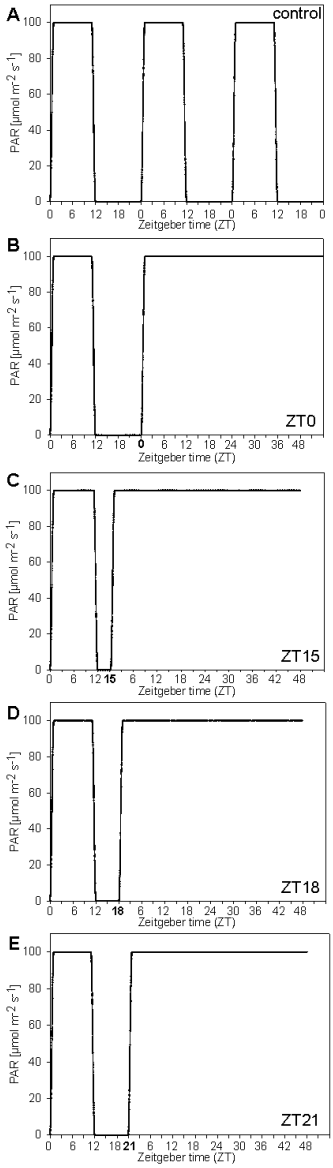

Figure 3.2: Light treatment applied to *N. gaditana* cultures. All cultures were entrained to the control condition (control) with 24 h photoperiod of 12 h/12 h light/dark (LD) cycles and a constant temperature of 23°C. Light intensity was gradually increased (or decreased) over an hour at the beginning (or at the end) of the light period. Time on the x-axis is shown as Zeitgeber time (ZT) which always starts at the point of light-on (ZT0). For experiments with constant light (LL), light regimes were switched from the LD to LL conditions at different phases of the dark period: after 12 h (ZT0), 3 h (ZT15), 6 h (ZT18) or 9 h (ZT21) of darkness.

LED, as in the experiment with LD cycles. However, the light regime of fluctuating light was different in this experiment: the PAR was switched between 10 µmol photons m^{-2} s^{-1} (3 min) and 770 µmol photons m^{-2} s^{-1} (1 min) to give the same amount of daily total PAR (≈17 mol m^{-2} d^{-1}) in both LL conditions. These experiments were run under a constant temperature of 23°C. The third experiment with varying day/night temperatures was conducted under 12 h/12 h LD cycles and daytime PAR of 200 µmol photons m^{-2} s^{-1} (as in Fig. 3.3A). The temperature regimes used were 23°C/15°C (light/dark) and 30°C/23°C. In all experiments, algae cultures were continuously aerated with 1% CO_2 in nearly CO_2 free ambient air (ambient CO_2 absorbtion with Soda Lime, Medisize Deutschland GmbH, Germany), which was filtered with activated charcoal filter and molecular filter (Chromatographie Service GmbH, Germany).

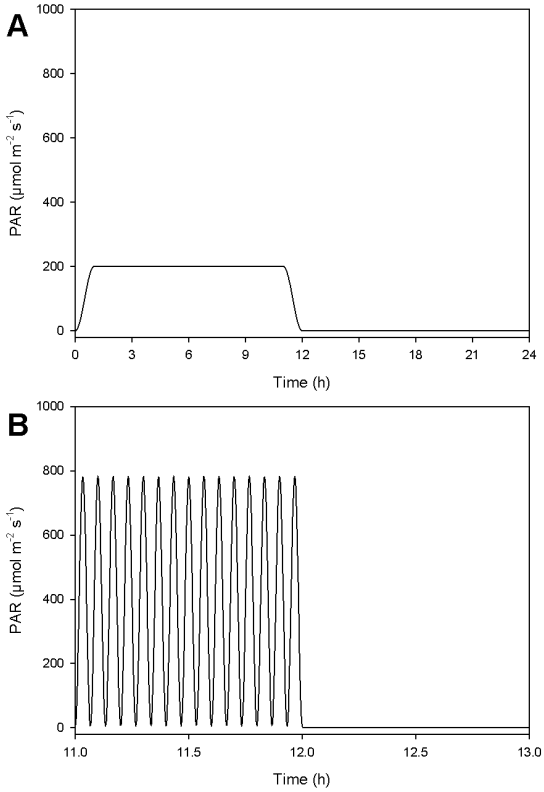

Figure 3.3: Light treatments applied to *N. gaditana* cultures. 12 h/12 h LD constant light with gradual increase (or decrease) over an hour at the beginning (or at the end) of the light period (A). 12 h/12 h LD fluctuating light (B). For (B) only the last and the first hour of LD period are shown.

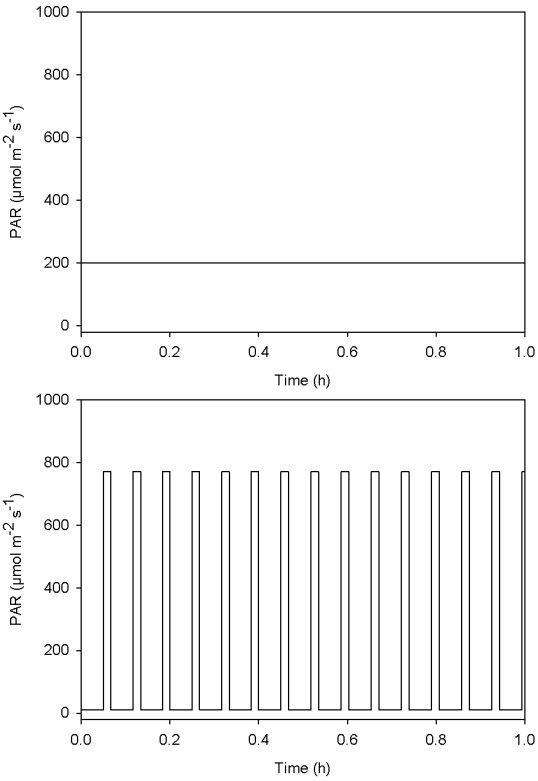

Figure 3.4: Light treatments applied to *N. gaditana* cultures. LL constant light (A). LL fluctuating light (B). For clarity, only a time course of an hour is shown for both treatments.

3.14 Cultivation in closed photobioreactors under greenhouse conditions

Four identical pilot-scale algae cultivation systems were set up in two small greenhouses (3 m x 4 m), two per greenhouse (Figs. 3.5 and 3.6). Each system consisted of two rows of four V-shaped PBRs (≈30 l per V-reactor, NOVA*green* - Projektmanagement GmbH, Germany) and a transparent mixing cylinder (≈25 l), connected with tubing. Every hour the whole content of the mixing cylinder was pumped with a peristaltic pump (Verderflex Smart L40, Pumphead S40, VERDER Deutschland GmbH, Germany) with a volume flow rate of 3.8 l min^{-1} into the

V-reactors through small tubes leading into the top of the reactors, during which a valve prevented algae culture from flowing into the mixing cylinder. After the cylinder was emptied, the valve was opened again and the microalgae from all V-reactors flowed through a tube at the bottom of the reactors into the mixing cylinder until the whole system was leveled off. During this process the pH-value of the culture was measured. A valve for CO_2 supply was automatically opened, if the pH was above 7.5. CO_2 was supplied with a volume flow rate of 4 l min^{-1}, mixed with air stream to have a CO_2 concentration of about 3%. Each V-reactor as well as the mixing cylinder was continuously aerated at 120 l min^{-1} by a compressor (LA-120A, Nitto Kohki Deutschland GmbH, Germany) which served two systems in the same greenhouse at the same time. Further, an air compressor (2 Zylinder Kompressor BT-AC 400/50, Einhell Germany AG, Germany) was turned on twice a day for 40 s in order to stir up algae settling at the bottom of V-reactors. Besides the pH, also temperature (PT 100, Hamilton Messtechnik GmbH, Germany) and conductivity (Conducell 4USF-PG-120, Hamilton Messtechnik GmbH, Germany) were measured and recorded every minute. The regulation of the devices was controlled by a programm created with Labview (National Instruments). The temperature in the greenhouse was controlled by a ventilation system which was turned on at 23°C and above to cool down or by an air heater (Helios STH 9T, Germany) which was turned on at 15°C and below to warm up. In order to protect the microalgae from extreme heat a spray cooling system was activated above 32°C.

PAR was continuously measured every minute with an optometer ($X1_2$ Optometer, Gigahertz-Optik GmbH, Germany). Data for sunshine duration, solar radiation and sunrise and sunset were kindly provided by Axel Knaps from S-UM, Forschungszentrum Jülich GmbH, Germany. Sunshine duration was calculated as the sum of all periods, in which the solar radiation exceeded a value of 120 W m^{-2}. Solar radiation was measured for wavelengths between 0.3 and about 30 µm [143].

For innoculation of each cultivation system, 500 ml of culture were taken from the stock cultivated in 5-l flasks in a climate cabinet with continuous aeration at constant temperature of 23°C and 12 h/12 h LD cycle. The light intensity during the light period was about 100 µmol photons m^{-2} s^{-1}. The optical density of the culture was adjusted to OD_{540}=0.5 before innoculation.

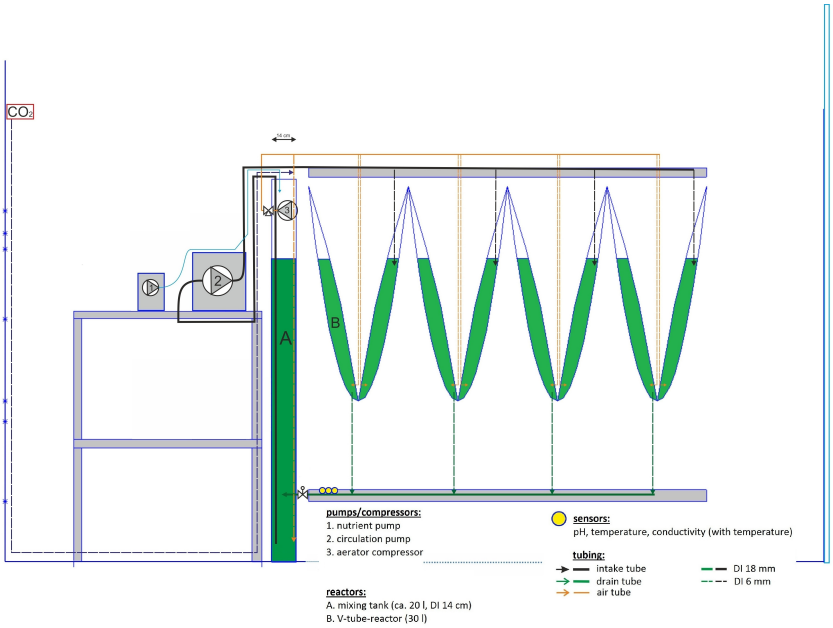

Figure 3.5: View from the side of the setup of photobioreactor system in the greenhouse *(created by Regina Braun with the assistance of Arthur Podosva)*.

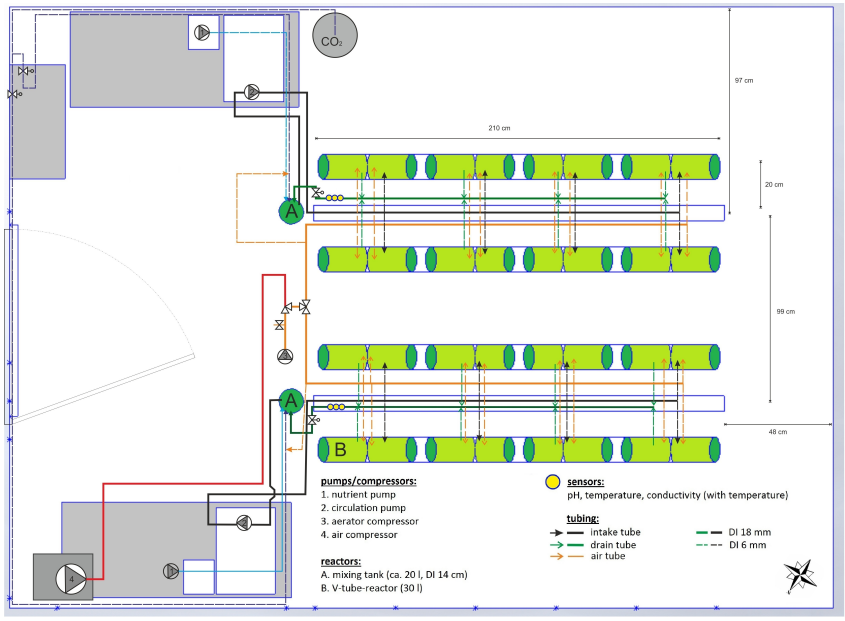

Figure 3.6: View from the top of the setup of photobioreactor system in the greenhouse *(created by Regina Braun with the assistance of Arthur Podosva)*.

3.15 Statistical analysis

The experiments in the laboratory were done in three or six replicates. Means and standard deviation (SD) were calculated for each treatment. Data between the treatments for each genotype or between WT and *npq3* or *npq21* were analyzed by using t-test where P values less than 0.05 were considered to be significant. The WT experiment in the greenhouse was done in four replicates with calculated means and SD, whereas the WT and *npq21* experiment was done in two replicates with calculated means.

4 Results

4.1 Experiments under controlled conditions

4.1.1 Effects of circadian clock

4.1.1.1 Comparison of different LD regimes

N. gaditana was grown under the 12 h/12 h or 18 h/6 h LD cycle to compare the two conditions (Fig. 4.1). In both LD regimes the values of OD_{680}, reflecting chlorophyll concentration and cell density of the culture (Fig. 4.2), increased steadily during the light periods and decreased slightly during the dark periods (Fig. 4.1A). Consequently, the values reached a higher level in the 18 h/6 h LD cycle in which the light periods were longer. At a closer look, the slope of OD_{680} increase was found to be significantly steeper in the first half of the light periods than in the second half under both LD cycles (Table 4.1). The rate of the OD_{680} increase was 32% (1^{st} cycle) and 28% (2^{nd} cycle) higher in the first 6 h than in the second 6 h of the light periods under the 12 h/12 h LD cycle, while the difference was further enhanced under the 18 h/6 h LD cycle to result in 47% (1^{st} cycle) and 46% (2^{nd} cycle) higher rates in the first 9 h than in the second 9 h of the light periods.

A similar picture was found when OD_{735}, a proxy of cell density (Fig. 4.3), was plotted instead of OD_{680} (Fig. 4.1B). Unlike OD_{680}, however, the slope of the daytime increase in OD_{735} did not differ significantly between the first and the second half of the light periods in both 12 h/12 h and 18 h/6 h LD cycles (Table 4.1).

The quantum yield of PS II was measured in the photobioreactors in parallel with the OD. The values were generally higher (0.65-0.70) during the dark periods (Fig. 4.4) in which primary quinone acceptors (Q_A) of the PS II complexes were more oxidized.

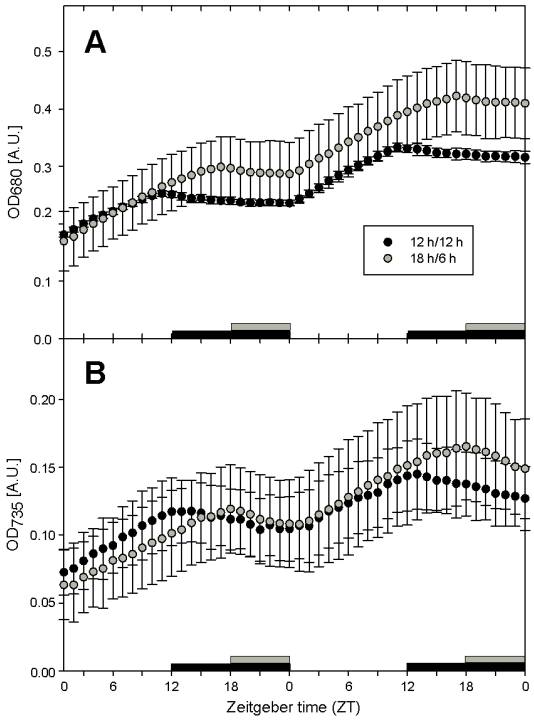

Figure 4.1: Changes in optical density monitored at 680 nm (OD_{680}, in arbitrary units, A.U.) (A) or at 735 nm (OD_{735}) (B) under the control conditions with 12 h/12 h (black circles) and 18 h/6 h (grey circles) LD cycles. Black and grey boxes above the x-axis show dark periods in 12 h/12 h and 18 h/6 h LD cycles, respectively. Data are means of three replicates and error bars indicate SD.

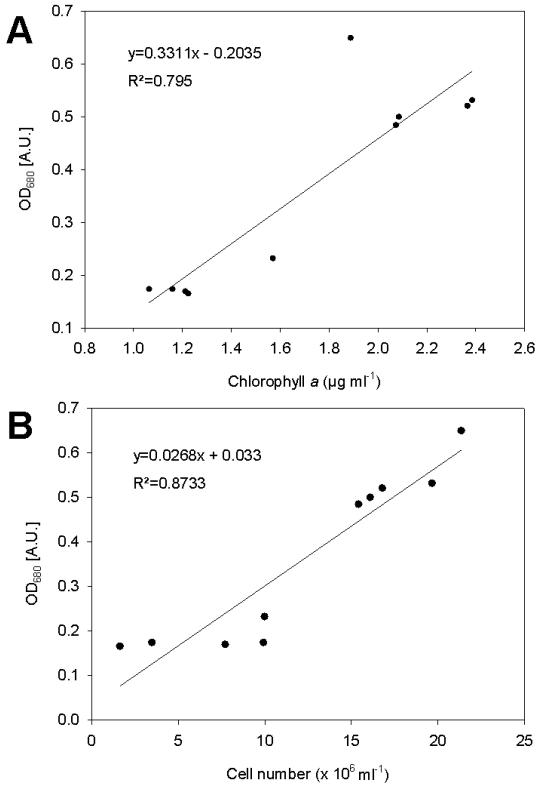

Figure 4.2: Correlation between OD_{680} and chlorophyll *a* concentration (A) or cell number of *N. gaditana* culture (B).

Table 4.1: Slopes (x100) of OD_{680} and OD_{735} increase during the first and second half of the light periods in the 12 h/12 h and 18 h/6 h LD cycles.

	12 h/12 h		18 h/6 h	
	OD_{680}	OD_{735}	OD_{680}	OD_{735}
light period 1				
1^{st} half	0.83 (±0.03)	0.42 (±0.07)	0.97 (±0.05)	0.36 (±0.05)
	***		***	
2^{nd} half	0.63 (±0.02)	0.43 (±0.10)	0.66 (±0.04)	0.33 (±0.04)
light period 2				
1^{st} half	1.01 (±0.04)	0.37 (±0.03)	0.95 (±0.03)	0.42 (±0.08)
	**		***	
2^{nd} half	0.79 (±0.04)	0.34 (±0.04)	0.65 (±0.02)	0.29 (±0.02)

Significant differences between the first and second half of the light periods are indicated by ** ($P \leq 0.01$) or *** ($P \leq 0.001$) for OD_{680}. The differences were not significant for OD_{735}. (n=3, ±SD)

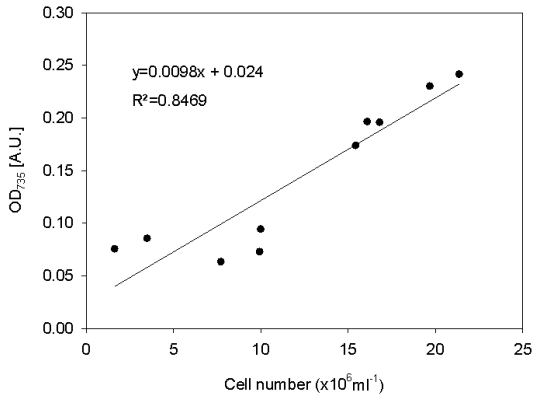

Figure 4.3: Correlation between OD_{735} and cell number of *N. gaditana* culture.

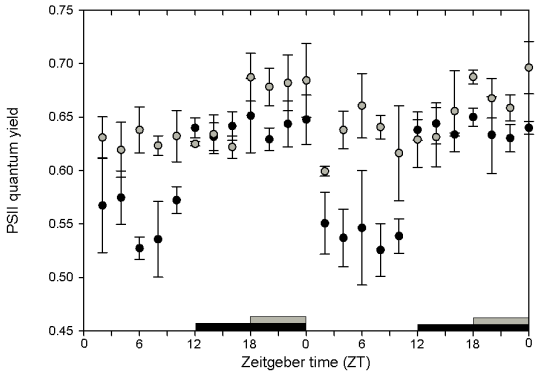

Figure 4.4: Changes in photosystem II (PS II) quantum yield under the control conditions with 12 h/12 h (black circles) and 18 h/6 h (grey circles) LD cycles. Data are from the same experiments as shown in Fig. 4.1. Black and grey boxes above the x-axis show dark periods in 12 h/12 h and 18 h/6 h LD cycle, respectively. Data are means of three replicates and error bars indicate SD.

During cultivation growth conditions were recorded via sensors. As an example, Figure 4.5 shows the pH-value during the experimental run with 12 h/12 h LD cycle; the pH-values stayed relatively constant at pH 7. The O_2 concentration, on the other hand, showed clear shifts between light and dark periods, reaching about 21% O_2 during the light and 20 to 20.4% O_2 during the dark periods (Fig. 4.6), reflecting oxygen evolution (photosynthesis) and oxygen consumption (respiration) by the algae during these periods.

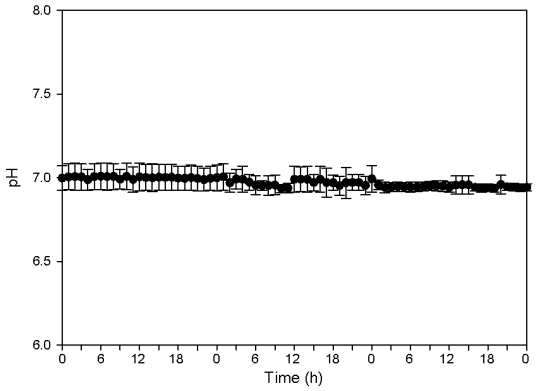

Figure 4.5: Changes in pH-value in culture during the 12 h/12 h LD cycle. Data are means of three replicates and error bars indicate SD.

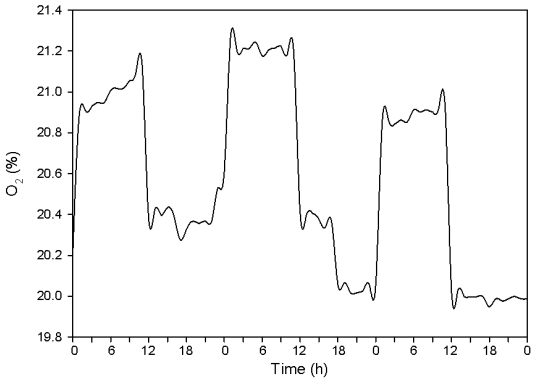

Figure 4.6: Changes in O_2 concentration in culture during the 12 h/12 h LD cycle. Data are means of three replicates.

4.1.1.2 Switch from 12 h/12 h and 18 h/6 h LD to LL

Figure 4.7 shows OD_{680} data in the 12 h/12 h LD control (A) and in the treatments in which the light regime was switched to LL at different time points during the dark period (B-E). A steady rise in OD_{680} was recorded in all LL conditions, which is in agreement with the observation of OD_{680} increase during the light periods under the LD conditions (Figs. 4.1 and 4.7A). Notably, the steepness of the slope declined after 12 h of LL illumination (i.e., at the beginning of the light period

III), irrespective of the timing of the LD-LL switch (Fig. 4.7B-E). Thereafter, the slope continued to increase in all LL treatments during the periods IV and V.

These changes in OD_{680} were quantified in Fig. 4.8 which shows relative increase in OD_{680} (% h^{-1}) calculated for each 12 h light period (I-V). A significantly lower value (≈90%) compared to the control was found during the period II when the LL treatment was started at ZT15 (i.e., after 3 h in the darkness), while no such decrease was observed for the other treatments in which the onset of LL was later in the dark period (i.e., after 6, 9 and 12 h in the darkness). Then in the period III, the increase in OD_{680} decelerated strongly and uniformly in all LL treatments; the values were around 50% of the control (Fig. 4.8B). This was followed by recovery in the periods IV and V, with the fastest recovery observed in ZT15 and the slowest in ZT0; in other words, the shorter the last dark period before switching to LL, the faster the recovery.

The quantum yield of PS II was always lower in the light than in the dark, regardless of the treatments (Fig. 4.9). Although the values during the last light period of the LD cycle (period I) varied between the different treatments, these values were maintained after switching to LL in all cases. Thus, no reduction or recovery of PS II quantum yield was found after the LD-LL switch in any of the LL treatments, which contrasts with the response of OD_{680} (Figs. 4.7 and 4.8).

Data of OD_{680} in the 18 h/6 h LD control (A) and in the treatment in which the light regime was switched to LL at ZT0 (B) is shown in Fig. 4.10. As for 12 h/12 h LD cycle steady rise in OD_{680} was recorded in the LL condition, as observed during the light periods under the LD conditions (Figs. 4.1 and 4.10A). Notably, the steepness of the slope already declined after 12 h of LL illumination in light period II. Thereafter, an increase of the slope in the LL treatment during the periods III and IV was found.

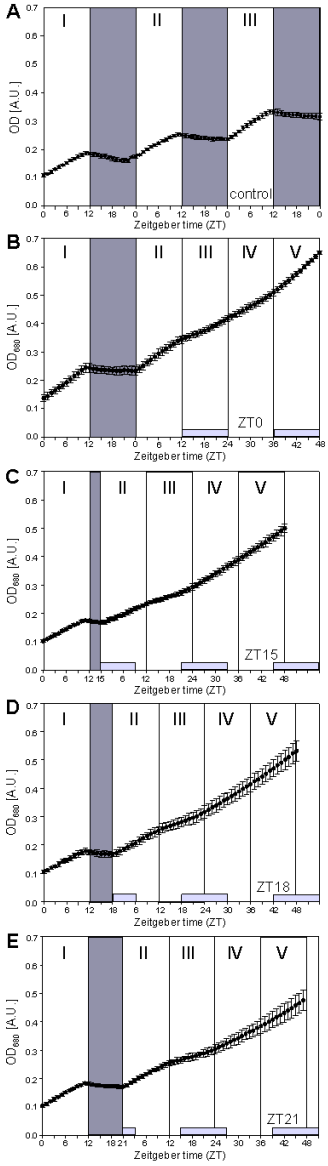

Figure 4.7: Changes in OD_{680} under the control condition (A) or after switching to LL at ZT0 (B), ZT15 (C), ZT18 (D) or ZT21 (E). Dark grey areas in the background show dark periods. Light boxes above the x-axis show dark periods in the original LD cycles to which the cultures were entrained prior to switching the light regime. Each 12 h light period of the LD or LL cycles is denoted by a roman number (I-V): the last period before switching the light regime (I) and the first (II), second (III), third (IV) and fourth (V) 12 h period in LL. For the control that remained in the LD condition throughout the experiment (A), the light periods were consecutively numbered from I to V (only I-III are shown). Data are means of three replicates and error bars indicate SD.

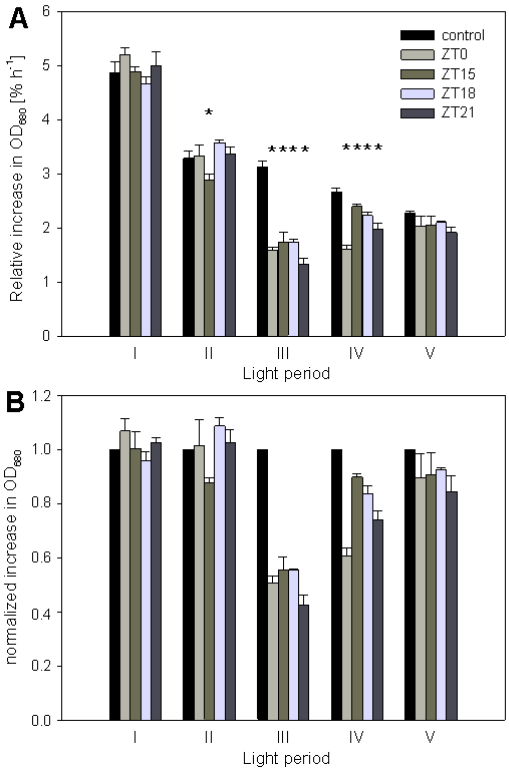

Figure 4.8: Relative increase in OD_{680} (% h^{-1}) during the 12 h light periods I-V shown in Fig. 4.7 (A). Within each light period, asterisks (*) above the bars show significant differences compared to the control ($P \leq 0.001$). In (B), all values are normalized to the corresponding data of the control in the same light period (control=1). Data are means of three replicates and error bars indicate SD.

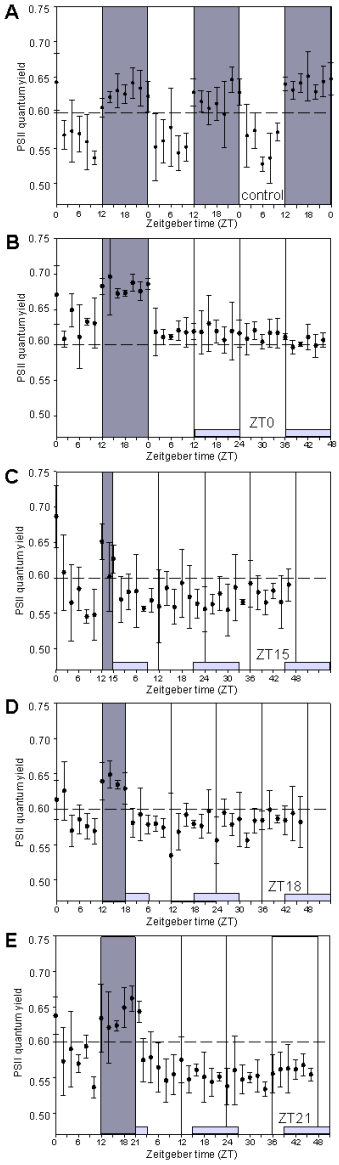

Figure 4.9: Changes in PS II quantum yield under the control conditions (A) or after switching to LL at ZT0 (B), ZT15 (C), ZT18 (D) or ZT21 (E). Data are from the same experiments as shown in Figs. 4.7 and 4.8. Dark grey areas in the background show dark periods. Light grey boxes above the x-axis show dark periods in the original LD cycles to which the cultures were entrained prior to switching the light regime. Data are means of three replicates and error bars indicate SD. Dashed lines show a reference value of 0.6.

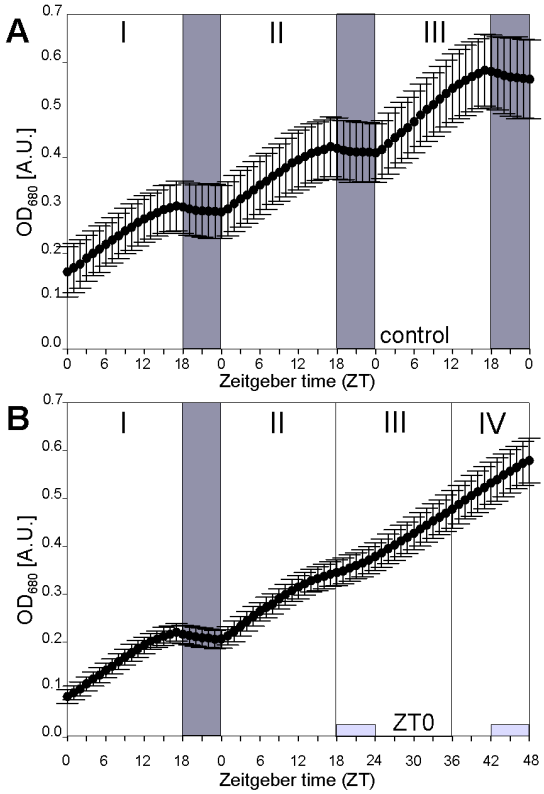

Figure 4.10: Changes in OD_{680} under the control condition with 18 h/6 h LD cycle (A) or after switching to LL at ZT0 (B). Dark grey areas in the background show dark periods. Light boxes above the x-axis show dark periods in the original LD cycles to which the cultures were entrained prior to switching the light regime. Each 18 h light period of the LD or LL cycles is denoted by a roman number (I-IV): the last period before switching the light regime (I) and the first (II) and second (III) 18 h period and third (IV) in LL. For the control that remained in the LD condition throughout the experiment (A), the light periods were consecutively numbered from I to IV (only I-III are shown). Data are means of three replicates and error bars indicate SD.

4.1.1.3 Effects of red and blue light

The oscillations of OD_{680} continuing in LL at least in the first 24 h suggested a role of the endogenous clock in controlling chlorophyll accumulation and growth in *N. gaditana*. The uniformly lower increase observed in all LL treatments during ZT12-24 (light period III), rather than during the dark periods according to the initial 12 h/12 h LD cycle prior to the switch to LL (indicated by light grey boxes in Fig. 4.7), suggests resetting of the circadian clock by light-on, making ZT12-24 "subjective" night. In order to find out whether red and blue light can both reset the clock equally well, some of the LL treatments were repeated by using only red or blue light for the LL illumination without changing the light intensity. The light regime was switched from 12 h/12 h LD (red + blue light) to LL (red or blue light) at ZT0 or ZT15 (Fig. 4.11).

Constant blue illumination induced strong oscillation of OD_{680}, which continued in the light periods IV and V with a cycle duration of >24 h (Figs. 4.11A and B). A reduction in the slope from the period II to III, as was seen in Figs. 4.7 and 4.8, could be clearly recognized after switching to blue LL at ZT0 as well as at ZT15. Constant red illumination also resulted in a lower increase in OD_{680} during the period III compared to the period II, but the changes were less obvious than in blue LL and the slope stayed nearly constant after the period III, with little or no sign of recovery during IV and V. The distinct patterns of OD_{680} changes under blue LL and red LL are also obvious in Fig. 4.12. The rate of hourly increase in OD_{680} indicates continuing oscillation in blue LL and no recovery after the period III in red LL (Figs. 4.12A and B). Changes in the slope were less evident for OD_{735} under blue or red LL (Figs. 4.11C and D). Lack of clear oscillation was also confirmed by the rate of hourly increase in OD_{735} (Figs. 4.12C and D).

The PS II quantum yield followed the patterns described for Figs. 4.4 and 4.9, i.e., higher during dark and lower during light periods (Fig. 4.13). Yet, after switching to LL at ZT0 and ZT15 the values remained higher in red LL than in blue LL in which the quantum yield gradually decreased to ≈0.55 by the end of the experiment.

At the end of the blue or red LL treatments the concentrations of pigments (vaucheriaxanthin, violaxanthin, chlorophyll *a* and β-carotene) were measured. Unknown peaks which appeared in the chromatograms, presumably vaucheriaxanthin

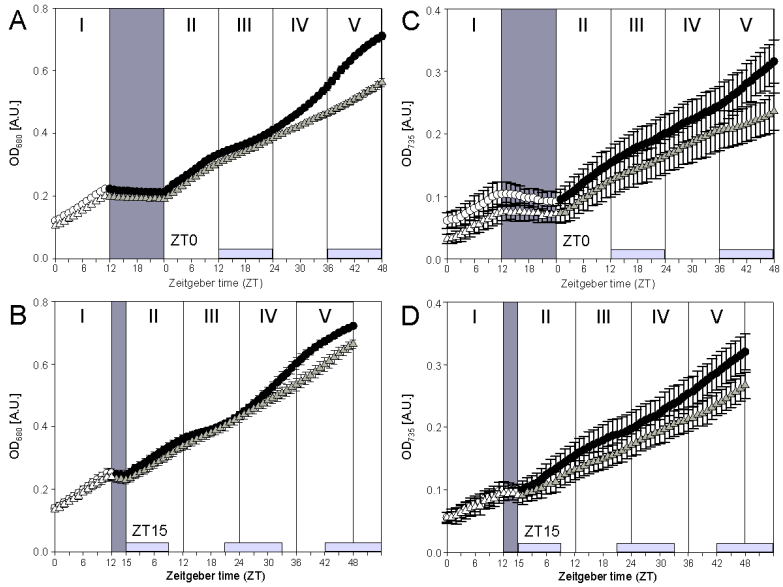

Figure 4.11: Changes in OD_{680} (A and B) and OD_{735} (C and D) after switching to LL with blue (black circles) or red (grey triangles) LED at ZT0 (A and C) or ZT15 (B and D). The cultures were entrained to the 12 h/12 h LD-cycles with both blue and red LED (white circles or triangles). The light intensity was about 100 µmol photons m^{-2} s^{-1} in both LD (blue + red) and LL (blue or red) conditions. Dark grey areas in the background show dark periods. Light grey boxes above the x-axis show dark periods of the original LD cycles to which the cultures were entrained prior to switching the light regime. Data are means of three replicates and error bars indicate SD.

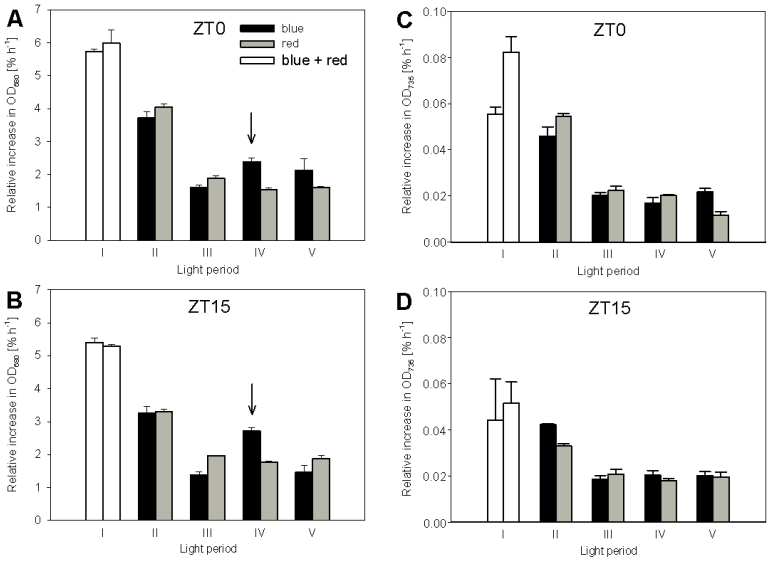

Figure 4.12: Relative increase (% h^{-1}) in OD_{680} (A and B) and OD_{735} (C and D) during the 12 h light periods I-V shown in Fig. 4.11. The light regime was switched from LD with blue + red LED to LL with only blue or only red LED at ZT0 (A and C) or ZT15 (B and D). The arrows above the black bars in A and B (OD_{680} in LL with blue LED) show significant increase of the values from the light period III to IV ($P \leq 0.001$). Data are means of three replicates and error bars indicate SD.

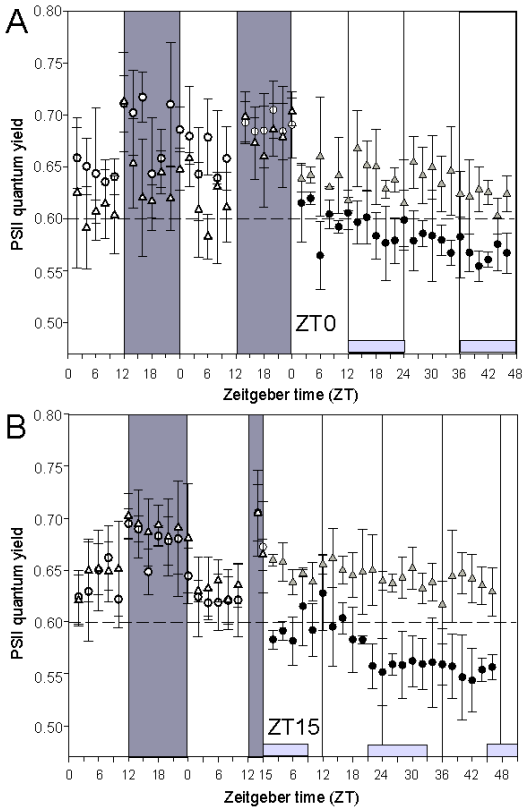

Figure 4.13: Changes in PS II quantum yield after switching to LL with blue (black circles) or red (grey triangles) LED at ZT0 (A) or ZT15 (B). Data are from the same experiments as shown in Figs. 4.11 and 4.12. The cultures were entrained to the 12 h/12 h LD-cycles with both blue and red LED (white circles or triangles). The light intensity was about 100 µmol photons m^{-2} s^{-1} in both LD (blue + red) and LL (blue or red) conditions. Dark grey areas in the background show dark periods. Light grey boxes above the x-axis show dark periods in the original LD-cycles to which the cultures were entrained prior to switching the light regime. Data are means of three replicates and error bars indicate SD. Dashed lines show a reference value of 0.6.

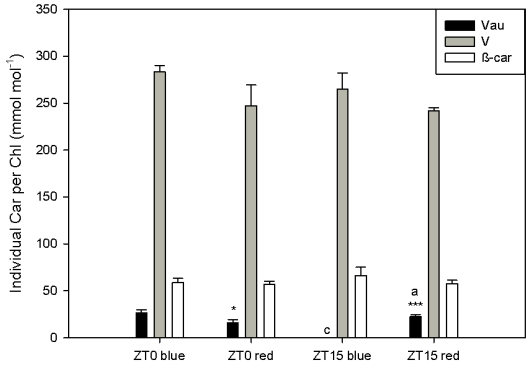

Figure 4.14: Ratio of vaucheriaxanthin (Vau), violaxanthin (V) or β-carotene (β-car) to chlorophyll (Chl) in culture at end of blue or red LL. Data are means of three replicates and error bars indicate SD. Asterisks indicate significant differences between the blue and red LL with the same ZT $P \leq 0.05$ (*) and $P \leq 0.001$ (***). Letters indicate significant differences between different ZT at which light was switched to blue or red LL $P \leq 0.05$ (a) and $P \leq 0.001$ (c).

esters, were not included in the analysis since they could not be identified. Figure 4.14 shows the levels of individual carotenoids on a chlorophyll basis. Violaxanthin was the major carotenoid pigment in *N. gaditana*, being ca. 78% of the total carotenoids. No significant differences were found for violaxanthin or β-carotene per chlorophyll *a* after switching to blue or red LL while vaucheriaxanthin per chlorophyll *a* differed significantly between the treatments.

The carotenoid to chlorophyll *a* ratios (Fig. 4.15) showed similar values after switching to red LL at ZT0 and ZT15 and to blue LL at ZT15. In contrast, a significantly higher ratio was found after switching to blue LL at ZT0 compared to all other treatments.

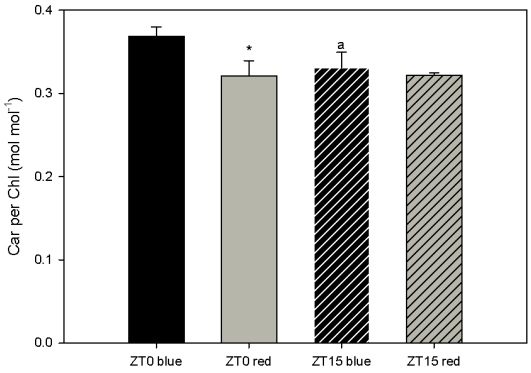

Figure 4.15: Ratio of carotenoids (Car) to chlorophyll (Chl) in culture at end of blue or red LL. Data are means of three replicates and error bars indicate SD. Asterisk indicates significant difference between the blue and red LL with the same ZT $P \leq 0.05$ (*). Letter indicates significant difference between different ZT at which light was switched to blue or red LL $P \leq 0.05$ (a).

4.1.2 Evaluation of NPQ mutants under fluctuating conditions

4.1.2.1 LD cycles with constant and fluctuating light

After receiving *N. gaditana* WT, *npq3* and *npq21* mutants, NPQ was measured during light induction and dark relaxation to check the low NPQ phenotypes originally identified for *npq3* and *npq21* during the mutant isolation and selection (Fig. 4.16) [137]. The NPQ phenotypes of the mutants were confirmed.

N. gaditana WT, *npq3* and *npq21* were grown under 12 h/12 h LD cycles, either with a constant light intensity (200 µmol photons m^{-2} s^{-1}) or with fluctuating light (from 10 to 770 and back to 10 µmol photons m^{-2} s^{-1} within 4 min) during the 12 h light period. The OD measured at 680 nm and 735 nm increased in all three genotypes during light periods for both treatments, yet higher mean values were measured under LD cycles with constant light for OD_{680}, whereas values of OD_{735} were similar after 84 h (Fig. 4.17). When comparing WT and mutants under LD cycle with constant light, mean OD_{680} values of *npq21* were slightly higher than WT, closely followed by *npq3* (Fig. 4.18A). OD_{735} showed similar behavior, except after 72 h WT showed slightly higher mean values than *npq3* (Fig. 4.18C). Under LD cycles with fluctuating light, WT and *npq21* had nearly the same OD_{680} values

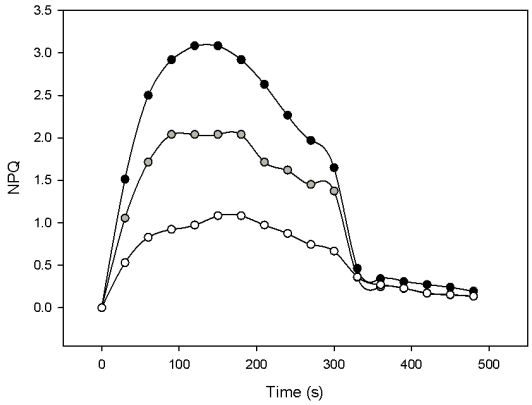

Figure 4.16: Non-photochemical quenching (NPQ) measured during light induction and dark relaxation after receiving the cultures of WT (black circles), *npq3* (grey circles) and *npq21* (white circles).

while the values for *npq3* were lower (Fig. 4.18B). OD_{735} showed similar behavior as under LD cycles with constant light (Fig. 4.18D).

In the constant light, the relative increase in OD_{680} (% d^{-1}) calculated for each 24 h period was lower in the first and the last 24 h. The mutant *npq21* had the highest and the lowest value of the three genotypes in the first and the last LD cycle, respectively (Fig. 4.19). In the second and the third 24 h the values of all treatments were more similar while minor differences were found between the genotypes. The relative increase in OD_{680} was significantly reduced in the first LD cycle with fluctuating light. However, the values recovered in the second LD cycle to exceed those in the constant light in the third cycle (WT and *npq21*) or the fourth cycle (*npq3*).

PS II quantum yield was measured 2 h before light-on and 2 h after light-off (Figs. 4.20 and 4.21). No striking difference was detected between the treatments for WT and mutuants. In all cases PS II quantum yields were slightly lower at the beginning of the experiments but reached steady state at ≈0.6 during the experiment. The three genotypes were also comparable under both conditions (Fig. 4.21).

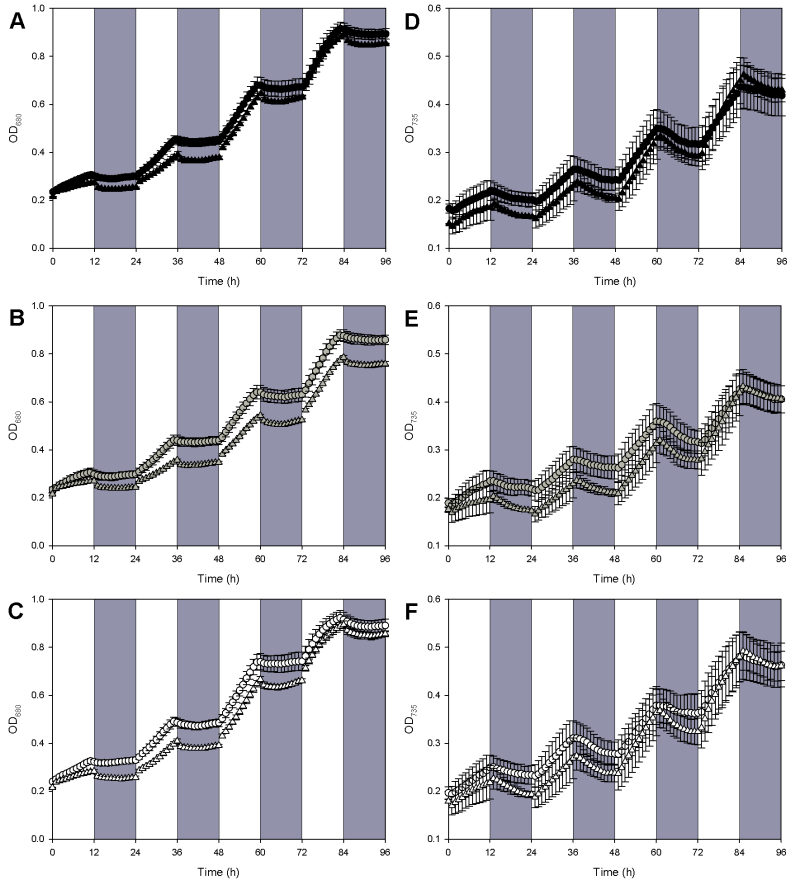

Figure 4.17: Changes in OD_{680} and OD_{735} under 12 h/12 h LD cycles of WT with constant light (black circles) and fluctuating light (black triangles) (A and D), *npq3* with constant light (grey circles) and fluctuating light (grey triangles) (B and E) and *npq21* with constant light (white circles) and fluctuating light (white triangles) (C and F). Dark grey areas in the background show dark periods. Data are means of three replicates and error bars indicate SD.

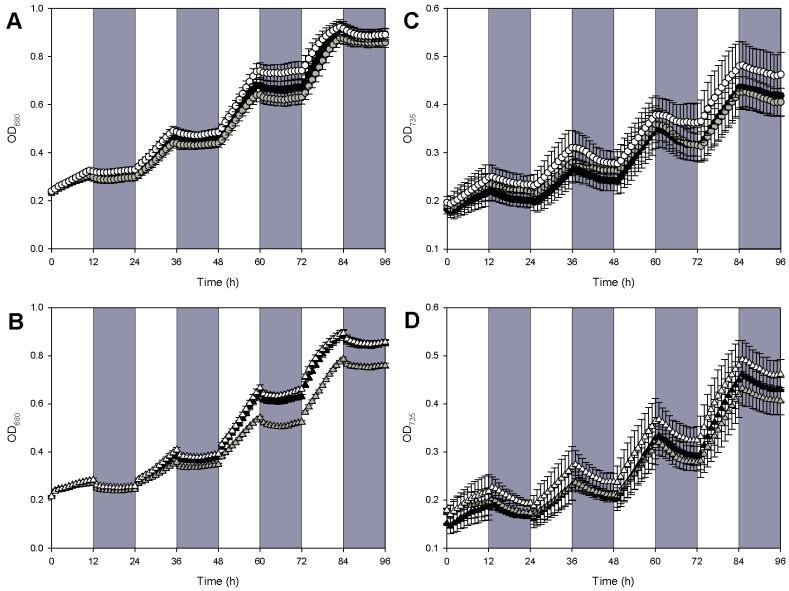

Figure 4.18: Changes in OD_{680} and OD_{735} under 12 h/12 h LD cycles with constant light (A and C) or with fluctuating light (B and D) for WT (black symbols), *npq3* (grey symbols) and *npq21* (white symbols). Dark grey areas in the background show dark periods. Data are means of three replicates and error bars indicate SD.

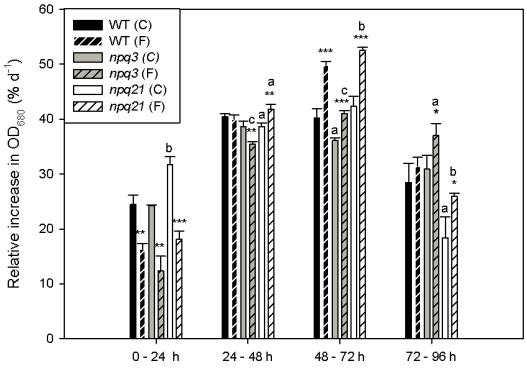

Figure 4.19: Relative increase in OD_{680} for 12 h/12 h LD cycle for WT, *npq3* and *npq21* with constant light (C) and fluctuating light (F). Data are means of three replicates and error bars indicate SD. Asterisks indicate significant differences between the treatments $P \leq 0.05$ (*), $P \leq 0.01$ (**) and $P \leq 0.001$ (***). Letters indicate significant differences compared to WT $P \leq 0.05$ (a), $P \leq 0.01$ (b) and $P \leq 0.001$ (c).

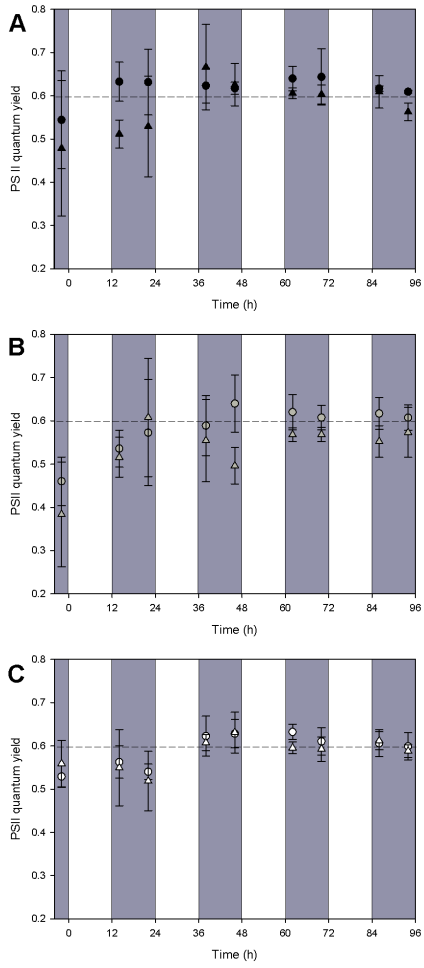

Figure 4.20: Changes in PS II quantum yield under 12 h/12 h LD cycles of WT (A), *npq3* (B) and *npq21* (C) under control conditions with constant light (circles) or with fluctuating light (triangles). Dark grey areas in the background show dark periods. Data are means of three replicates and error bars indicate SD. Dashed lines show a reference value of 0.6.

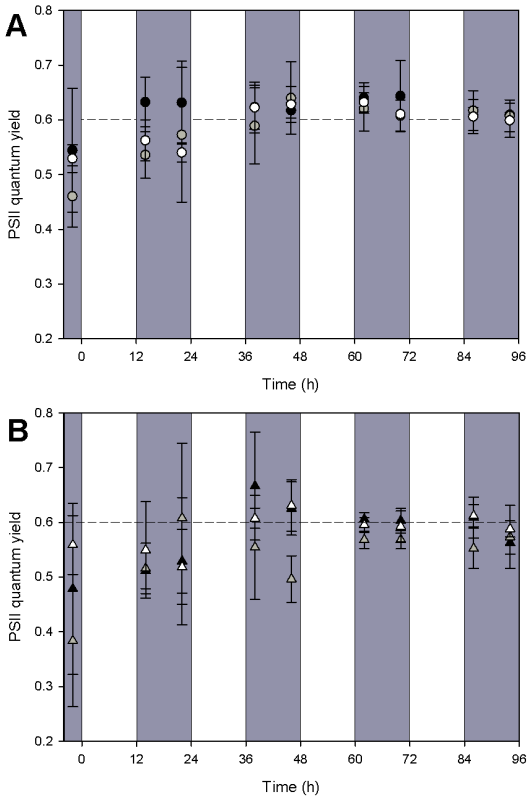

Figure 4.21: Changes in PS II quantum yield under 12 h/12 h LD cycles with constant light (A) or fluctuating light (B) for WT (black symbols), *npq3* (grey symbols) and *npq21* (white symbols). Dark grey areas in the background show dark periods. Data are means of three replicates and error bars indicate SD. Dashed lines show a reference value of 0.6.

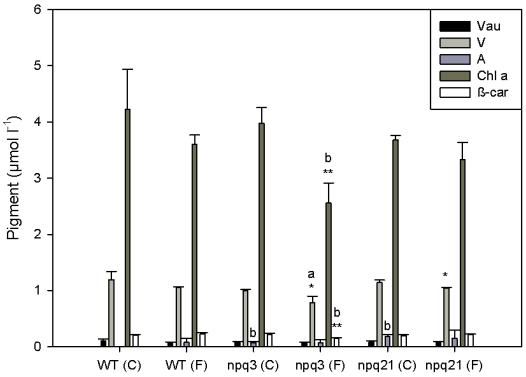

Figure 4.22: Molar pigment concentration of vaucheriaxanthin (Vau), violaxanthin (V), antheraxanthin (A), chlorophyll *a* (Chl *a*) and β-carotene (β-car) after 96 h in culture of WT, *npq3* and *npq21* under 12 h/12 h LD cycles with constant light (C) and fluctuating light (F). Data are means of three replicates and error bars indicate SD. Asterisks indicate significant differences between the treatments $P \leq 0.05$ (*) and $P \leq 0.01$ (**). Letters indicate significant differences compared to WT $P \leq 0.05$ (a) and $P \leq 0.01$ (b).

The concentrations of vaucheriaxanthin, violaxanthin, antheraxanthin, chlorophyll *a* and β-carotene were measured after 96 h (Fig. 4.22). For chlorophyll *a* the mean values tended to be higher under LD cycle with constant light than with fluctuating light, with a significant difference found for *npq3*. The highest among the carotenoids, albeit by a factor of three to four lower than chlorophyll *a*, was violaxanthin which also exhibited a similar pattern as chlorophyll *a*, with both mutants showing significantly lower concentrations under fluctuating light compared to WT. Molar concentrations of vaucheriaxanthin, antheraxanthin, and β-carotene were always below 0.3 µmol l^{-1}.

For chlorophyll-based contents of individual carotenoids (Fig. 4.23), the values of *npq3* under LD cycle with constant light were significantly lower than under fluctuating light whereas this was true only for β-carotene in WT and *npq21*. Significant differences compared to WT were found for antheraxanthin under constant light conditions; both mutants accumulated antheraxanthin in both constant and fluctuating light regimes while WT had antheraxanthin only under fluctuating light.

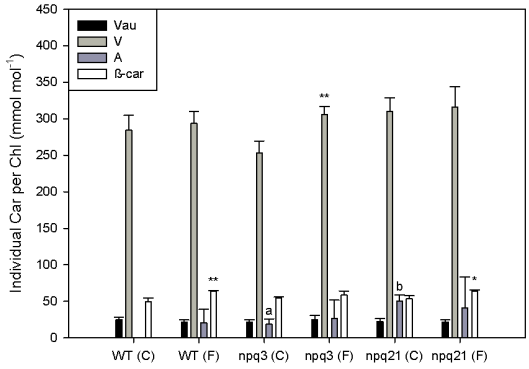

Figure 4.23: Ratio of vaucheriaxanthin (Vau), violaxanthin (V), antheraxanthin (A) or β-carotene (β-car) to chlorophyll (Chl) after 96 h in culture of WT, *npq3* and *npq21* under 12 h/12 h LD cycles with constant light (C) and fluctuating light (F). Data are means of three replicates and error bars indicate SD. Asterisks indicate significant differences between the treatments $P \leq 0.05$ (*) and $P \leq 0.01$ (**). Letters indicate significant differences compared to WT $P \leq 0.05$ (a) and $P \leq 0.01$ (b).

Figure 4.24 shows that mean ratios of total carotenoid to chlorophyll *a* were higher under LD cycles with fluctuating light for WT and *npq3* while ratios were the same for *npq21* which always showed significantly higher values than WT.

Mean values of biomass production were significantly higher under LD cycles with fluctuating light for WT (+16%) and *npq21* (+38%) (Fig. 4.25). Under fluctuating light *npq3* showed significantly lower biomass production than WT.

The chlorophyll *a* content per biomass after 96 h (Fig. 4.26) showed lower values under LD cycles with fluctuating light, and this was significant for *npq3* and *npq21*. The latter mutant also showed a significantly lower chlorophyll *a* content under fluctuation light compared to WT.

A similar pattern was also found for the total nitrogen content per biomass dry weight with significantly lower values for LD cycles with fluctuating light (-0.23% for WT, -0.16% for *npq3*, -0.29% for *npq21*). Again *npq21* showed significant differences to WT, having lower values than WT under both treatments (Fig. 4.27).

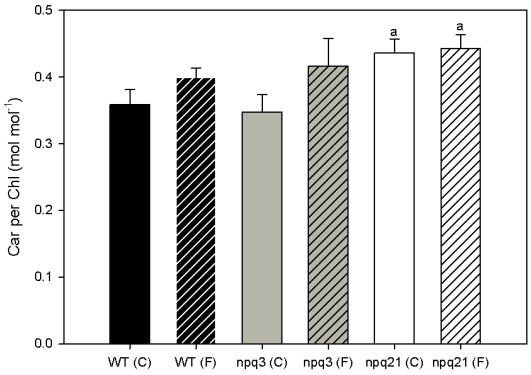

Figure 4.24: Ratio of carotenoids (Car) to chlorophyll (Chl) after 96 h in culture of WT, *npq3* and *npq21* under 12 h/12 h LD cycles with constant light (C) and fluctuating light (F). Data are means of three replicates and error bars indicate SD. Letters indicate significant differences compared to WT $P \leq 0.05$ (a).

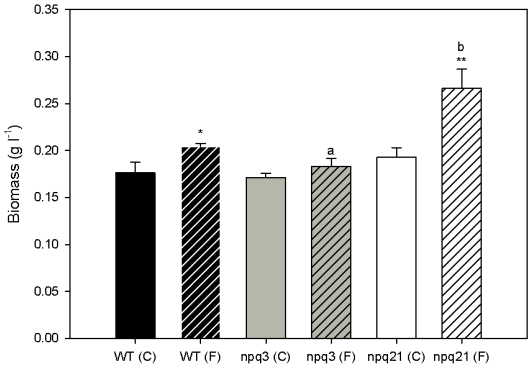

Figure 4.25: Biomass dry weight per liter after 96 h of WT, *npq3* and *npq21* under 12 h/12 h LD cycles with constant light (C) and fluctuating light (F). Data are means of three replicates and error bars indicate SD. Asterisks indicate significant differences between the treatments $P \leq 0.05$ (*) and $P \leq 0.01$ (**). Letters indicate significant differences compared to WT $P \leq 0.05$ (a) and $P \leq 0.01$ (b).

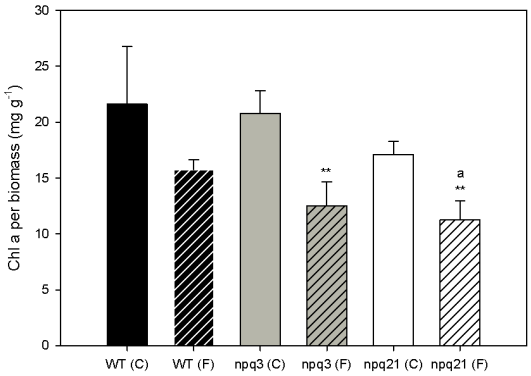

Figure 4.26: Chlorophyll a (Chl a) content per dry biomass after 96 h of WT, *npq3* and *npq21* under 12 h/12 h LD cycles with constant light (C) and fluctuating light (F). Data are means of three replicates and error bars indicate SD. Asterisks indicate significant differences between the treatments $P \leq 0.01$ (**) and letter indicates significant difference compared to WT $P \leq 0.05$ (a).

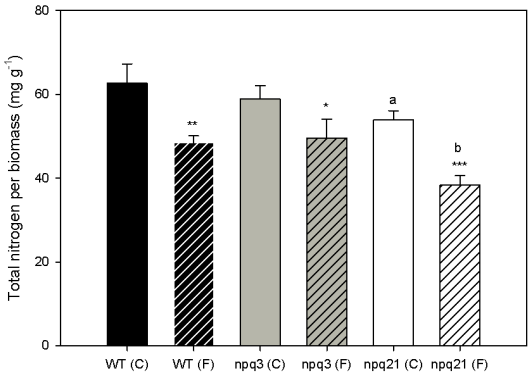

Figure 4.27: Total-nitrogen content per dry biomass after 96 h of WT, *npq3* and *npq21* under 12 h/12 h LD cycles with constant light (C) and fluctuating light (F). Data are means of three replicates and error bars indicate SD. Asterisks indicate significant differences between the treatments $P \leq 0.05$ (*), $P \leq 0.01$ (**) and $P \leq 0.001$ (***). Letters indicate significant differences compared to WT $P \leq 0.05$ (a) and $P \leq 0.01$ (b).

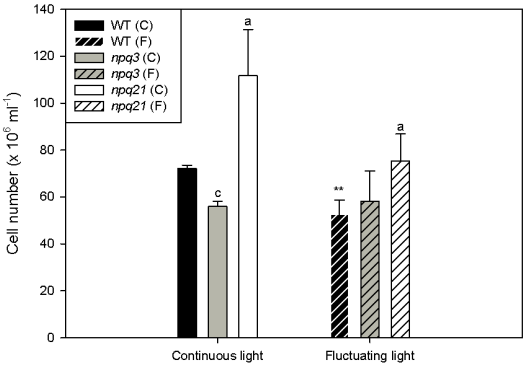

Figure 4.28: Cell number after 96 h of WT, *npq3* and *npq21* under 12 h/12 h LD cycles with constant light (C) and fluctuating light (F). Data are means of three replicates and error bars indicate SD. Asterisks indicate significant difference between the treatments $P \leq 0.01$ (**). Letters indicate significant differences compared to WT $P \leq 0.05$ (a) and $P \leq 0.001$ (c).

The cell numbers shown in Fig. 4.28 were significantly lower for WT under LD cycles with fluctuating light than constant light. While *npq3* had significantly less cells than WT under constant light, its cell number did not change under fluctuating light. The cell numbers of *npq21* were the highest among the three genotypes under both conditions.

Chlorophyll *a* per cell were not significantly different between the treatments for WT and *npq21* while *npq3* had significantly lower chlorophyll *a* per cell under fluctuating light (Fig. 4.29). *npq3* and *npq21* showed significantly lower chlorophyll *a* per cell under fluctuating light compared with WT as well as lower values were found for *npq21* under constant light.

Before and after the experiment with 12 h/12 h LD cycles with constant light and fluctuating light NPQ induction and relaxation was measured (Fig. 4.30). In all cases higher NPQ values were found at the end of the experiment compared with the values measured at the beginning. Under the illumination of 1000 µmol photons m^{-2} s^{-1} NPQ values were ≈1.0 higher after the experiment than before and values during relaxation stayed higher, except for *npq3* under 12 h/12 h LD cycles with fluctuating light where NPQ sustained in the dark was nearly the same

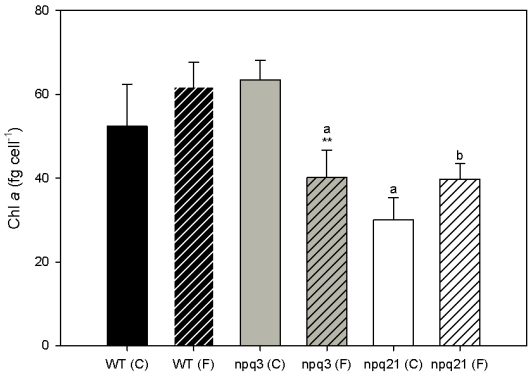

Figure 4.29: Chlorophyll *a* (Chl a) per cell after 96 h of WT, *npq3* and *npq21* under 12 h/12 h LD cycles with constant light (C) and fluctuating light (F). Data are means of three replicates and error bars indicate SD. Asterisks indicate significant differences between the treatments $P \leq 0.01$ (**). Letters indicate significant differences compared to WT $P \leq 0.05$ (a) and $P \leq 0.01$ (b).

for both treatments. Unlike in Fig. 4.16, NPQ values did not show clear differences between the genotypes (Fig. 4.31). Before and after 12 h/12 h LD cycles with constant light NPQ of WT and *npq21* were similar while NPQ of *npq3* was lower. Before 12 h/12 h LD cycles with fluctuating light NPQ of *npq3* and *npq21* were similar while NPQ of WT was slightly lower, yet after the experiment WT showed slightly higher NPQ than the other two genotypes.

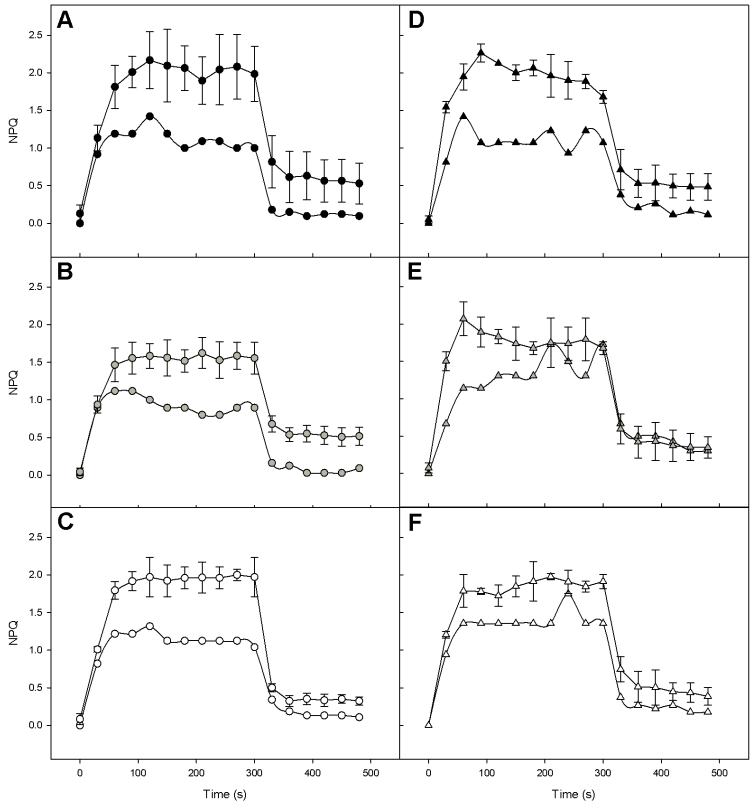

Figure 4.30: NPQ during light induction and dark relaxation before and after 12 h/12 h LD cycles with constant light (circles) (A, B and C) and fluctuating light (triangles) (D, E and F) of WT (black symbols), *npq3* (grey symbols) and *npq21* (white symbols). Data before treatment are without error bars, data after treatment are means of three replicates and error bars indicate SD.

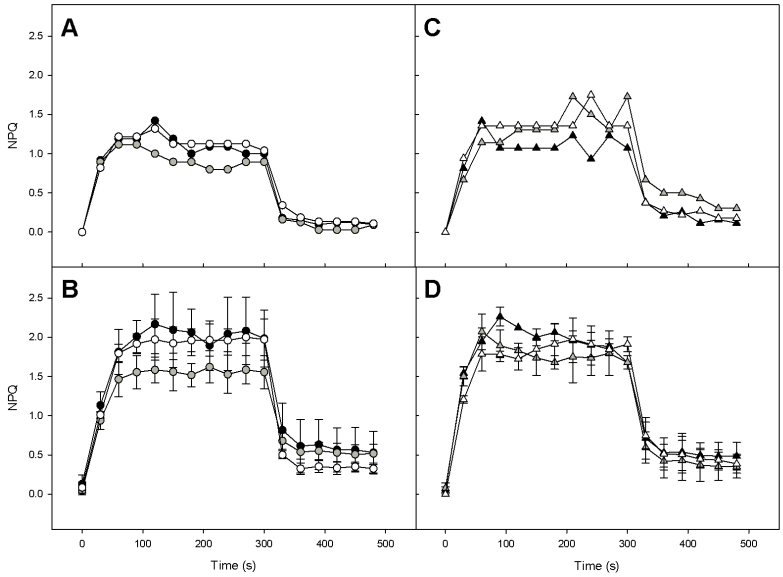

Figure 4.31: NPQ during light induction and dark relaxation before and after 12 h/12 h LD cycles with constant light (circles) (A and B) and fluctuating light (triangles) (C and D) of WT (black symbols), *npq3* (grey symbols) and *npq21* (white symbols). Data before treatment are without error bars (A and C), data after treatment are means of three replicates (B and D) and error bars indicate SD.

4.1.2.2 Continuous light with constant and fluctuating light

N. gaditana WT, *npq3* and *npq21* were grown under LL with either a constant light intensity (200 µmol photons m^{-2} s^{-1}) or periodic light switching between very low light (10 µmol photons m^{-2} s^{-1} for 3 min) and high light (770 µmol photons m^{-2} s^{-1} for 1 min). Under LL constant light the values of OD_{680} increased exponentially for approximately 37 h for WT and *npq21* before reaching the stationary phase; the curves of these two genotypes were very similar (Fig. 4.32A). For *npq3* the inflection point of the OD_{680} curve was approximately 10 h later than the others (i.e. after 47 h of growth) and from the time point of approximately 24 h OD_{680} values of *npq3* were lower than those of WT and *npq21*, leading to a lower end-OD_{680} at 96 h. In contrast, under the continuously fluctuating light condition all three strains grew extremely slowly throughout 96 h. Even though values were rather low, *npq21* showed a trend of faster density increase followed by WT, while *npq3* showed lowest values.

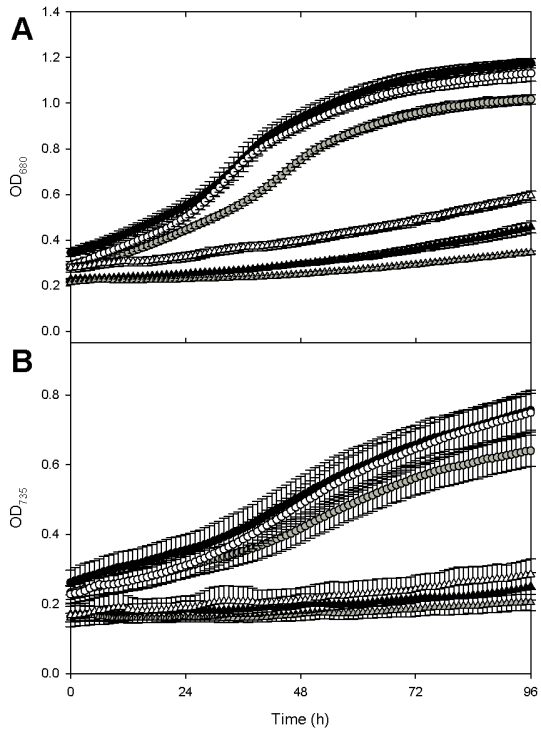

Figure 4.32: Changes in OD_{680} (A) and OD_{735} (B) under constant LL of WT (black circles), *npq3* (grey circles) and *npq21* (white circles) and under fluctuating LL of WT (black triangles), *npq3* (grey triangles) and *npq21* (white triangles). Data are means of three replicates and error bars indicate SD.

A similar picture was found for OD_{735}, yet the inflection points of the curves under constant LL were approximately after 47 h of growth for all three genotypes and again from the time point of approximately 24 h OD_{735} values of *npq3* were lower than those of WT and *npq21* (Fig. 4.32B). Under the fluctuating LL, OD_{735} values showed a similar behavior as OD_{680}.

The relative increase in OD_{680} (Fig. 4.33) calculated from OD_{680} values in Fig. 4.32 indicated rapid growth during the first 48 h under constant LL, followed by a drastic decrease between 48 and 72 h. During the last 24 h the values were very low. A different picture of slow and gradual increase in OD_{680} was observed un-

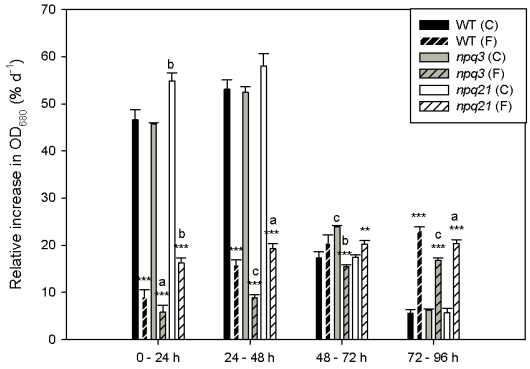

Figure 4.33: Relative increase in OD_{680} per day for WT, *npq3* and *npq21* under constant LL (C) and fluctuating LL (F). Data are means of three replicates and error bars indicate SD. Asterisks indicate significant differences between the treatments $P \leq 0.01$ (**) and $P \leq 0.001$ (***). Letters indicate significant differences compared to WT $P \leq 0.05$ (a), $P \leq 0.01$ (b) and $P \leq 0.001$ (c).

der fluctuating LL. Thus, the values of the fluctuating LL exceeded those of the constant LL between 72 and 96 h. Yet, the relative increase values were always significantly different between the treatments except for WT between 48 and 72 h. When comparing the mutants with the WT, significant differences under constant LL were found for *npq21* (*npq21*>WT) in the first 24 h and for *npq3* (*npq3*>WT) in the third 24 h period. Under fluctuating LL *npq21* had higher rates of relative increase than WT in the first 48 h while *npq3* always had lower rates than WT. Also for *npq21* the values became lower than WT in the last 24 h (72 - 96 h).

PS II quantum yield was recorded only in the experiment with constant LL, as the timing of fluorescence measurements and light fluctuations in the fluctuating LL were not synchronized, which resulted in strong fluctuations also of fluorescence signal (Fig. 4.34). Under the constant LL WT and *npq21* showed very similar PS II quantum yields whereas yield for *npq3* was clearly lower. After the first 24 h PS II quantum yields started to decrease to reach a steady state after ≈40 h for WT and *npq21* and ≈52 h for *npq3*. Thereafter PS II quantum yield remained unchanged until the end of the experiments with the values of WT and *npq21* still lying higher than those of *npq3* by ca. 0.1.

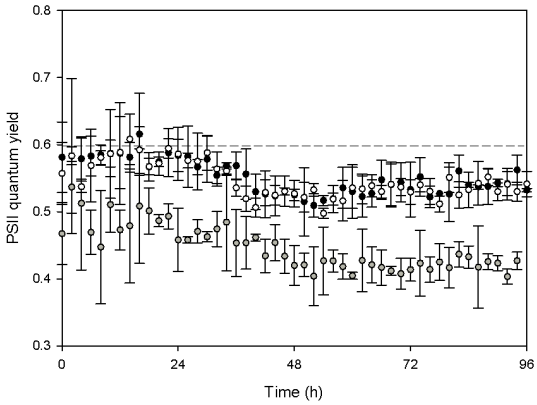

Figure 4.34: Changes in PS II quantum yield under constant LL of WT (black circles), *npq3* (grey circles) and *npq21* (white circles). Data are means of three replicates and error bars indicate SD. Dashed lines show a reference value of 0.6.

The mean values of the molar pigment concentration per liter of vaucheriaxanthin, violaxanthin, antheraxanthin, chlorophyll *a* and β-carotene were all lower under fluctuating LL compared to constant LL (Fig. 4.35). When looking at the ratios of each carotenoid to chlorophyll *a*, violaxanthin values were lower under fluctuating light for WT and *npq3* (Fig. 4.36). Unlike in the constant light with LD cycles (Fig. 4.23), WT accumulated antheraxanthin in constant LL, even though the level was significantly lower than in the mutants. Again, *npq21* had the highest amount of antheraxanthin among the three strains under constant LL. Figure 4.37 shows that the ratios of carotenoids per chlorophyll *a* increased strongly in *npq3* under constant LL, reaching the values of about 0.5 (i.e. carotenoids:chlorophylls 1:2), which is much higher than the values found in this mutant in the fluctuating LL or in the two light regimes with LD cycles (Fig. 4.24). The values were around 0.4 for WT and *npq21* in LL, with or without light fluctuation.

In accordance to Fig. 4.32, cell numbers were significantly lower after fluctuating LL treatment than after constant LL treatment (Fig. 4.38). Compared to WT, *npq3* showed a significantly lower cell number under constant light whereas *npq21* showed a significantly high cell number under fluctuating light.

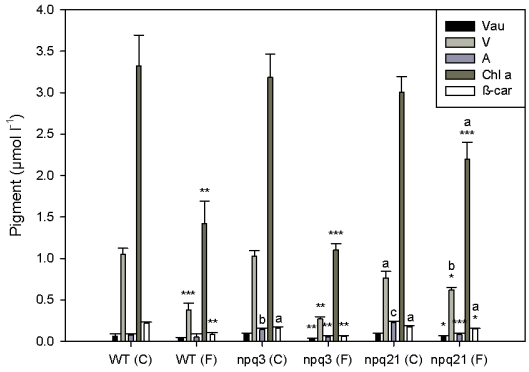

Figure 4.35: Molar pigment concentration of vaucheriaxanthin (Vau), violaxanthin (V), antheraxanthin (A), chlorophyll *a* (Chl *a*) and β-carotene (β-car) after 96 h in culture of WT, *npq3* and *npq21* under constant LL (C) and fluctuating LL (F). Data are means of three replicates and error bars indicate SD. Asterisks indicate significant differences between the treatments $P \leq 0.05$ (*), $P \leq 0.01$ (**) and $P \leq 0.001$ (***). Letters indicate significant differences compared to WT $P \leq 0.05$ (a), $P \leq 0.01$ (b) and $P \leq 0.001$ (c).

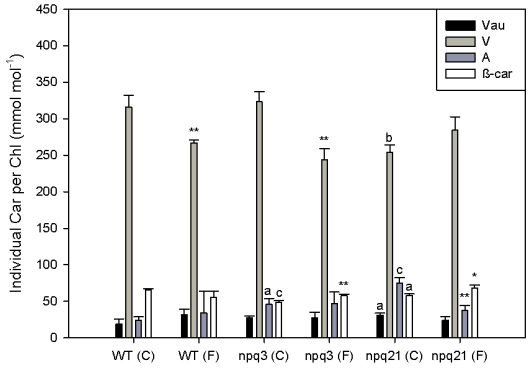

Figure 4.36: Ratio of vaucheriaxanthin (Vau), violaxanthin (V), antheraxanthin (A) or β-carotene (β-car) to chlorophyll (Chl) after 96 h in culture of WT, *npq3* and *npq21* under constant LL (C) and fluctuating LL (F). Data are means of three replicates and error bars indicate SD. Asterisks indicate significant differences between the treatments $P \leq 0.05$ (*) and $P \leq 0.01$ (**). Letters indicate significant differences compared to WT $P \leq 0.05$ (a), $P \leq 0.01$ (b) and $P \leq 0.001$ (c).

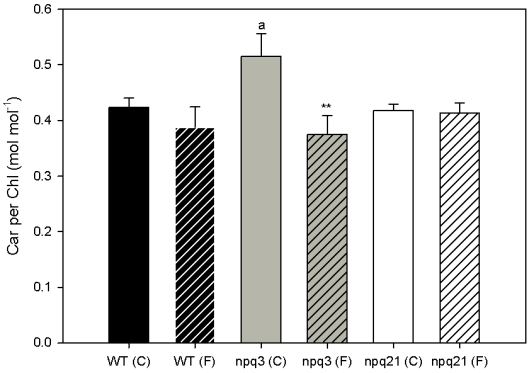

Figure 4.37: Ratio of carotenoids (Car) to chlorophyll (Chl) after 96 h in culture of WT, *npq3* and *npq21* under constant LL (C) and fluctuating LL (F). Data are means of three replicates and error bars indicate SD. Asterisks indicate significant difference between the treatments $P \leq 0.01$ (**). Letter indicates significant difference compared to WT $P \leq 0.05$ (a).

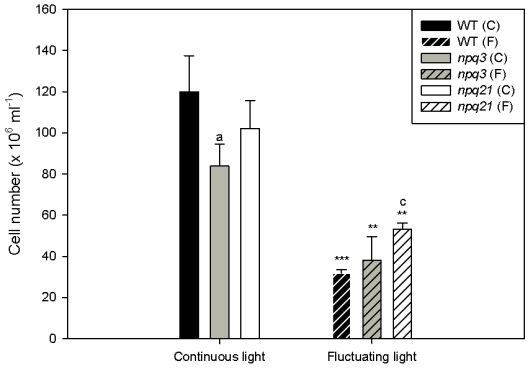

Figure 4.38: Cell number after 96 h of WT, *npq3* and *npq21* under constant LL (C) and fluctuating LL (F). Data are means of three replicates and error bars indicate SD. Asterisks indicate significant differences between the treatments $P \leq 0.01$ (**) and $P \leq 0.001$ (***). Letters indicate significant differences compared to WT $P \leq 0.05$ (a) and $P \leq 0.001$ (c).

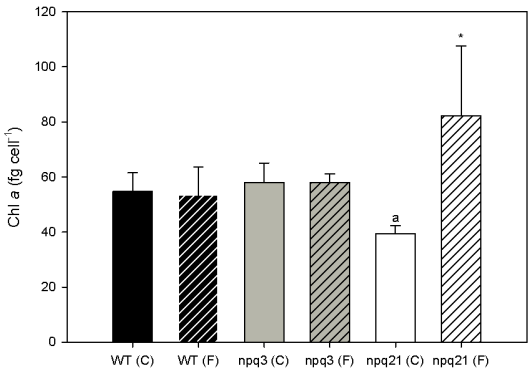

Figure 4.39: Chlorophyll *a* (Chl *a*) per cell after 96 h of WT, *npq3* and *npq21* under constant LL (C) and fluctuating LL (F). Data are means of three replicates and error bars indicate SD. Asterisk indicates significant difference between the treatments $P \leq 0.05$ (*). Letter indicates significant difference compared to WT $P \leq 0.05$ (a).

For WT and *npq3* no differences were found in chlorophyll *a* per cell between the treatments (Fig. 4.39) whereas *npq21* showed higher chlorophyll *a* per cell under fluctuating LL and a significantly lower value under constant LL compared with WT.

4.1.2.3 Temperature cycles

The above results for *npq3* did not suggest a better performance under different light regimes compared to WT or *npq21*, whereas *npq21* had similar or higher growth than WT. Thus, *npq3* was excluded from the following experiments with temperature cycles.

Cultures of WT and *npq21* were grown under LD cycles, with temperature cycles of either 23°C/15°C or 30°C/23°C. Figure 4.40 shows an increase of OD_{680} and OD_{735} values during the light periods. For WT the increase in OD values was strongly suppressed under 23°C/15°C unlike under 30°C/23°C. The difference between the two temperature regimes was not very pronounced for *npq21*.

While the relative increase in OD_{680} continued to rise for WT under 23°C/15°C in the first three LD cycles and stagnated in the fourth, it started to decrease

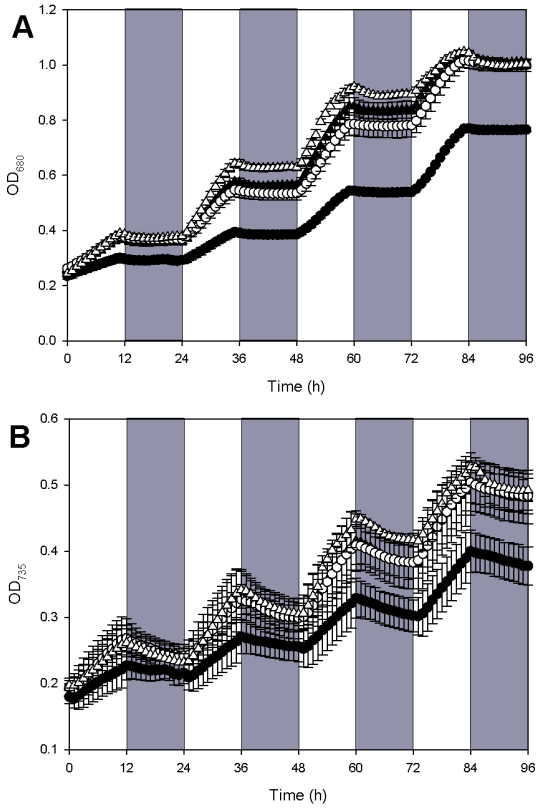

Figure 4.40: Changes in OD_{680} (A) and OD_{735} (B) under 12 h/12 h LD cycles and temperature cycles with either 23°C/15°C (circles) or 30°C/23°C (triangles) of WT (black symbols) and *npq21* (white symbols). Dark grey areas in the background show dark periods. Data are means of six replicates and error bars indicate SD.

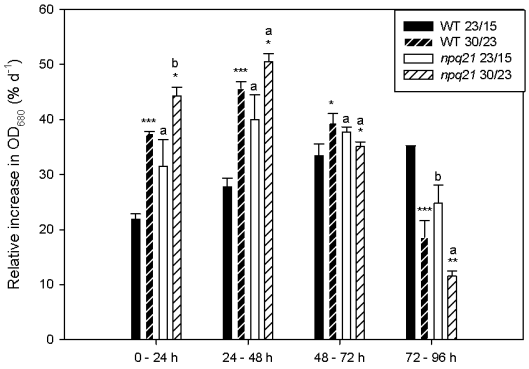

Figure 4.41: Relative increase in OD_{680} per 24 h period for WT and *npq21* under 12 h/12 h LD cycles and temperature cycles with either 23°C/15°C or 30°C/23°C. Data are means of six replicates and error bars indicate SD. Asterisks indicate significant differences between the treatments $P \leq 0.05$ (*), $P \leq 0.01$ (**) and $P \leq 0.001$ (***). Letters indicate significant differences compared to WT $P \leq 0.05$ (a) and $P \leq 0.01$ (b).

under 30°C/23°C in the third LD cycle (Fig. 4.41). Similar to WT, *npq21* decreased in the relative increase in OD_{680} between 48 and 72 h whereas under the control conditions the second and third 24 h periods showed nearly the same values. When comparing WT and *npq21* the values of *npq21* were higher in the first two LD cycles while in the third they were similar and in the fourth lower than WT.

Contrary to the pictures for OD_{680} (Figs. 4.40 and 4.41), Fig. 4.42A-B shows higher PS II quantum yields during light and dark periods for 23°C/15°C compared to 30°C/23°C for both WT and *npq21*. The differences between the two strains were only minor, if any, in 23°C/15°C or 30°C/23°C (Fig. 4.42C-D).

The concentrations of chlorophyll *a*, violaxanthin and β-carotene were higher under 30°C/23°C compared to 23°C/15°C and values were higher for *npq21* than for WT (Fig. 4.43). When looking at the ratios of individual carotenoids to chlorophyll *a*, significant differences between the treatments were detected for WT for all carotenoids except vaucheriaxanthin while no significant differences were found for *npq21* (Fig. 4.44). Under 23°C/15°C conditions *npq21* showed significantly higher levels of violaxanthin and antheraxanthin than WT while under 30°C/23°C they were similar. Accumulation of antheraxanthin was found only in 30°C/23°C

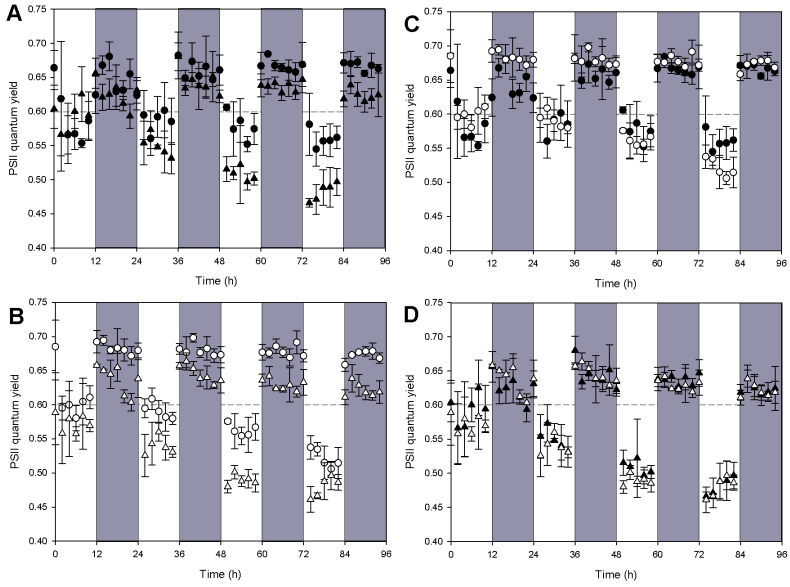

Figure 4.42: Changes in PS II quantum yield of WT under 23°C/15°C (black circles) and under 30°C/23°C (black triangles) (A), *npq21* under 23°C/15°C (white circles) and under 30°C/23°C (white triangles) (B), WT (black circles) and *npq21* (white circles) under 23°C/15°C (C) and WT (black triangles) and *npq21* (white triangles) under 30°C/23°C (D). Data are means of six replicates and error bars indicate SD. Dashed lines show a reference value of 0.6.

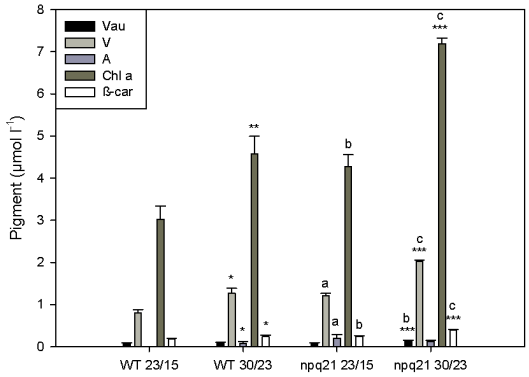

Figure 4.43: Molar pigment concentration of vaucheriaxanthin (Vau), violaxanthin (V), antheraxanthin (A), chlorophyll *a* (Chl *a*) and β-carotene (β-car) after 96 h in culture of WT and *npq21* under 12 h/12 h LD cycles and temperature cycles with either 23°C/15°C or 30°C/23°C. Data are means of six replicates and error bars indicate SD. Asterisks indicate significant differences between the treatments $P \leq 0.05$ (*), $P \leq 0.01$ (**) and $P \leq 0.001$ (***). Letters indicate significant differences compared to WT $P \leq 0.05$ (a), $P \leq 0.01$ (b) and $P \leq 0.001$ (c).

for WT, whereas *npq21* always had some antheraxanthin, as was seen in the experiments with fluctuating light (Figs. 4.23 and 4.36). The total caroteniods to chlorophyll *a* ratio was nearly the same as measured in the LD cycle with constant light and temperature (Fig. 4.24) for WT under both treatments (Fig. 4.45). Likewise, the values of *npq21* under 23°C/15°C were comparable with those in the LD cycle with constant temperature (Fig. 4.24), while they decreased in 30°C/23°C.

Figure 4.46 shows lower cell numbers under 30°C/23°C than 23°C/15°C for both genotypes, with significant differences for the WT. Between WT and *npq21* the values of *npq21* were higher than WT under 30°C/23°C.

Chlorophyll *a* per cell was significantly higher under 30°C/23°C than 23°C/15°C for WT and *npq21*, yet no differences were found between the genotypes (Fig. 4.47).

Table 4.2 gives an overview of the highest values of relative OD_{680} increase in WT, *npq3* and *npq21* under the different light and temperature treatments. Under all treatments highest relative OD_{680} increase was found for *npq21*, except under fluctuating LL WT had a significant higher value. On the other hand, *npq3* showed

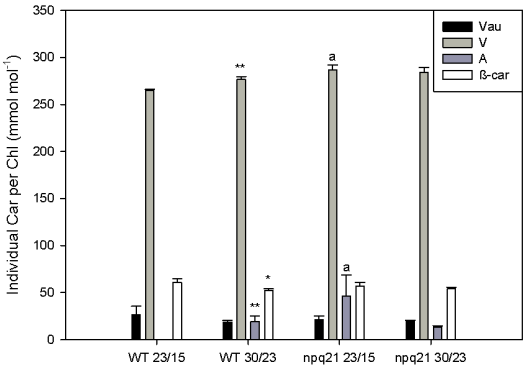

Figure 4.44: Ratio of vaucheriaxanthin (Vau), violaxanthin (V), antheraxanthin (A) or β-carotene (β-car) to chlorophyll *a* (Chl) after 96 h in culture of WT and *npq21* under 12 h/12 h LD cycles and temperature cycles with either 23°C/15°C or 30°C/23°C. Data are means of six replicates and error bars indicate SD. Asterisks indicate significant differences between the treatments $P \leq 0.05$ (*) and $P \leq 0.01$ (**). Letters indicate significant differences compared to WT $P \leq 0.05$ (a).

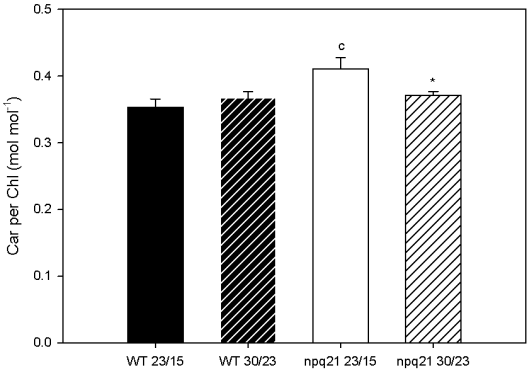

Figure 4.45: Ratio of carotenoids (Car) to chlorophyll (Chl) after 96 h in culture of WT and *npq21* under 12 h/12 h LD cycles and temperature cycles with either 23°C/15°C or 30°C/23°C. Data are means of six replicates and error bars indicate SD. Asterisk indicates significant difference between the treatments $P \leq 0.05$ (*). Letter indicates significant difference compared to WT $P \leq 0.001$ (c).

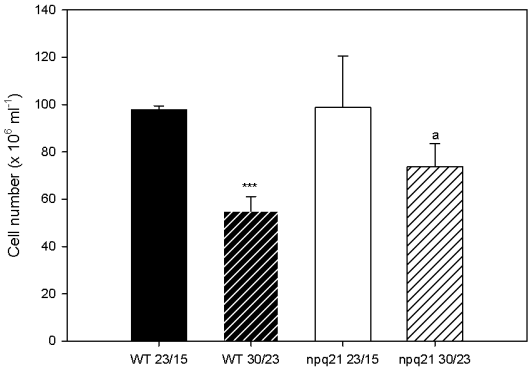

Figure 4.46: Cell number at end of fourth day of WT and *npq21* under 12 h/12 h LD cycles and temperature cycles with either 23°C/15°C or 30°C/23°C. Data are means of six replicates and error bars indicate SD. Asterisks indicate significant difference between the treatments $P \leq 0.001$ (***). Letter indicates significant difference compared to WT $P \leq 0.05$ (a).

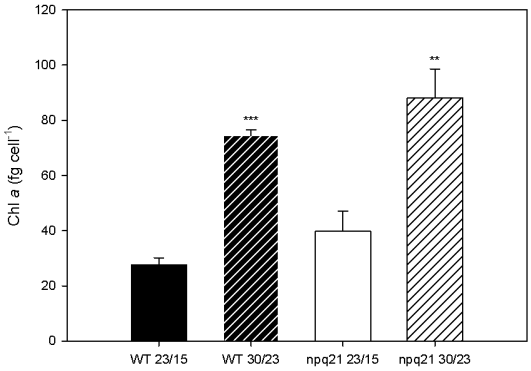

Figure 4.47: Chlorophyll *a* (Chl *a*) per cell at end of fourth day of WT and *npq21* under 12 h/12 h LD cycles and temperature cycles with either 23°C/15°C or 30°C/23°C. Data are means of six replicates and error bars indicate SD. Asterisks indicate significant differences between the treatments $P \leq 0.01$ (**) and $P \leq 0.001$ (***).

lower values under all treatments compared with the other two genotypes, which were significant under fluctuating LD and fluctuating LL. The levels of carotenoids per chlorophyll *a* (Table 4.3) were highest for *npq21* under most treatments except under constant LL and constant LD with 30°C/23°C where *npq21* and WT had similar values. Under fluctuating LD *npq3* achieved a slightly higher value than WT and in addition had the significantly highest carotenoids per chlorophyll *a* value under constant LL.

Table 4.2: Highest values of relative OD_{680} increase of WT, *npq3* and *npq21* under different light (C-constant, F-fluctuating) and temperature treatments. Letters indicate significant differences compared to WT $P \leq 0.05$ (a), $P \leq 0.01$ (b) and $P \leq 0.001$ (c).

light	**temp. (°C)**	**WT (% d^{-1})**	***npq3*** **(% d^{-1})**	***npq21*** **(% d^{-1})**
LD (C)	23	40 (±0.59)	39 (±1.1)	42 (±1.9)
LD (F)	23	50 (±0.62)	41 (±0.51) (c)	53 (±0.57) (b)
LL (C)	23	53 (±2.0)	52 (±1.1)	58 (±2.6)
LL (F)	23	23 (±0.75)	17 (±0.41) (c)	20 (±0.84) (a)
LD (C)	23/15	35 (±0.24)		40 (±4.5)
LD (C)	30/15	46 (±1.3)		51 (±1.4) (a)

Table 4.3: Highest values of carotenoids (Car) per chlorophyll (Chl) of WT, *npq3* and *npq21* under different light (C-constant, F-fluctuating) and temperature treatments. Letters indicate significant differences compared to WT $P \leq 0.05$ (a).

light	**temp. (°C)**	**WT**	***npq3***	***npq21***
LD (C)	23	0.36 (±0.023)	0.35 (±0.026)	0.44 (±0.021) (a)
LD (F)	23	0.4 (±0.014)	0.42 (±0.042)	0.44 (±0.021) (a)
LL (C)	23	0.42 (±0.017)	0.52 (±0.041) (a)	0.42 (±0.011)
LL (F)	23	0.39 (±0.037)	0.38 (±0.033)	0.41 (±0.018)
LD (C)	23/15	0.35 (±0.013)		0.41 (±0.017) (a)
LD (C)	30/15	0.37 (±0.0093)		0.37 (±0.0062)

4.2 Experiments under greenhouse conditions

4.2.1 Comparison of WT in four PBRs

N. gaditana was continuously cultivated under greenhouse conditions in four pilot-scale closed PBR systems, which were set up in two small greenhouses with a constructed area of 12 m^2 each. The PBRs were numbered according to the greenhouse, thus PBR 1.1 and PBR 1.2 were located in greenhouse 1, whereas PBR 2.1 and PBR 2.2 were located in greenhouse 2. To investigate the comparability of the four systems, they were run in parallel from middle of October until middle of December 2012. The sunshine duration per day varied between 0 and about 500 min whereas maximal solar radiation reached 1,600 Wh m^{-2} d^{-1} (Fig. 4.48) [143]. Further growth conditions were monitored by recording the temperature (Fig. 4.50) in the culture. The day length (Fig. 4.49) decreased during the cultivation period from 11 h mid of October till 8 h mid of December [143], whereby temperatures rarely exceed 23°C during the day and the heater was turned on, preventing temperatures from falling below 14°C during the night. The pH-values (Fig. 4.51) were mostly around 7.5, with transient fluctuations up to 9 or down to 7 depending on the rate of CO_2 uptake by the algae and addition of CO_2.

During cultivation OD was measured at three different wavelengths: 540 nm (OD_{540}), 680 nm (OD_{680}) and 735 nm (OD_{735}) (Fig. 4.52). To ensure sufficient light for algae inside the PBR, OD_{540} was maintained within a range between ≈0.5 and ≈0.7; at these OD_{540} values growth curves of *N. gaditana* culture (obtained by measuring OD_{540}) seldom reached saturation under the greenhouse conditions in the experimental period. When OD_{540} exceeded a value of ≈0.7 the culture was diluted to ≈0.5 by discarding culture and refilling the system with fresh f/2 medium containing 2% sea salt. Due to the harvesting, OD values fluctuate in Fig. 4.52 but with very similar patterns for all three wavelengths. A technical problem occurred on November 8^{th} where the pump hose of PBR 1.2 leaked, so that the system was filled with fresh medium leading to a dilution and thus a change of OD_{540} values for the samples taken prior to the following harvest.

The biomass dry weight was determined at each harvest for every cultivation system (Fig. 4.53). There is a variation between the data, yet no clear trend for any reactor producing more or less compared to the others. On November 12^{th}

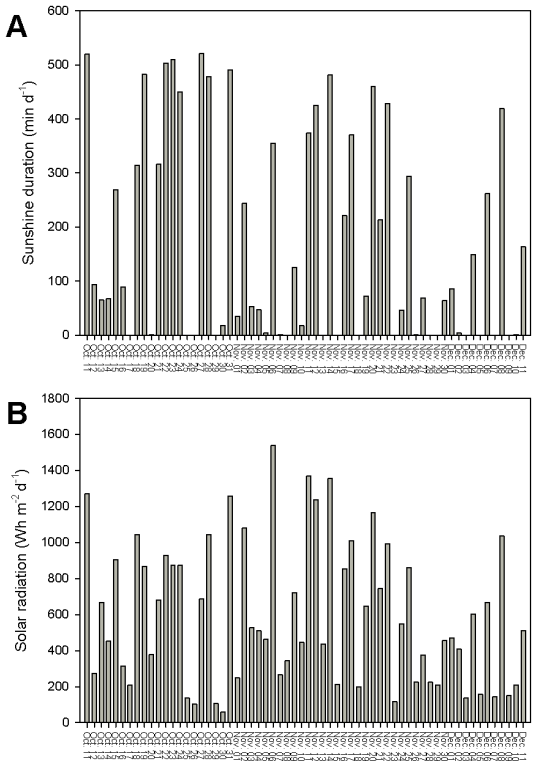

Figure 4.48: Changes in daily light in greenhouse from October until December 2012. Sunshine duration (A) and solar radiation (B) [143].

there was a strong decrease in biomass for PBR 1.2, as four days before the system had been filled up with fresh medium due to the leaking pump hose. In general, the biomass concentration on the harvesting days lied between 0.05 and 0.2 g l^{-1}, on average ≈0.1 g l^{-1} at OD_{540} of ≈0.7. This corresponds to an aerial productivity of ≈2 g m^{-2} at each harvest, except for the last day on which the whole system (≈300 l) was harvested.

The variation in cell numbers (Fig. 4.54) as well as chlorophyll *a* concentrations (Fig. 4.55) often showed a similar pattern as biomass concentrations. On average, the cell numbers within the PBRs was ≈5 x 10^9 cells l^{-1}. The average chlorophyll *a* concentration was ≈3.7 mg l^{-1} (Fig. 4.55), leading to ca. 3% chlorophyll *a* content in dry biomass with an average of ≈33 g kg^{-1} (Fig. 4.56).

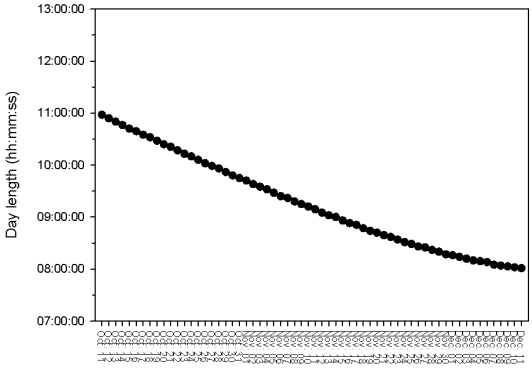

Figure 4.49: Changes in day length in Jülich (Germany) from October until December 2012 [143].

The total amount of nitrogen was determined in the biomass, which is an important macronutrient needed for growth and metabolic processes within the algae. Figure 4.57 shows the total nitrogen content in the algae per liter of the culture which lied between 9 and 15 mg l^{-1}, except on November 6th where the average was ≈19 mg l^{-1}. A particularly low nitrogen concentration was measured in PBR 1.2 on November 12th due to the dilution resulting from the technical defect. When looking at the total nitrogen content in the biomass (Fig. 4.58), the values were higher in the first half of the experimental period (except for November 12th), lying between 120 to 170 g kg^{-1}, while later values were between 70 to 100 g kg^{-1}.

As algae were harvested by discarding a certain volume of the culture and refilling the cultivation system with fresh medium, water was needed. In Fig. 4.59 the addition of water is given. At the beginning of the experiment the systems were filled with a volume of 300 l each. The added volumes of water at each harvest ranged between 90 and 144 l.

Sea salt was needed for cultivation as *N. gaditana* is a marine alga. Therefore salt was added to the f/2 medium to obtain 2% saline water. Thus, 6 kg of salt were added to the initial volume of the system, then salt was given in the systems according to the volume of water added after harvest, which lied around 2 kg (Fig. 4.60).

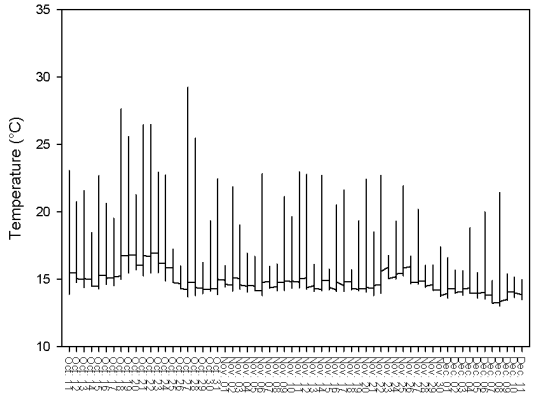

Figure 4.50: Changes in temperature of WT culture cultivated under greenhouse conditions from October until December 2012. Data are means of four replicate PBRs.

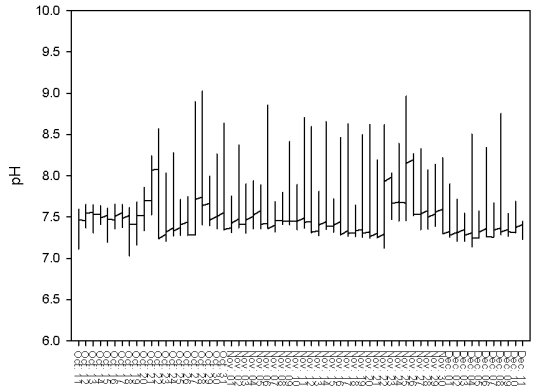

Figure 4.51: Changes in pH of WT culture cultivated under greenhouse conditions from October until December 2012. Data are means of four replicate PBRs.

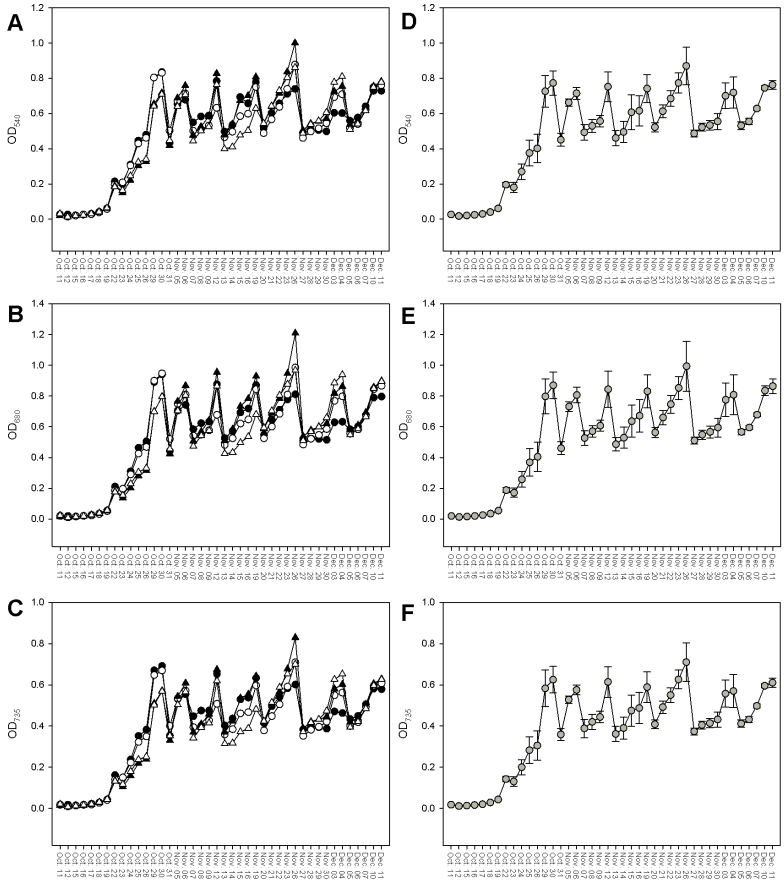

Figure 4.52: Changes in optical density monitored at 540 nm (OD_{540}) (A and D), 680 nm (OD_{680}) (B and E) and 735 nm (OD_{735}) (C and F) of WT cultivated under greenhouse conditions from October until December 2012 of PBR 1.1 (black circles), PBR 1.2 (white circles), PBR 2.1 (black triangles), PBR 2.2 (white triangles) and means (grey circles). Data (D-F) are means of four replicate PBRs and error bars indicate SD.

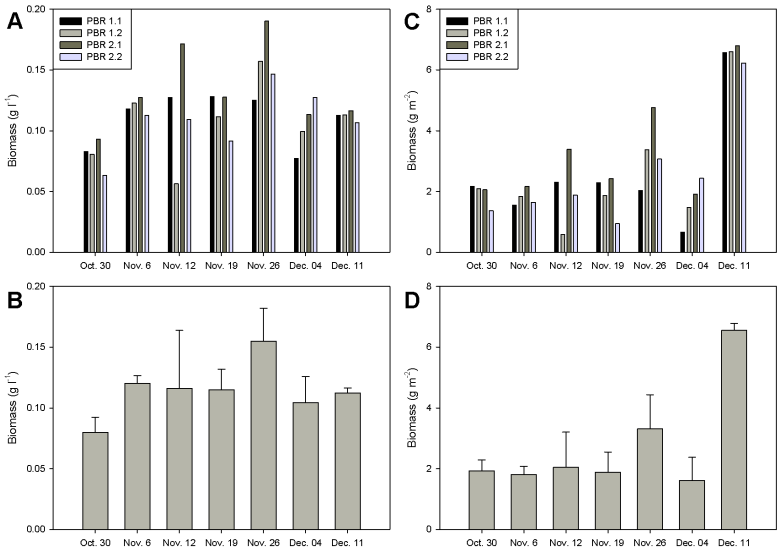

Figure 4.53: Biomass dry weight per liter (A and B) or area (C and D) at each harvest of WT cultivated under greenhouse conditions from October until December 2012. Data (B and D) are means of four replicate PBRs with error bars indicating SD.

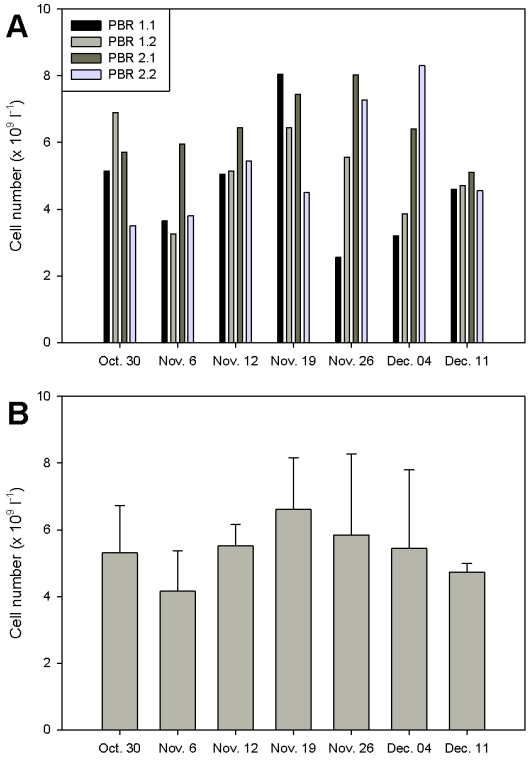

Figure 4.54: Cell number per liter at each harvest of WT cultivated under greenhouse conditions from October until December 2012. Data (B) are means of four replicate PBRs with error bars indicating SD.

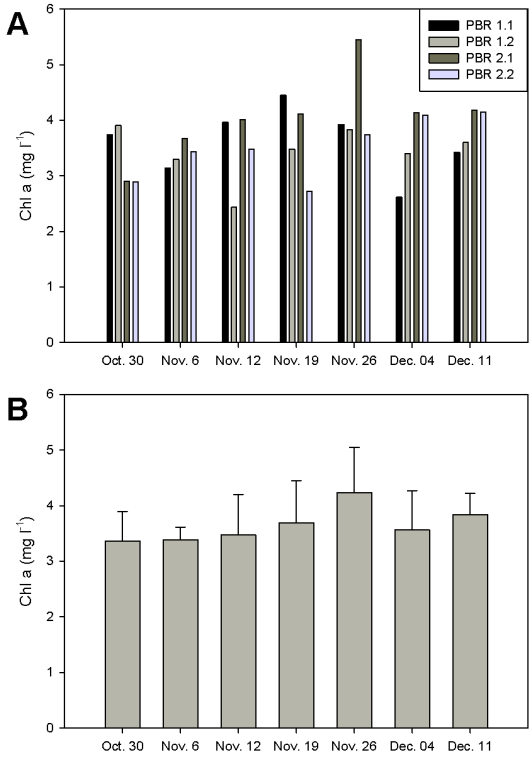

Figure 4.55: Chlorophyll *a* (Chl *a*) content per liter at each harvest of WT cultivated under greenhouse conditions from October until December 2012. Data (B) are means of four replicate PBRs with error bars indicating SD.

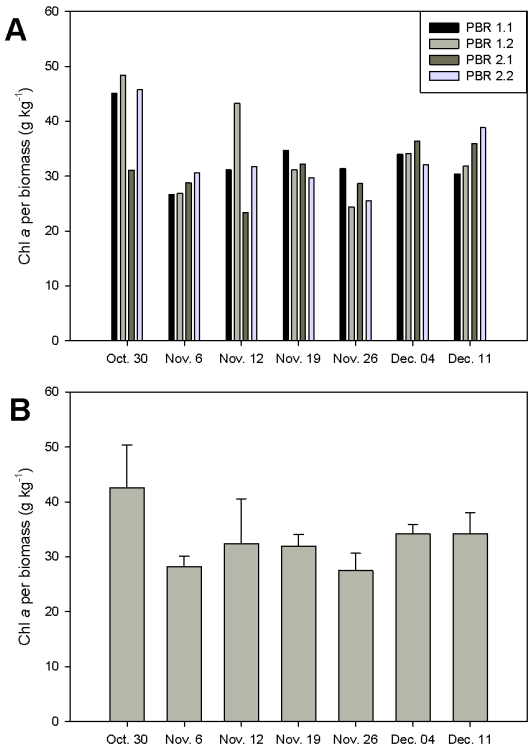

Figure 4.56: Chlorophyll *a* (Chl *a*) in dry biomass at each harvest of WT cultivated under greenhouse conditions from October until December 2012. Data (B) are means of four replicate PBRs with error bars indicating SD.

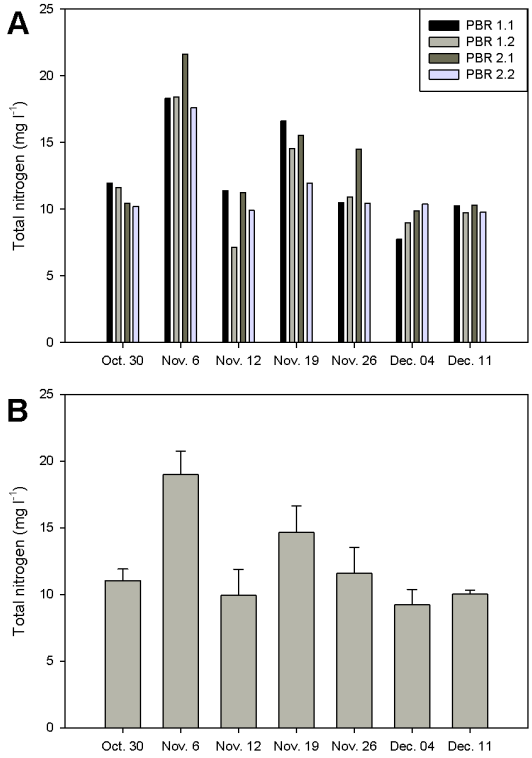

Figure 4.57: Total nitrogen in biomass per liter at each harvest of WT cultivated under greenhouse conditions from October until December 2012. Data (B) are means of four replicate PBRs with error bars indicating SD.

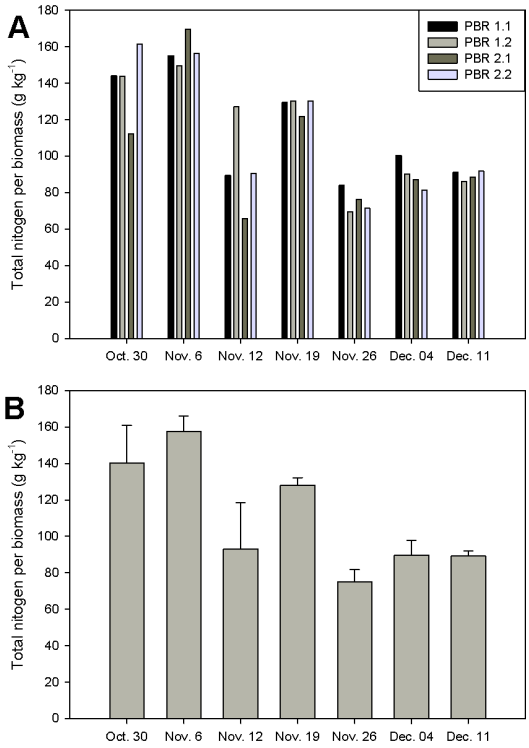

Figure 4.58: Total nitrogen per dry biomass at each harvest of WT cultivated under greenhouse conditions from October until December 2012. Data (B) are means of four replicate PBRs with error bars indicating SD.

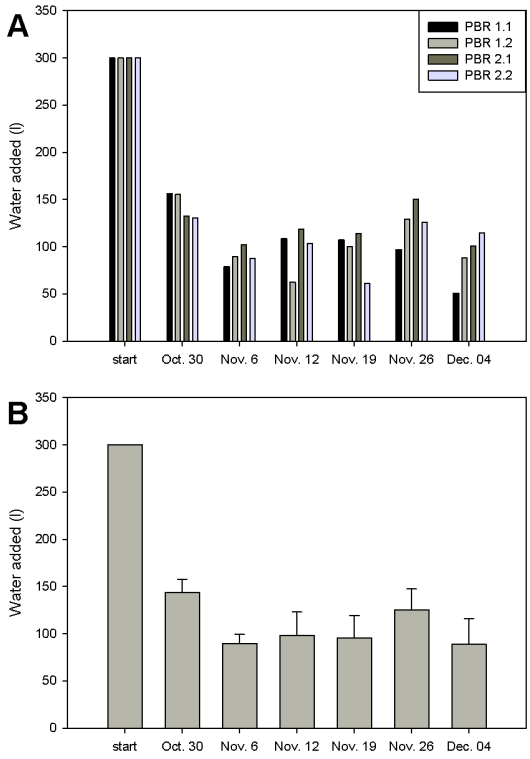

Figure 4.59: Water added during cultivation of WT under greenhouse conditions from October until December 2012. Values from October 30th and onwards show the volume of water needed to fill up each PBR to the starting volume (300 l). Data (B) are means of four replicate PBRs with error bars indicating SD.

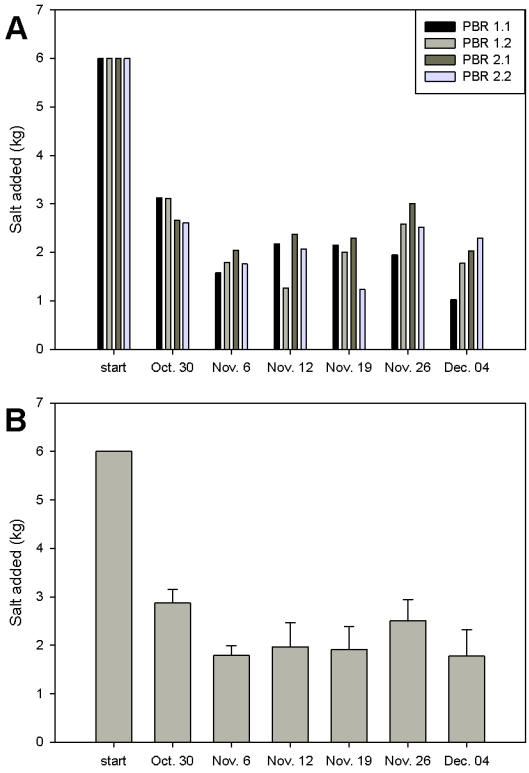

Figure 4.60: Sea salt added during cultivation of WT under greenhouse conditions from October until December 2012. Data (B) are means of four replicate PBR with error bars indicating SD.

On day of harvest the nitrate concentration was measured as a representative compound in the medium to determine the amount of the f/2 nutrient stock solution which needed to be added to reach the initial concentration. The added volume was calculated as a sum of the volume missing in the remaining culture in the PBRs after discarding and the volume needed for the fresh medium with which the PBRs were filled up again or, if it was not a day of harvest then the difference to the initial concentration was added (Fig. 4.61). Therefore values varied strongly between 11 and 223 ml containing 0.5 to 2.5 g NO_3-N.

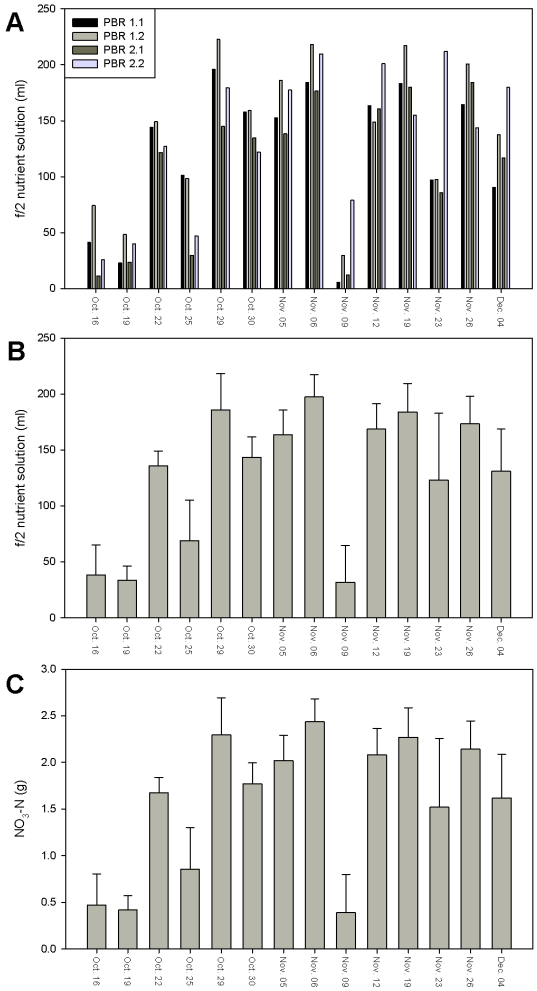

Figure 4.61: Addition of f/2 nutrient stock solution (A and B) and nitrogen (C) during cultivation of WT under greenhouse conditions from October until December 2012. Data (B and C) are means of four replicate PBRs with error bars indicating SD.

Throughout the whole production period 115 g biomass were produced on average per PBR with a content of 3.7 g chlorophyll *a* (Table 4.4). Based on the constructed area, 19 g m^{-2} biomass and 0.62 g m^{-2} chlorophyll *a* were produced. The main components used were needed for the composition of the medium, including 942 l water, 19 kg salt and 2.1 l f/2 nutrient stock solution. Referring the addition of the components to the production of 1 g biomass 8.3 l water, 0.17 kg salt and 18.5 ml f/2 nutrient stock solution were needed. During cultivation and harvest period a biomass production of 450 mg m^{-2} with 12 mg m^{-2} chlorophyll *a* was achieved (Table 4.5). Higher amounts of nitrogen were found in the biomass compared to nitrogen added in f/2 nutrient solution (excluding the added f/2 nutrient solution before first harvest), yet it is unsure if nitrogen was also available in the sea salt as well as how much was available in the fresh water. It is also possible that differences occur due to the use of two different kits. During cultivation an average of 14 l water per day were added to each PBR.

Table 4.4: Total biomass and chlorophyll *a* (Chl *a*) production and total consumption of medium components during cultivation of WT in a greenhouse PBR from October 10th until December 11th, 2012. Data are means of four replicate PBRs (±SD).

	WT
production	
biomass (g PBR^{-1}) / (g m^{-2})	115 (±18) / 19 (±2.9)
Chl *a* (g PBR^{-1}) / (g m^{-2})	3.7 (±0.46) / 0.62 (±0.076)
addition	
water (l PBR^{-1}) / (l $g_{biomass}^{-1}$)	942 (±53) / 8.3 (±0.72)
salt (kg PBR^{-1}) / (kg $g_{biomass}^{-1}$)	19 (±1.1) / 0.17 (±0.014)
f/2 stock solution (l PBR^{-1}) / (ml $g_{biomass}^{-1}$)	2.1 (±0.21) / 18.5 (±3.9)

Table 4.5: Average daily cultivation parameters for WT in a greenhouse PBR from October 28th until December 11th, 2012. Data are means of four replicate PBRs.

average daily	**WT**
biomass (mg l^{-1}) / (mg m^{-2})	8.5 / 450
Chl *a* (mg l^{-1}) / (mg m^{-2})	0.23 / 15
NO_3-N consumption (mg l^{-1}) / (mg m^{-2})	1.4 / 67
N in biomass (mg l^{-1}) / (mg m^{-2})	2.4 / 117
water added (l PBR^{-1})	14

4.2.2 Comparison of WT and npq21

After selecting *npq21* as a promising strain under lab-conditions, it was cultivated in the greenhouse systems in comparison to WT. Both genotypes were cultivated in each greenhouse, *npq21* in PBR 1.1 and PBR 2.1, and WT in PBR 1.2 and PBR 2.2. The inoculation was done end of January 2013 and as the PBRs were filled, data was recorded until end of March 2013. The cultivation conditions were again recorded including PAR as well as sunshine duration and solar radiation (Fig. 4.62) [143], temperature (Fig. 4.64) and pH (Fig. 4.65) of the culture. Higher PAR values were recorded in March with a peak value of 19 mol m^{-2} d^{-1}, whereas highest sunshine duration reached about 600 min d^{-1} and solar radiation 2,800 Wh m^{-2} d^{-1}, while day length increased throughout the cultivation period from ≈9.5 up to 12 h (Fig. 4.63). Temperatures varied between 14°C in the night and 32°C (transiently) during the day and pH values varied between 7 and 9.5, showing less variation at the beginning of February and higher variation throughout March.

In Fig. 4.66 the optical densities of the four systems are shown during cultivation and continuous harvest. At the beginning *npq21* showed higher increase in OD compared with WT. Therefore, harvest was performed earlier for *npq21* than for WT, yet in March all four systems had similar OD values and thus harvested on the same days.

On most days of harvest the biomass concentration lied around 0.1 g l^{-1} while on March 6^{th}, 13^{th} and 18^{th} biomass concentrations were about double (Fig. 4.67). Only on three days harvest was performed in parallel for all four PBR, while in most cases only one system was harvested. The aerial production was mostly between 2 and 6 g m^{-2} whereas on the last day it was ≈11 g m^{-2}. A similar picture is found for cell numbers in Fig. 4.68. The number of cells was between 3 and 9 x 10^9 cells l^{-1}. The chlorophyll *a* content in the culture ranged from 2.7 to 7 mg l^{-1} with higher values measured on the days when all PBRs were harvested (Fig. 4.69). The chlorophyll *a* content in the biomass ranged from 20 to 50 mg kg^{-1} with higher content in February and lower in March (Fig. 4.70).

During harvest 100 to 150 l of water were discarded and the PBRs needed to be filled up again with the same volume of fresh water (Fig. 4.71). This led to an addition of salt of 2 to 3 kg per refilling (Fig. 4.72) and an addition of 180 to

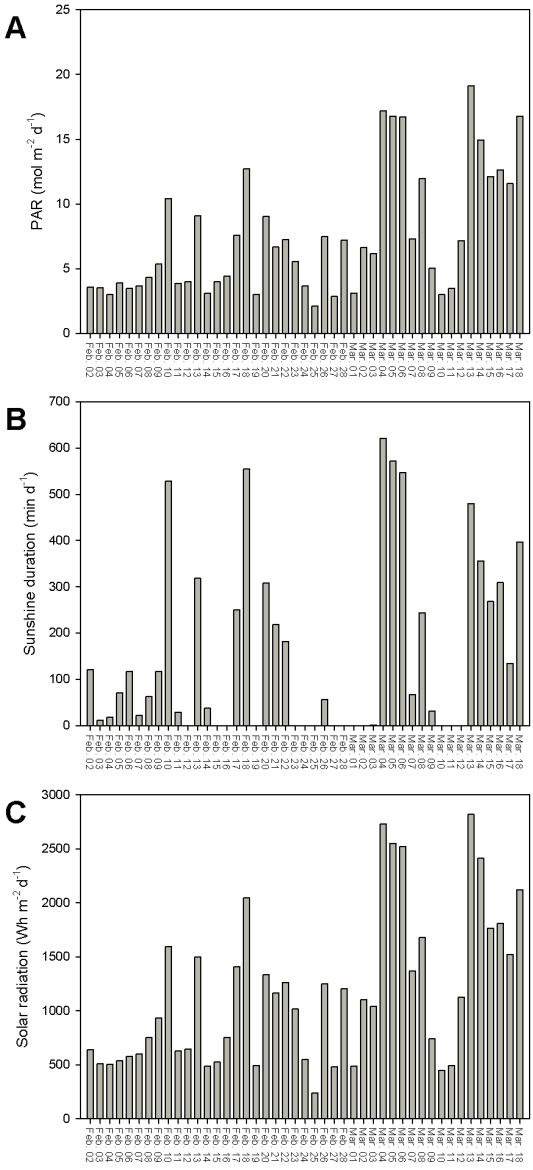

Figure 4.62: Changes in daily light in greenhouse from February until March 2013. Photosynthetic active radiation (PAR) (A), sunshine duration (B) and solar radiation (C) [143].

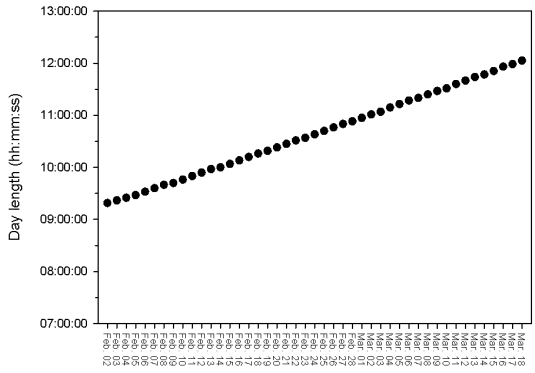

Figure 4.63: Changes in day length in Jülich (Germany) from February until March 2013 [143].

300 ml f/2 nutrient stock solution containing less than one to over 3 g NO_3-N (Fig. 4.73).

For the entire duration of the cultivation period slightly more biomass was produced by *npq21* (164 g) compared to WT (146 g) and therefore a slightly higher aerial productivity of 26 g m^{-2} in *npq21* in comparison to 24 g m^{-2} in WT (+8%; Table 4.6). Higher chlorophyll *a* was produced in total by the *npq21* culture (3.6 g or 0.60 g m^{-2}) whereas WT produced 3.3 g (0.55 g m^{-2}). Higher productivity also resulted in greater consumption of nutrients for *npq21* compared to WT. The average daily PAR was 7.5 mol m^{-2} during cultivation and harvest period. Slightly higher daily biomass and chlorophyll *a* production was achieved by *npq21* compared to WT (Table 4.7). Higher amounts of nitrogen were found in the biomass compared to nitrogen added in f/2 nutrient solution as in Table 4.5, assuming the same reasons as mentioned before for cultivation of WT including additional nitrogen sources as sea salt and fresh water as well as differences due to the utilization of two different kits. For cultivation of WT 23 l water were added to each 300 l PBR per day, whereas for *npq21* water addition was 26 l.

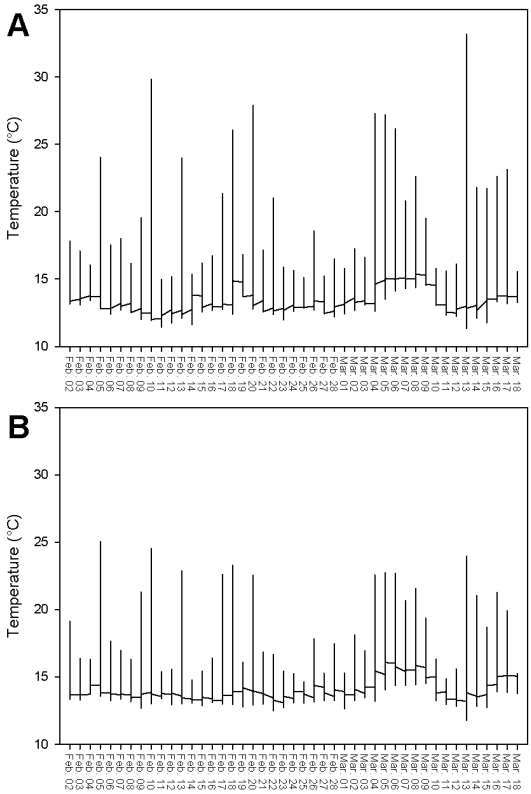

Figure 4.64: Changes in temperature of WT (A) and *npq21* (B) culture under greenhouse conditions from February until March 2013. Data are means of two replicate PBRs.

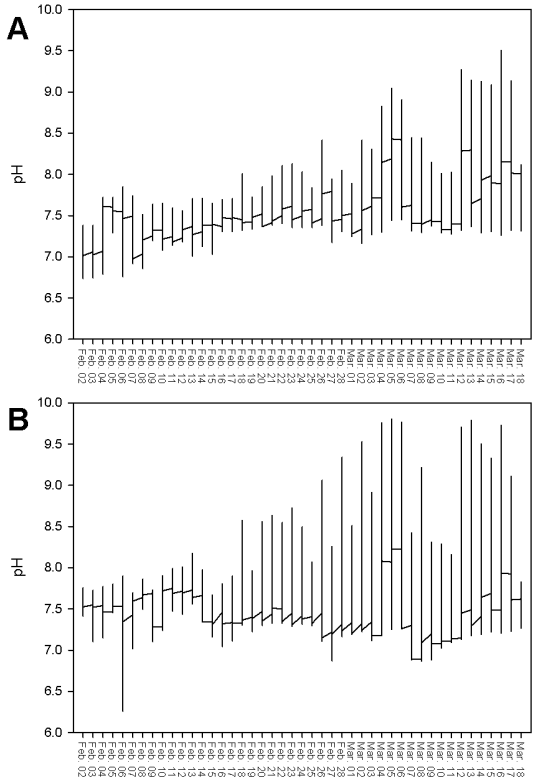

Figure 4.65: Changes in pH of WT (A) and *npq21* (B) culture cultivated under greenhouse conditions from February until March 2013. Data are means of two replicate PBRs.

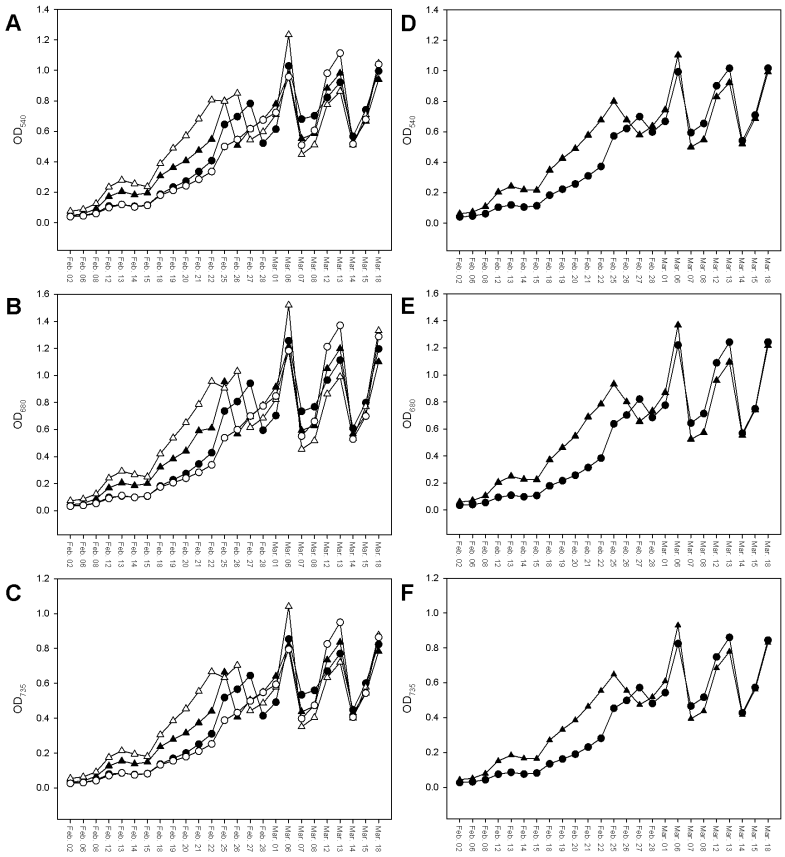

Figure 4.66: Changes in optical density monitored at 540 nm (OD_{540}) (A and D), 680 nm (OD_{680}) (B and E) and 735 nm (OD_{735}) (C and F) under greenhouse conditions from February until March 2013 of PBR 1.1 *npq21* (black triangles), PBR 1.2 WT (black circles), PBR 2.1 *npq21* (white triangles), PBR 2.2 WT (white circles) and means of WT (black circles) and *npq21* (black triangles). Data (D-F) are means of two replicate PBRs.

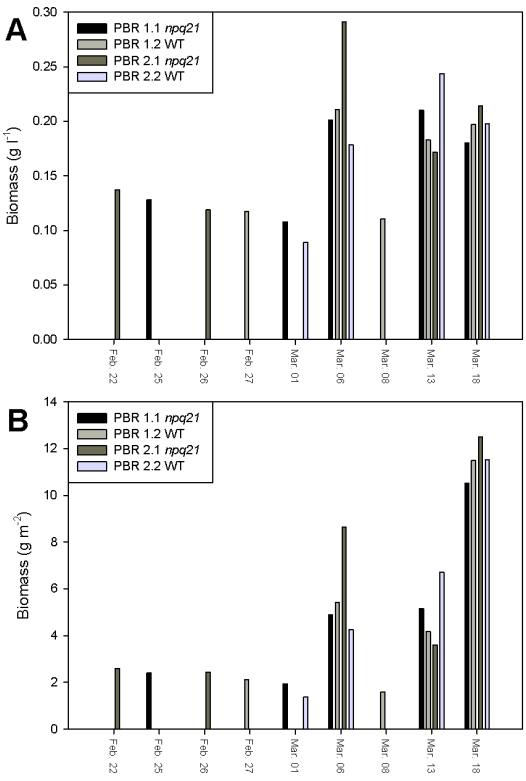

Figure 4.67: Biomass dry weight per liter (A) or area (B) at each harvest of WT and *npq21* cultivated under greenhouse conditions from February until March 2013.

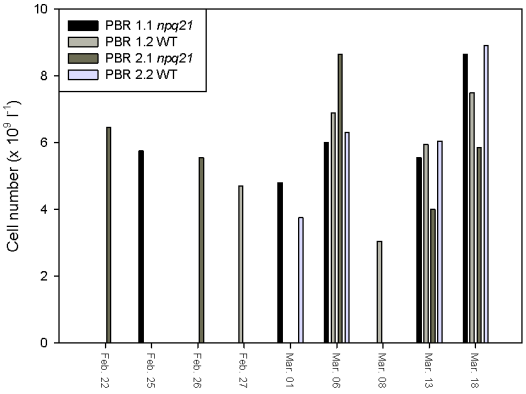

Figure 4.68: Cell number per liter at each harvest of WT and *npq21* cultivated under greenhouse conditions from February until March 2013.

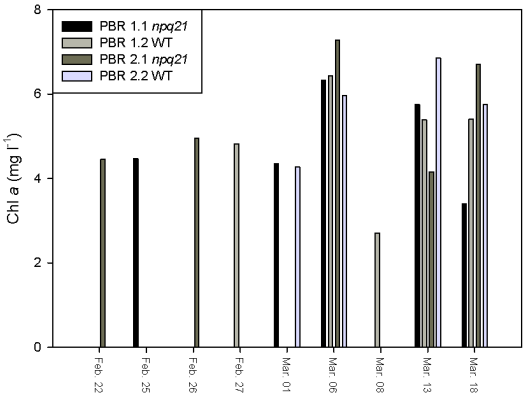

Figure 4.69: Chlorophyll *a* (Chl a) content per liter at each harvest of WT and *npq21* cultivated under greenhouse conditions from February until March 2013.

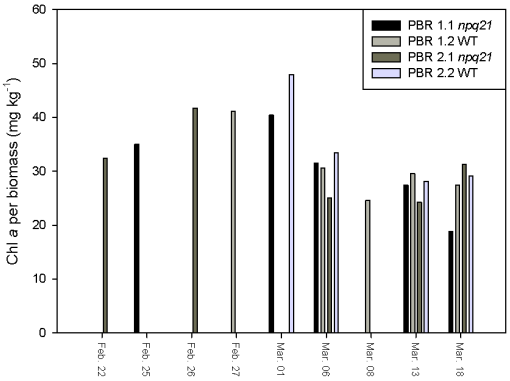

Figure 4.70: Chlorophyll *a* (Chl *a*) in dry biomass at each harvest of WT and *npq21* cultivated under greenhouse conditions from February until March 2013.

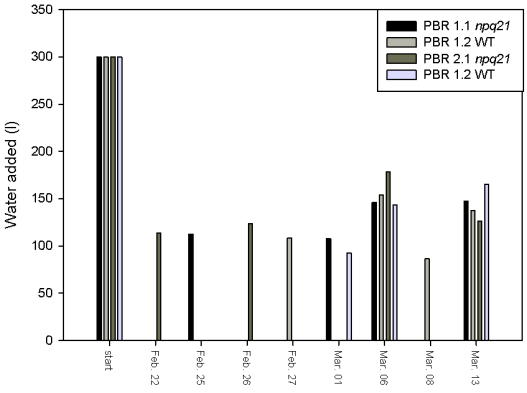

Figure 4.71: Water added during cultivation of WT and *npq21* under greenhouse conditions from February until March 2013.

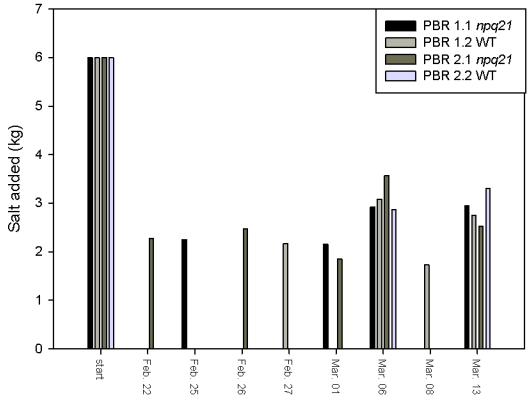

Figure 4.72: Sea salt added during cultivation of WT and *npq21* under greenhouse conditions from February until March 2013.

Table 4.6: Total biomass and chlorophyll *a* (Chl *a*) production and consumption of medium components for WT and *npq21* from January 31st until March 18th, 2013. Data are means of two replicates.

	WT	***npq21***
production		
biomass (g PBR^{-1}) / (g m^{-2})	146 / 24	164 / 27
Chl *a* (mg/PBR^{-1}) / (g m^{-2})	3.3 / 0.55	3.6 / 0.60
addition		
water (l PBR^{-1}) / (l $g_{biomass}^{-1}$)	896 / 4.1	976 / 4.1
salt (kg PBR^{-1}) / (kg $g_{biomass}^{-1}$)	20 / 0.14	22 / 0.13
f/2 stock solution (l PBR^{-1}) / (ml $g_{biomass}^{-1}$)	1.7 / 11.5	1.8 / 11.6

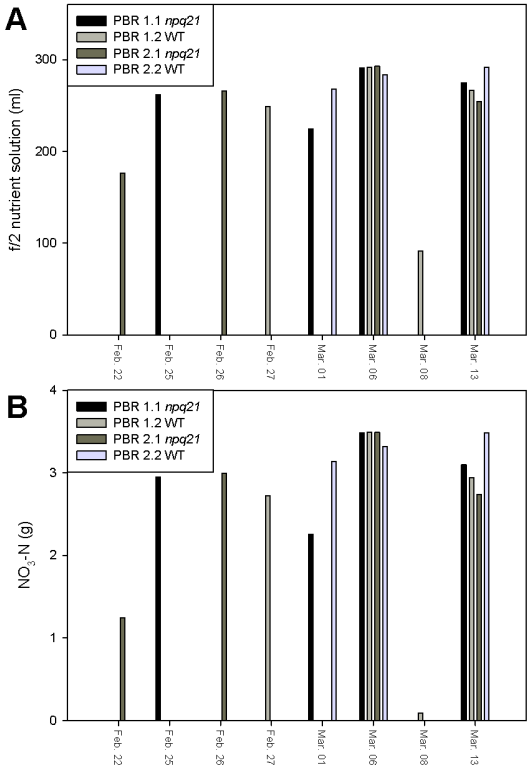

Figure 4.73: Addition of f/2 nutrient stock solution during cultivation of WT and *npq21* under greenhouse conditions from February until March 2013.

Table 4.7: Average daily cultivation parameters for WT and *npq21* per PBR from February 21st until March 18th, 2013. Data are means of two replicate PBRs.

average daily	**WT**	***npq21***
PAR (mol m^{-2})	7.5	7.5
biomass (mg l^{-1}) / (g m^{-2})	19 / 0.94	21 / 1.1
Chl *a* (mg l^{-1}) / (mg m^{-2})	0.42 / 21	0.46 / 23
NO_3-N consumption (mg l^{-1}) / (mg m^{-2})	1.8 / 92	2.0 / 103
N in biomass (mg l^{-1}) / (mg m^{-2})	2.0 / 101	2.4 / 119
water added (l PBR^{-1})	23	26

5 Discussion

5.1 Laboratory experiments

5.1.1 Circadian and light control of chlorophyll accumulation and growth in N. gaditana

The growth of *N. gaditana*, as assessed by measurements of OD_{680} and OD_{735}, was confined to the light periods; the OD_{680} and OD_{735} values never increased, or even decreased, during the dark periods (Figs. 4.1, 4.7, 4.10 and 4.11). Thus, the growth of *N. gaditana* is a function of light duration, as has been described for *N. oceanica* cultivated in greenhouse photobioreactors [144]. It appears that chlorophyll accumulation and growth processes, which give rise to an increase in OD_{680} and OD_{735} in *N. gaditana* cultures, are regulated by light and/or require assimilates provided by photosynthesis. On the other hand, persistent oscillation could be observed at least in the first 24 h after switching to the LL conditions, especially for OD_{680} (Figs. 4.7 and 4.8), suggesting endogenous regulation of the processes. Oscillations of OD_{680} were found in the first 24 h in LL even when the algae were entrained to the 18 h/6 h LD cycle (Fig. 4.10). The time courses of OD_{680} in both 12 h/12 h and 18 h/6 h LD cycles, i.e. rapid increase in the first half of the light period followed by slowing down in the second half and no increase during the dark period (Fig. 4.1, Table 4.1), most likely arise from the interactions between the external conditions (LD cycles) and internal regulation of algae.

The circadian clocks allow organisms to synchronize physiological and metabolic processes (and also behavioral patterns) to daily environmental cycles [48]. Persistent oscillation in constant light and temperature conditions are a hallmark of circadian processes. In photosynthetic organisms such "free-running" oscillations continuing for several days have been demonstrated, e.g. for rhythmic gene expression of the *kaiBC* reporter in *Synechococcus elongatus* [50] or light-harvesting

antenna complex *Lhcb1.1* (also called *cab2*) and catalase *CAT3* in *A. thaliana* [49]. In the case of *Arabidopsis* stomatal conductance and CO_2 assimilation in leaves also exhibit free-running oscillations in LL [145]. In contrast, rhythmic changes in OD_{680} faded away in *N. gaditana* after 24 h in LL (Fig. 4.7). The continuous illumination with red + blue LED may not be optimal for monitoring OD_{680} oscillation in *N. gaditana*; compared with red + blue LL, strong oscillation of OD_{680} continued longer (for >50 h) in blue LL, albeit not in red LL (Figs. 4.11 and 4.12). Furthermore, oscillations of OD_{680} and OD_{735} were detectable for >50 h even in red + blue LL when the algae were growing slowly (10-15% of the growth rates in Figs. 4.7 and 4.8). Thus, growth enhancement in LL may have obscured the endogenous oscillations in the experiments in Figs. 4.7 and 4.8. This is reminiscent of the previous report in the green macroalga *Ulva pseudocurvata*, in which rhythmic growth of thalli could be observed for 3-4 days at low growth rates in constant darkness, whereas the rhythmicity quickly vanished in constant light [146]. These findings are also in line with the notion that cells cannot maintain circadian rhythms when they divide more than once a day [50].

Circadian oscillation of δ-aminolevulinic acid (δ-ALA) accumulation, which is an early regulatory step in chlorophyll biosynthesis, has been reported in leaves of *Hordeum vulagare* (barley) under LL, with pronounced δ-ALA accumulation during the subjective night and a gradual decline concomitant with a chlorophyll increase during the subjective day [147, 148]. In these studies the amplitude of rhythmic oscillation of the δ-ALA level diminished during the first 24 to 48 h in LL, in much the same way as seen for OD_{680} in *N. gaditana* in the present study (Figs. 4.7 and 4.11). The circadian clocks in flowering plants are supposed to coordinate synthesis of chlorophylls and chlorophyll-binding proteins (especially light-harvesting antenna complexes) by regulating the accumulation of chlorophyll precursor δ-ALA [147, 148] and *Lhc* gene expression that peaks at early to mid-morning [52, 147, 149, 150]. In addition, the light-dependent reduction of protoChlide to Chlide catalized by the enzyme NADPH:protoChlide oxydoreductase (POR) represents an environmental control step to suppress chlorophyll synthesis in the dark, although the light-independent POR found in photosynthetic bacteria, algae and gymnosperms can catalyze the same reaction in the dark [151]. While circadian regulation of *Lhc* gene expression awaits demonstration in *Nannochloropsis*, it has been reported in the green microalga *C. reinhardtii* [152, 153]. Interestingly,

N. gaditana does show diurnal increase in cellular chlorophyll *a* content [87], as do natural phytoplankton populations [154]. Furthermore, the draft genome sequence of *N. gaditana* contains two gene models for light-dependent, nuclear-encoded POR but two out of the three subunits of the light-independent, plastid-encoded POR are missing [44]. The results showing the strictly diurnal increase of OD_{680} and OD_{735} in LD cycles and persistent oscillation of OD_{680} in LL support both circadian and light control of chlorophyll accumulation and growth in *N. gaditana*.

The slope of OD_{680} declined in all treatments after 12 h in LL (the light period III; Figs. 4.7 and 4.8), which falls on the first subjective night, assuming resetting of the clock by light-on. The capacity of *N. gaditana* to grow and accumulate chlorophyll in the period III was no more than 50% of the control, regardless of the timing to switch to LL during the last dark period (Fig. 4.8B). Hence, the processes associated with OD_{680} increase, which normally take place in the light period of LD cycles (Figs. 4.1A and 4.7A), are likely programmed to synchronize with the daylight and photosynthesis, hence not for the subjective night. The slightly lower increase in OD_{680} found in the period II after switching to LL at ZT15 (Fig. 4.8A) may be indicative of strong suppression of these processes in the early night. In flowering plants the expression of *Lhc* genes is the lowest in the early night [52, 149]. The correlation between the onset of LL during the dark period and the recovery in the period IV (Fig. 4.8) seems to reflect different "phase shifts" [48] induced by clock resetting with respect to the original LD phases; the larger the phase shift (e.g. ZT15), the greater the OD_{680} increase in the second subjective day. The OD_{680} oscillation in LL was not accompanied by rhythmic changes in the PS II quantum yield (Fig. 4.9), underscoring the dominant effect of light environment on photosynthetic electron transport ("light" reactions), as opposed to the circadian oscillation described for leaf stomatal conductance and gas exchange [145].

Besides chlorophyll accumulation, cell division and growth are also under the circadian control in many photosynthetic organisms, such as *Synechococcus PCC* 7942 [57], *C. reinhardtii* [56], diatom *Skeletonema costatum* [155], macroalgae *U. pseudocurvata* [146] and *Porphyra umbilicalis* [156], or hypocotyl and leaves of *A. thaliana* [51, 53, 157, 158]. The studies in macroalgae [146, 156] and leaves of different dicotyledonous plants [159, 160] have shown that the timing of the highest growth in LD cycles can vary substantially between different species. Nevertheless,

mitosis occurs predominantly during the dark periods in both macroalgae *U. pseudocurvata* and *P. umbilicalis* [146, 156] as well as in shoots of different plant species [55], which coincides with the timing of mitotic activities in *C. reinhardtii* [56] or *Euglena gracilis* [161].

Although neither OD_{680} nor OD_{735} increased in the dark in our experiments (Fig. 4.1), cell number can increase in *N. gaditana* cultures during the dark period (supplementary Fig. 7.1; [87]) or at the beginning of the light period [162]. Despite the reasonable correlations with the cell number (Fig. 4.2B and 4.3), it thus seems that OD_{680} and OD_{735} of *N. gaditana* are strongly influenced by cellular compounds that accumulate during the light period, such as pigments, proteins, sugars and lipids [87]. By analogy with starch which serves as transient carbohydrate storage and for which circadian turnover has been described in *Arabidopsis* leaves [53, 54], turnover of triacylglycerides in *N. gaditana* may well be subject to the circadian clock regulation. Whether the much weaker oscillation of OD_{735} compared to OD_{680} (Fig. 4.12, Table 4.1) is due to the relatively poor signal-to-noise ratio of OD_{735} and/or a minor impact of the circadian clock on the cellular processes/constituents detected at OD_{735} is yet to be clarified.

5.1.2 Distinct effects of blue and red light on N. gaditana

Light signal input for clock entrainment is conferred by photoreceptors, such as the blue-light photoreceptor cryptochromes and the red-light photoreceptor phytochromes in plants [49]. Clock resetting by blue as well as red light has been documented for circadian phototaxis of *C. reinhardtii* [163, 164]. However, involvement of phytochrome for red-light signaling seemed unlikely in this green alga because far-red light did not reverse the action [164]. In fact, no phytochrome-like gene sequence was found in the *Chlamydomonas* genome, whereas two putative cryptochromes and another blue-light photoreceptor phototropin have been identified [62]. The genomes of the marine diatoms *P. tricornutum* and *Thalassiosira pseudonana*, to which *N. gaditana* is more closely related than to *Chlamydomonas*, contain seven or eight putative blue-light photoreceptors of the cryptochrome/photolyase family and four blue-light regulated transcription factors aureochromes [104]. Interestingly, *P. tricornutum* and *T. pseudonana* seem to have a new variant of phytochrome-like red-light photoreceptor [104].

In the present study the oscillation of OD_{680} was more pronounced after switching to blue LL than red LL at both ZT0 and ZT15 (Figs. 4.11 and 4.12). Moreover, the increase in the OD values was larger in blue LL, indicating better growth of *N. gaditana* in blue light than in red light [165]. While a role of photosynthesis in clock entrainment has been postulated for illuminated cells of *C. reinhardtii* [163], the data of PS II efficiency (Fig. 4.13) can explain neither the stronger oscillation nor the enhanced growth in blue LL. Rather, the decreasing PS II quantum yield measured during the blue-LL treatment appears to be a result of an increasing reduction state of the Q_A in PS II due to greater absorption of blue light by PS II compared to PS I and/or higher susceptibility of PS II to photoinhibition and photo-damage under continuous blue light than continuous red light.

The genome analysis of *N. gaditana* [44] will reveal potential blue-light photoreceptors and the presence or absence of phytochrome-like genes in this alga. Since blue light is prevailing in aquatic environments [104], blue-light photoreceptors may play an important role for growth and survival of algae. The strong and persistent oscillation of OD_{680} found in *N. gaditana* under constant blue light (Fig. 4.11) invites further investigations.

The carotenoid to chlorophyll ratios showed significantly higher values for vaucheriaxanthin (Fig. 4.14) as well as for the total carotenoids (Fig. 4.15) after switching to blue light compared to red light at ZT0, suggesting a higher need of these pigments. This is reminiscent of increased carotenoid accumulation relative to chlorophyll found in species of *Leptolyngby* under blue light [166] or higher levels of xanthophyll-cycle pigments observed in the diatom *P. tricornutum* under blue light [167]. Blue light-induced upregulation of gene expression for carotenogenic enzymes has been found in *C. reinhardtii* [168], which also supports the link between blue light illumination and carotenoid accumulation. In contrary, no vaucheriaxanthin was detected after switching to blue light in early night (at ZT15), although the three replicate chromatograms showed a peak putatively identified as vaucheriaxanthin ester, indicating accumulation in lower quantity. Blue light illumination during subjective night may suppress vaucheriaxanthin accumulation in *N. gaditana*. Further investigation is needed for a better understanding of interactions between blue light, circadian clock and carotenoid metabolism.

5.1.3 Growth of NPQ mutants

5.1.3.1 Light regimes

Light is essential for growth of microalgae as light energy is needed for photosynthetic processes [66]. Depending on the design of a photobioreactor for large-scale production, algae can be exposed to fluctuating light conditions by circulation of the culture between the high light exposed outside layer and the light-limited inside layer [169]. To select algae which can outperform WT under such conditions, two NPQ mutants of *N. gaditana*, *npq3* and *npq21*, were selected by the collaboration partner at University of Verona based on their lower NPQ values compared to the WT (Fig. 4.16); reduced heat dissipation capacities in these mutants could potentially allow better light use efficiency and growth [170] provided that they can cope with fluctuating light and other environmental changes. In order to assess the growth performance of *npq3* and *npq21* mutants under variable conditions, these genotypes were cultivated in photobioreactors along with WT under different light and temperature regimes in this study.

Cultivation under LD cycles with either constant light or fluctuating light led to increase in OD during the light periods and constant to slightly decreasing OD values during the night (Fig. 4.17), confirming the strict dependence of growth on light as seen in the experiments with 12 h/12 h and 18 h/6 h LD cycles (Fig. 4.1). The OD_{680} and OD_{735} values were higher most of the time under constant LD than under fluctuating LD, suggesting more efficient utilization of light energy in growth under constant light, despite lower amount of photons available. When comparing the genotypes with each other, *npq21* showed slightly larger increase in OD_{680} compared to WT (Fig. 4.18), whereas *npq3* showed lower values. As found for *npq21*, xanthophyll cycle mutants of *Chlamydomonas* showed no impairment of growth compared to the wild type under various light conditions [101], whereas *npq3* showed some impairment. Similar results were found under continuous light, where *npq3* showed less increase in OD values, indicating its smaller energy utilization capacity for growth (Fig. 4.32). No differences were found for PS II quantum yield under LD cycles between the genotypes or between constant and fluctuating light (Figs. 4.20 and 4.21), suggesting equal PS II efficiencies under these conditions.

Unlike under LD cycles, however, constant LL led to similar PS II quantum yields for *npq21* and WT, whereas the values for *npq3* were obviously lower (Fig. 4.34). This is in accordance with the lower OD values found in this mutant under constant LL. The mutation in *npq3* seems to impair not only the NPQ capacity but also the capacity to maintain high PS II activity in LL, resulting in reduced growth capacity.

A pigment trait of *N. gaditana* is the absence of chlorophyll *c* and *b*; chlorophyll *a* is the only form of chlorophyll in this alga [40, 74, 171] (Fig. 3.1). Violaxanthin is a major carotenoid in *Nannochloropsis* [74, 172] showing far higher concentrations compared with vaucheriaxanthin, antheraxanthin or β-carotene (Fig. 4.22). Violaxanthin as well as vaucheriaxanthin (including its ester) are of importance for light harvesting [40, 173], with a violaxanthin-chlorophyll *a* protein complex being the major light harvesting complex in *Nannochloropsis* [78]. Besides functioning for light harvesting, it appears that violaxanthin can also provide photoprotection after de-epoxidation to antheraxanthin under high light, as it is described in the violaxanthin cycle [40]. The unknown peaks found in the chromatograms are likely vaucheriaxanthin-ester (Fig. 3.1), as have been found in *Nannochloropsis* [74, 173] and generally in Eustigmatophyceae [174]. Under fluctuating LD higher mean carotenoid to chlorophyll ratios, though statistically not significant, were found for WT and *npq3* (Fig. 4.24), as has been reported also for *H. pluvialis* under high light [175], suggesting enhanced need for protection against photooxidative stress [176]. *npq21* showed similar carotenoid to chlorophyll ratios under both treatments, which, however, were always higher compared with WT. The increased accumulation of carotenoid pigments may have allowed this mutant to better cope with photooxidative stress and outperform WT under the fluctuating light conditions. In *N. gaditana* the violaxanthin cycle operates to provide photoprotection under changing environments [40, 171]. Under non-stressful constant LD conditions no antheraxanthin or zeaxanthin was found in WT (Fig. 4.22), whereas under fluctuating LD accumulation of antheraxanthin was detected. Antheraxanthin is an intermediate pigment in the xanthophyll cycle, which is produced by deepoxidation of violaxanthin or epoxidation of zeaxanthin [90]. The accumulation of antheraxanthin in both mutants under constant and fluctuating LD conditions may suggest higher degrees of light stress perceived by these mutants. Constitutive accumulation of antheraxanthin was found in *npq2* mutants of *C. reinhardtii* and this has been associated with an impaired activity of zeaxanthin epoxidase [176]. Given the

presence of a large amount of violaxanthin and the lack of zeaxanthin (Fig. 4.22), however, the enzyme zeaxanthin epoxidase must have been functional in the *npq21* and *npq3* mutants. Detection of antheraxanthin in all genotypes under constant or fluctuating LL (Fig. 4.35) also indicates functional but lower apparent activity of zeaxanthin epoxidase under these conditions.

Chlorophyll content per biomass was similar for all genotypes under constant light whereas under fluctuating LD significantly lower mean values were found for the mutants (Fig. 4.26). Pale green phenotypes under high light were also found for *Chlamydomonas* WT, *npq1* and *npq2* [101] or *H. pluvialis* [175]. The reduction in chlorophyll per biomass was accompanied by the lower chlorophyll content per cell for *npq3*, as described by [40] for *N. gaditana* under high light treatment, yet not for *npq21* (Fig. 4.29). Although this may imply that cells of *npq21* were larger under fluctuating LD, it should be noted that the cell number data may not be reliable given the high variability, possibly due to different cell division stages occurring during cell counting (Fig. 4.28). Based on carotenoid to chlorophyll ratios, light-induced stress is similar under constant LL with continuous or fluctuating light, except for *npq3* in which a higher carotenoid to chlorophyll ratio was measured under constant LL (Fig. 4.37). The chlorophyll content per cell showed no difference for WT and *npq3*, whereas *npq21* showed lower chlorophyll content under constant LL, suggesting bleaching or less accumulation of chlorophyll. Under fluctuating LL, on the other hand, *npq21* tended to have higher chlorophyll content per cell than the other two genotypes. This could indicate that *npq21* is able to protect chlorophyll and tolerate photooxidative stress better than WT and *npq3* under fluctuating light.

Interestingly, higher biomass production was found under fluctuating LD than constant LD, especially for WT and *npq21* (Fig. 4.25). The reason for this growth improvement by fluctuating light under LD conditions is unknown and deserves further investigations. *npq21* showed the highest biomass production under fluctuating LL (+30% compared with WT), which, in addition to the chlorophyll content, also points to greater tolerance of this mutant to stress associated with fluctuating LL. Decrease in nitrogen content per biomass shown for several microalgae under high light conditions [177] was confirmed in the three genotypes under fluctuating

LD (Fig. 4.27), indicating reduced uptake of nitrogen relative to carbon assimilation under light stress conditions.

During the different light treatments NPQ values increased in all three genotypes compared to the beginning of the experiment (Figs. 4.30 and 4.31), which demonstrates the ability to upregulate NPQ also in the two mutants. Furthermore, unlike in Fig. 4.16 which was obtained shortly after the arrival of the three genotypes from Verona, only *npq3* showed lower pre-treatment levels of NPQ than WT, whereas the NPQ capacity of *npq21* was found to be comparable with WT. Thus, the phenotypic differences found between *npq21* and WT in this study cannot be explained by different NPQ capacities of these genotypes. As EMS-induced mutants can have several mutations, it is possible that mutation related to a factor other than NPQ led to the better performance of *npq21*. Whatever the mutation(s) contributing to increased growth and tolerance to fluctuating light in *npq21* may be, it can be concluded that NPQ, with its high plasticity and variability under changing environments, may not be an ideal trait by which mutants should be selected for higher biomass production under natural/variable conditions.

5.1.3.2 Temperature regimes

Growth rates of microalgae depend on the temperature [178, 179], thus temperature variations in greenhouses can influence growth of microalgae. On the other hand, when cultivating microalgae in industrial-scale under greenhouse conditions, temperatures are difficult to regulate. Depending on the heating and cooling systems installed, temperatures can rise in summer especially when the sun shines while during winter less sun is common in high-latitude regions, which leads to lower temperatures. Further, temperatures vary between day and night. After the finding of improved performance for *npq21* compared with WT under different light regimes, while *npq3* never showed any growth advantages, only WT and *npq21* were examined further under different temperature regimes which are likely to occur in greenhouses. *npq21* showed less pronounced differences in OD increase between 23°C/15°C and 30°C/23°C than WT (Fig. 4.40). Higher temperatures seem to have little influence on growth of *npq21*, whereas enhanced growth was recorded for WT under 30°C/23°C, although PS II quantum yield of WT was higher under 23°C/15°C (Fig. 4.42). Increasing growth rates from 13°C up to 26°C have been found for *N. salina* [180] and higher growth rates at 30°C compared to 20°C have

also been found for *Ostreopsis ovate* [181]. Further, elevated biomass production has been found for *N. oculata* under 30°C [182]. Also in this study the temperature of 30°C was apparently not impairing growth of *N. gaditana*.

Even though light conditions were the same for all treatments, differences were found in antheraxanthin accumulation. No antheraxanthin was found for WT under 23°C/15°C (Fig. 4.43), as under LD cycles with constant temperature of 23°C (Fig. 4.22), whereas it was found under 30°C/23°C; *npq21* contained antheraxanthin under both temperature treatments (Fig. 4.43). The influence of temperature on the xanthophyll-cycle pigments has been shown in *N. gaditana* Lubián [183] where higher accumulation of antheraxanthin (and zeaxanthin, but in lower quantity) were found under 35°C compared with 25°C. The same was found in *N. gaditana* under 30°C and 23°C [40]. Higher temperature of 40°C has been shown to damage the photosynthetic apparatus [183]. When looking at the carotenoid to chlorophyll ratio, only *npq21* under 23°C/15°C showed an increased value, indicating some kind of stress (Fig. 4.45). Higher temperatures seemed to increase chlorophyll production in the *Nannochloropsis* cells as the concentration was higher under 30°C/23°C for both genotypes (Fig. 4.47), as also reported for other microalgae [179]. These observations are also consistent with the higher growth rates of the two genotypes under 30°C/23°C (Figs. 4.40, 4.41).

The lower cell number under 30°C/23°C (Fig. 4.46), yet similar OD as under 23°C/15°C, indicated larger cell volumes and/or higher chlorophyll content per cell (Fig. 4.47) under higher temperatures. This has also been found for some other microalgae [179, 184].

Summarizing the results from the comparison under variable light and temperature regimes, the highest relative OD_{680} increase was found for *npq21* for all experiments except one, where WT had a slightly higher value under fluctuating LL (Table 4.2), indicating a higher growth performance for *npq21*. On the contrary, *npq3* showed lowest values, presumably due to negative effects of reduced NPQ on the ability to acclimate to changing environments. The carotenoid to chlorophyll ratio varied between the experiments and the genotypes independent of the growth rates (Table 4.3). Because the carotenoid to chlorophyll ratio not only shows a sign of stress (negative attribute) but also reflects the capacity of algae to respond

to the stress (positive attribute), it is difficult to evaluate genotypes based on this parameter without more detailed examination.

5.2 Greenhouse experiments

5.2.1 Production of N. gaditana biomass in the greenhouse PBRs

Up-scaling from laboratory to commercial-scale systems is one of the recent main objectives in studies on algal biomass production. To scale up observations in small PBRs in the laboratory to more realistic conditions, pilot-scale commercial PBRs were setup in greenhouses to test productivity under conditions resembling industrial production sites, which are characterized by natural fluctuations in light and temperature. First, the comparability of the four PBRs (Table 4.4 and 4.5) was checked for the purpose. Variations were mostly attributable to manual harvest which is not as accurate and reproducible as a mechanically controlled and monitored harvest procedure. The volume capacity of the pilot PBRs used in this study was 50 l m^{-2} which is double the volume capacity given for flat panel photobioreactors, but only one third of an open pond or less than one third of a tubular reactor as described in Table 1.4.

The optical density at which the culture of *N. gaditana* was harvested as well as the average optical density during the cultivation were much lower than the values given in the literature as the optimal culture densities for production with *Spirulina* or other microalgae (Tables 1.3 and 1.4, [185]). In the present study high relative growth rates of *N. gaditana* were found at low optical densities in the greenhouse PBRs, due partly to low light availability in late fall and winter time in Germany. Thus, the lower densities were chosen to allow better light penetration and reduce self-shading, which is a major problem in PBRs [95]. The productivity at higher densities (i.e. much higher than the average harvest density of 0.115 g l^{-1} reached during the autumn-winter experiment conducted in this study) needs to be tested during sunnier seasons.

When comparing with the value previously reported for *Nannochloropsis* sp. cultivated in horizontal tube reactors in September in central Italy (Table 1.7), the

productivity measured in the greenhouse PBRs in this study was extremely low (1.2% of the value in central Italy). Considering the different experimental locations and PBR shapes, comparability of the productivity data is not given. Yet, further investigations are needed to check if changed growth conditions, e.g. higher densities used during cultivation, would lead to higher productivities as given in the literature.

The water footprint of 8.3 l $g_{biomass}^{-1}$ could be reduced by a longer production period as well as by recycling water by e.g. using a centrifuge [5, 10, 23, 26, 135] for separation of biomass and medium which could then be transferred back into the PBRs. Thereby the costs for nutrient addition could also be reduced; for the experiment in this study, 19 ml of f/2 nutrient stock solution (corresponding to 0.23 g N and 0.021 g P) were needed per gram biomass production because a high proportion of nutrients was discarded at every harvest.

The pH-value increased with increasing culture density (Fig. 4.51) as more CO_2 was taken up by the algae. *Nannochloropsis* is able to grow in a broad pH range from pH 6.5 to 10 [165] so that the pH values stayed within the acceptable region during cultivation in the greenhouse PBRs. Addition of more CO_2 could have had a positive effect on growth provided that enough light was available.

The production of WT in February to March 2013 with October to December 2012 was found to be not comparable, as the conditions were different and the duration of cultivation was shorter for the second experiment. Nevertheless, it is conspicuous that biomass production was clearly higher and also higher biomass densities were reached in February-March than in October-November. The longer light periods in February-March (Fig. 4.63) compared to October-December (Fig. 4.49) may have allowed higher growth (Fig. 4.1; [144]), even though temperatures were lower on most days during February-March. Also, the higher OD values used at harvest in the second experiment, and hence higher biomass concentrations contained in the cultures, could have contributed to higher biomass yield. This would indicate that higher culture density can lead to a higher overall productivity, even though light penetration is reduced. The right balance needs to be found between culture density and light penetration, which would be dependent on the interaction of the different factors of the cultivation conditions.

5.2.2 Comparison between WT and npq21

After cultivation of WT and NPQ mutants under laboratory conditions *npq21* was selected as the promising candidate for higher productivity as it outcompeted *npq3* and often also WT under different light and temperature treatments in the laboratory. The conditions for growth were not optimal as the average PAR was as low as 7.5 mol m^{-2} d^{-1} during the experiment (Table 4.7), but temperatures rising over 23°C (Fig. 4.64) could have improved growth. The pH-values increased with increasing density, yet higher pH-values were reached earlier for *npq21* (Fig. 4.65), suggesting a higher CO_2 uptake and faster culture growth compared to WT (Fig. 4.66). This was also reflected by the higher biomass production of *npq21* throughout the cultivation including higher chlorophyll *a* production (Table 4.6 and 4.7): 12% more biomass was produced by *npq21* compared to WT during 29 days of cultivation between January and March, 2013. The higher production of *npq21* and thus larger harvest volume also led to increased total amounts of water, salt and nutrient stock solution added to the culture, while these additions were nearly the same for both genotypes when expressed for gram biomass production (Table 4.6). These results are basically in line with the observations found under laboratory conditions. Based on the results of this study, it can be said that, under low light conditions in winter, *npq21* achieves higher productivity than WT in commercially available PBRs under greenhouse conditions and is therefore a promising candidate for higher yields in an industrial-scale production. Clearly, the productivity should be tested also under high irradiance and high temperature conditions prevailing in summer. Attempts to evaluate the productivity of *npq21* and WT during the spring-summer 2013 failed due to repeated problems with contamination and infection of the culture in the PBRs. These problems with contamination, common in non-sterile systems outside the laboratory, represent a major challenge for large-scale continuous biomass production with algae.

6 Conclusion and Outlook

Bio-based economy is the new direction in which our society is headed, as fossil resources and agricultural land are limited while global population is increasing. Besides crops, other biomass sources need investigation for optimal production and economic resource utilization. Being an alternative biomass source, algae need to be further improved for "domestication" as production costs, as they currently stand, are too high because of high initial investment and energy input needed for cultivation and low biomass yields from WT strains. *N. gaditana*, containing high amounts of lipids, is an interesting species for biodiesel production.

The results of this study show that chlorophyll accumulation and growth of *N. gaditana* is under the control of both circadian clock and light, as manifested by diurnal increase of OD_{680} and OD_{735} in LD cycles and persistent oscillation of OD_{680} in blue LL, but not in red LL. In comparison to OD_{680}, free-running oscillations could not be clearly recognized for OD_{735} and the PS II quantum yield was determined primarily by light conditions. Understanding the interactions between endogenous regulation (clock) and environmental signals (e.g. light, nutrients, stress) in *N. gaditana* could contribute to development of genetic engineering strategies and cultivation protocols for improved biomass and lipid production in this alga under dynamic outdoor environments.

Similar or improved growth performance was found for the *N. gaditana* mutant *npq21*, compared with WT or *npq3*. The presence of antheraxanthin in both mutants, *npq3* and *npq21*, indicates a possible defect in the violaxanthin cycle or increased level of light-induced stress in these mutants. As violaxanthin was present in large amounts in *npq3* and *npq21*, a functional zeaxanthin epoxidase must have been present. Lower activity of zeaxanthin epoxidase may explain the constitutive accumulation of antheraxanthin. Higher chlorophyll contents per cell under fluctuating light suggest the capacity of *npq21* to activate efficient protection against

photooxidative stress. The improved growth under varying temperatures, especially lower stress symptoms under high temperatures, make *npq21* an interesting candidate for large-scale cultivation in warmer regions, or in greenhouses, where it is difficult to reduce temperatures during intensive solar radiation. Further, the tolerance to fluctuating light, which is unavoidable due to circulation in the PBRs, is another advantageous characteristic of *npq21* for large-scale production in PBRs.

Indeed, the experiments in the PBRs under the greenhouse conditions have confirmed these findings in the laboratory experiments; also in the greenhouse PBRs *npq21* showed higher biomass production in the same period of time under the same conditions compared to WT. This was achieved at the same production costs as WT, based on the equal amounts of water, salt and nutrient solution needed for a unit biomass production. Together, *npq21* seems to have interesting traits, such as high tolerance to changing light and temperature as well as improved biomass yield compared to WT, thus inviting further tests at a larger scale for potential use in industrial biomass or oil production.

It remains to be investigated whether the higher growth and biomass production of *npq21* under stressful light conditions may arise from mutations that are not directly related to NPQ or pigment composition. The metabolic processes and pathways which are suppressed or enhanced in this alga may shed light on its physiology. Given the availability of the genome sequence, rapid sequencing technologies in combination with bioinformatics tools could help identify the mutations in *npq21*, which can then be used, e.g. for genetic engineering. Better understanding of regulatory processes of growth and metabolism within the algal cell, such as the circadian clock, would also be essential to develop strategies for targeted genetic modifications and to optimize cultivation conditions.

Collection of monthly, seasonal or annual data on biomass production and yield of other high-value products are needed, especially for Central Europe where the climate conditions are characterized by long but not too hot days during summer and limited solar radiation and temperature during winter. Despite some technical and climatic bottlenecks, the potential of these photosynthetic microorganisms as producers of fuels, raw materials and high-value products in bio-based economy is high. The quest for optimal strains and cultivation protocols is worth continuing.

7 Supplementary

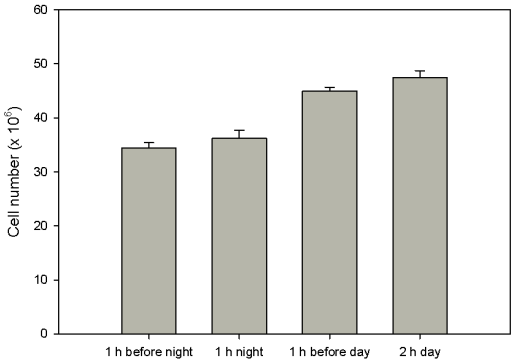

Figure 7.1: Changes in cell number during dark period under the control conditions with 12 h/12 h LD cycles. Data are means of three replicates and error bars indicate SD.

Bibliography

[1] D.G. Ugarte, M.E. Walsh, H. Shapouri, and S.P. Slinsky. The Economic Impacts of Bioenergy Crop Production on U.S. Agriculture. *USDA Agricultural Economic Report*, 2000.

[2] L.M. Brown and K.G. Zeiler. Aquatic Biomass and Carbon-dioxide Trapping. *Energy Conversion and Management*, 34(9-11):1005–1013, SEP 1993.

[3] FAO. The State of Food and Agriculture. *Food and Agriculture Organization of the United Nations*, 2008.

[4] L. Brennan and P. Owende. Biofuels from microalgae - A review of technologies for production, processing, and extractions of biofuels and co-products. *Renewable & Sustainable Energy Reviews*, 14(2):557–577, FEB 2010.

[5] T.M. Mata, A.A. Martins, and N.S. Caetano. Microalgae for biodiesel production and other applications: A review. *Renewable & Sustainable Energy Reviews*, 14(1):217–232, JAN 2010.

[6] M.F. Demirbas. Biofuels from algae for sustainable development. *Applied Energy*, 88(10):3473–3480, OCT 2011.

[7] Y.M. Gong and M.L. Jiang. Biodiesel production with microalgae as feedstock: from strains to biodiesel. *Biotechnology Letters*, 33(7):1269–1284, JUL 2011.

[8] P.M. Foley, E.S. Beach, and J.B. Zimmerman. Algae as a source of renewable chemicals: opportunities and challenges. *Green Chemistry*, 13(6):1399–1405, 2011.

[9] A. Demirbas. Use of algae as biofuel sources. *Energy Conversion and Management*, 51(12):2738–2749, DEC 2010.

[10] C.Y. Chen, K.L. Yeh, R. Aisyah, D.J. Lee, and J.S. Chang. Cultivation, photobioreactor design and harvesting of microalgae for biodiesel production: A critical review. *Bioresource Technology*, 102(1):71–81, JAN 2011.

[11] Y. Chisti. Biodiesel from microalgae. *Biotechnology Advances*, 25(3):294–306, MAY 2007.

[12] S.H. Ho, C.Y. Chen, D.J. Lee, and J.S. Chang. Perspectives on microalgal CO_2-emission mitigation systems - A review. *Biotechnology Advances*, 29(2):189–198, MAR 2011.

[13] E.W. Wilde, J.R. Benemann, J.C. Weissman, and D.M. Tillett. Cultivation of algae and nutrient removal in a waste heat utilization process. *Journal of Applied Phycology*, 3:159–167, JUN 1991.

[14] A. Kumar, S. Ergas, X. Yuan, A. Sahu, Q.O. Zhang, J. Dewulf, F.X. Malcata, and H. van Langenhove. Enhanced CO_2 fixation and biofuel production via microalgae: recent developments and future directions. *Trends In Biotechnology*, 28(7):371–380, JUL 2010.

[15] S.-Y. Chiu, C.-Y. Kao, M.-T. Tsai, S.-C. Ong, C.-H. Chen, and C.-S. Lin. Lipid accumulation and CO_2 utilization of Nannochloropsis oculata in response to CO_2 aeration. *Bioresource Technology*, 100(2):833–838, JAN 2009.

[16] http://protist.i.hosei.ac.jp/pdb/images/Prokaryotes/Oscillatoriaceae/ Oscillatoria/princeps/, Mar. 26th 2013.

[17] B.J. Schmidt, X. Lin-Schmidt, A. Chamberlin, K. Salehi-Ashtiani, and J.A. Papin. Metabolic systems analysis to advance algal biotechnology. *Biotechnology Journal*, 5(7):660–670, JUL 2010.

[18] H. Masukawa, M. Mochimaru, and H. Sakurai. Disruption of the uptake hydrogenase gene, but not of the bidirectional hydrogenase gene, leads to enhanced photobiological hydrogen production by the nitrogen-fixing cyanobacterium Anabaena sp PCC 7120. *Applied Microbiology and Biotechnology*, 58(5):618–624, APR 2002.

[19] R. Radakovits, R.E. Jinkerson, A. Darzins, and M.C. Posewitz. Genetic engineering of algae for enhanced biofuel production. *Eukaryotic Cell*, 9(4):486–501, APR 2010.

[20] Z.T. Wang, N. Ullrich, S. Joo, S. Waffenschmidt, and U. Goodenough. Algal lipid bodies: Stress induction, purification, and biochemical characterization in wild-type and starchless Chlamydomonas reinhardtii. *Eukaryotic Cell*, 8(12):1856–1868, DEC 2009.

[21] D.E. Robertson, S.A. Jacobson, F. Morgan, D. Berry, G.M. Church, and N.B. Afeyan. A new dawn for industrial photosynthesis. *Photosynthesis Research*, 107(3):269–277, MAR 2011.

[22] A.L. Stephenson, E. Kazamia, J.S. Dennis, C.J. Howe, S.A. Scott, and A.G. Smith. Life-cycle assessment of potential algal biodiesel production in the united kingdom: A comparison of raceways and air-lift tubular bioreactors. *Energy & Fuels*, 24:4062–4077, JUL 2010.

[23] Y. Li, M. Horsman, N. Wu, C.Q. Lan, and N. Dubois-Calero. Biofuels from microalgae. *Biotechnology Progress*, 24(4):815–820, JUL 2008.

[24] U. Schmid-Staiger, R. Preisner, W. Trsch, and P. Marek. Kultivierung von Mikroalgen im Photobioreaktor zur stofflichen und energetischen Nutzung. *Chemie Ingenieur Technik*, 81(11):1783–1789, 2009.

[25] M.J. Cooney, G. Young, and R. Pate. Bio-oil from photosynthetic microalgae: Case study. *Bioresource Technology*, 102(1):166–177, JAN 2011.

[26] J.K. Pittman, A.P. Dean, and O. Osundeko. The potential of sustainable algal biofuel production using wastewater resources. *Bioresource Technology*, 102(1):17–25, JAN 2011.

[27] L. Rodolfi, G.C. Zittelli, N. Bassi, G. Padovani, N. Biondi, G. Bonini, and M.R. Tredici. Microalgae for oil: Strain selection, induction of lipid synthesis and outdoor mass cultivation in a low-cost photobioreactor. *Biotechnology and Bioengineering*, 102(1):100–112, JAN 2009.

[28] R. Huerlimann, R. de Nys, and K. Heimann. Growth, lipid content, productivity, and fatty acid composition of tropical microalgae for scale-up production. *Biotechnology and Bioengineering*, 107(2):245–257, OCT 2010.

[29] J.J. Milledge. Commercial application of microalgae other than as biofuels: a brief review. *Reviews In Environmental Science and Bio-technology*, 10(1):31–41, MAR 2011.

[30] S. Singh, S. Arad, and A. Richmond. Extracellular polysaccharide production in outdoor mass cultures of Porphyridium sp in flat plate glass reactors. *Journal of Applied Phycology*, 12(3-5):269–275, OCT 2000.

[31] R. Chaiklahan, N. Chirasuwan, W. Siangdung, K. Paithoonrangsarid, and B. Bunnag. Cultivation of Spirulina platensis using pig wastewater in a semi-continuous process. *Journal of Microbiology and Biotechnology*, 20(3):609–614, MAR 2010.

[32] A. Makri, S. Bellou, M. Birkou, K. Papatrehas, N.P. Dolapsakis, D. Bokas, S. Papanikolaou, and G. Aggelis. Lipid synthesized by micro-algae grown in laboratory- and industrial-scale bioreactors. *Engineering In Life Sciences*, 11(1):52–58, FEB 2011.

[33] J.M. Sandnes, T. Kallqvist, D. Wenner, and H.R. Gislerod. Combined influence of light and temperature on growth rates of Nannochloropsis oceanica: linking cellular responses to large-scale biomass production. *Journal of Applied Phycology*, 17(6):515–525, DEC 2005.

[34] J.Y. An, S.J. Sim, J.S. Lee, and B.W. Kim. Hydrocarbon production from secondarily treated piggery wastewater by the green alga Botryococcus braunii. *Journal of Applied Phycology*, 15(2-3):185–191, MAR 2003.

[35] J.M.S. Rocha, J.E.C. Garcia, and M.H.F. Henriques. Growth aspects of the marine microalga Nannochloropsis gaditana. *Biomolecular Engineering*, 20(4-6):237–242, JUL 2003.

[36] M.M. Rebolloso-Fuentes, A. Navarro-Perez, F. Garcia-Camacho, J.J. Ramos-Miras, and J.L. Guil-Guerrero. Biomass nutrient profiles of the microalga Nannochloropsis. *Journal of Agricultural and Food Chemistry*, 49(6):2966–2972, JUN 2001.

[37] J.K. Volkman, Malcolm R. Brown, G.A. Dunstan, and S.W. Jeffrey. The biochemical composition of marine microalgae from the class Eustigmatophyceae. *Journal of Phycology*, 29:69–78, 1993.

[38] A. Sukenik, J. Beardall, J.C. Kromkamp, J. Kopecky, J. Masojidek, S. van Bergeijk, S. Gabai, E. Shaham, and A. Yamshon. Photosynthetic performance

of outdoor Nannochloropsis mass cultures under a wide range of environmental conditions. *Aquatic Microbial Ecology*, 56(2-3):Int Soc Limnol; Int Assoc Ecol; Grp Aquat Primary Productiv, 2009.

[39] L.M. Lubián, O. Montero, I. Moreno-Garrido, I.E. Huertas, C. Sobrino, M. Gonzalez-del Valle, and G. Pares. Nannochloropsis (Eustigmatophyceae) as source of commercially valuable pigments. *Journal of Applied Phycology*, 12(3-5):249–255, OCT 2000.

[40] M.P. Gentile and H.W. Blanch. Physiology and xanthophyll cycle activity of Nannochloropsis gaditana. *Biotechnology and Bioengineering*, 75(1):1–12, OCT 2001.

[41] L.M. Lubián. Nannochloropsis gaditana sp.nov., una nueva Eustigmatophyceae marina. 4:287–293, 1982.

[42] A. Carrero, G. Vicente, R. Rodriguez, M. Linares, and G. L. del Peso. Hierarchical zeolites as catalysts for biodiesel production from Nannochloropsis microalga oil. *Catalysis Today*, 167:148–153, JUN 2011.

[43] M. Ferreira, P. Coutinho, P. Seixas, J. Fabregas, and A. Otero. Enriching rotifers with "premium" microalgae Nannochloropsis gaditana. *Marine Biotechnology*, 11:585–595, OCT 2009.

[44] R. Radakovits, R.E. Jinkerson, S.I. Fuerstenberg, H. Tae, R.E. Settlage, J.L. Boore, and M.C. Posewitz. Draft genome sequence and genetic transformation of the oleaginous alga Nannochloropis gaditana. *Nature Communications*, 3, FEB 2012.

[45] A. Vieler, G. Wu, C.-H. Tsai, B. Bullard, A.J. Cornish, C. Harvey, I.-B. Reca, C. Thornburg, R. Achawanantakun, C.J. Buehl, M.S. Campbell, D. Cavalier, K.L. Childs, T.J. Clark, R. Deshpande, E. Erickson, A.A. Ferguson, W. Handee, Q. Kong, X. Li, B. Liu, S. Lundback, C. Peng, R.L. Roston, Sanjaya, Jeffrey P. Simpson, A. TerBush, J. Warakanont, S. Zaeuner, E.M. Farré, E.L. Hegg, N. Jiang, M.-H. Kuo, Y. Lu, K.K. Niyogi, J. Ohlrogge, K.W. Osteryoung, Y. S.Shacher-Hill, B.B. Sears, Y. Sun, H. Takahashi, M. Yandell, S.-H. Shiu, and C. Benning. Genome, Functional Gene Annotation, and Nuclear Transformation of the Heterokont Oleaginous Alga Nannochloropsis oceanica CCMP1779. *Plos Genetics*, 8(11), NOV 2012.

[46] R. Jinkerson, R. Radakovits, and M. Posewitz. Genomic insights from the oleaginous model alga Nannochloropsis gaditana. *Bioengineered*, 4:37 – 43, 2013.

[47] R. Radakovits, R. Jinkerson, and M. Posewitz. Use of endogenous promoters in genetic engineering of Nannochloropsis gaditana, APR 2013.

[48] C.S. Pittendrigh. Temporal organization: Reflection of a Darwinain Clock-Watcher. *Annual Review of Physiology*, pages 16–54, 1993.

[49] C.R. McClung. Circadian rhythms in plants. *Annual Review of Plant Physiology and Plant Molecular Biology*, 52, 2001.

[50] L. Suzuki and C.H. Johnson. Algae know the time of day: Circadian and photoperiodic programs. *Journal of Phycology*, 37:933–942, DEC 2001.

[51] E. M. Farré. The regulation of plant growth by the circadian clock. *Plant Biology*, 14:401–410, MAY 2012.

[52] S.L. Harmer, J.B. Hogenesch, M. Straume, H.S. Chang, B. Han, T. Zhu, X. Wang, J. A. Kreps, and S A. Kay. Orchestrated transcription of key pathways in Arabidopsis by the circadian clock. *Science*, 290:2110–2113, 2000.

[53] A. Graf, A. Schlereth, M. Stitt, and A.M. Smith. Circadian control of carbohydrate availability for growth in Arabidopsis plants at night. *Proceedings of the National Academy of Sciences of the United States of America*, 107:9458–9463, MAY 2010.

[54] M. Stitt and S.C. Zeeman. Starch turnover: pathways, regulation and role in growth. *Current Opinion in Plant Biology*, 15:282–292, JUN 2012.

[55] E. Bünning. Über den Tagesrhythmus der Mitosehäufigkeit in Pflanzen. *Zeitschrift für Botanik*, 40:193–199, 1952.

[56] K. Goto and C.H. Johnson. Is the cell-division cycle gated by a circadian clock - the case of Chlamydomonas reinhardtii. *Journal of Cell Biology*, 129:1061–1069, MAY 1995.

[57] T. Mori, B. Binder, and C.H. Johnson. Circadian gating of cell division in cyanobacteria growing with average doubling times of less than 24 hours. *Proceedings of the National Academy of Sciences of the United States of America*, 93:10183–10188, SEP 1996.

[58] D.E. Somers, P.F. Devlin, and S.A. Kay. Phytochromes and cryptochromes in the entrainment of the Arabidopsis circadian clock. *Science*, 282(5393):1488–1490, NOV 1998.

[59] L. Rensing and P. Ruoff. Temperature effect on entrainment, phase shifting, and amplitude of circadian clocks and its molecular bases. *Chronobiology International*, 19:807–864, 2002.

[60] J. Aschoff. Exogenous and endogenous components in circadian rhythms. *Cold Spring Harbor Symposia on Quantitative Biology*, 25:11–28, 1960.

[61] S.S. Golden and S.R. Canales. Cyanobacterial circadian clocks - Timing is everything. *Nature Reviews Microbiology*, 1:191–199, DEC 2003.

[62] M. Mittag, S. Kiaulehn, and C.H. Johnson. The circadian clock in Chlamydomonas reinhardtii. What is it for? What is it similar to? *Plant Physiology*, 137:399–409, 2005.

[63] T. Matsuo and M. Ishiura. Chlamydomonas reinhardtii as a new model system for studying the molecular basis of the circadian clock. *FEBS Letters*, 585:1495–1502, 2011.

[64] S. Hwang, R. Kawazoe, and D.L. Herrin. Transcription of tufA and other chloroplast-encoded genes is controlled by a circadian clock in Chlamydomonas. *Proceedings of the National Academy of Sciences*, 93(3):996–1000, 1996.

[65] T. Kondo, C.A. Strayer, R.D. Kulkarni, W. Taylor, M. Ishiura, S.S. Golden, and C.H. Johnson. Circadian rhythms in prokaryotes: luciferase as a reporter of circadian gene expression in cyanobacteria. *Proceedings of the National Academy of Sciences*, 90(12):5672–5676, 1993.

[66] A.P. Carvalho, S.O. Silva, J.M. Baptista, and F.X. Malcata. Light requirements in microalgal photobioreactors: an overview of biophotonic aspects. *Applied Microbiology and Biotechnology*, 89:1275–1288, 2010.

[67] M. Ballottari, J. Girardon, L. Dall'Osto, and R. Bassi. Evolution and functional properties of photosystem II light harvesting complexes in eukaryotes. *Biochimica Et Biophysica Acta-bioenergetics*, 1817(1):143–157, JAN 2012.

[68] E.J. Boekema, B. Hankamer, D. Bald, J. Kruip, J. Nield, A.F. Boonstra, J. Barber, and M. Rogner. Supramolecular structure of the photosystem II complex from green plants and cyanobacteria. *Proceedings of the National Academy of Sciences of the United States of America*, 92:175–179, JAN 1995.

[69] A. Ben-Shem, F. Frolow, and N. Nelson. Crystal structure of plant photosystem I. *Nature*, 426:630–635, 2003.

[70] E. Gantt. Phycobilisomes. *Annual Review of Plant Physiology*, 32(1):327–347, 1981.

[71] Z.F. Liu, H.C. Yan, K.B. Wang, T.Y. Kuang, J.P. Zhang, L.L. Gui, X.M. An, and W.R. Chang. Crystal structure of spinach major light-harvesting complex at 2.72 angstrom resolution. *Nature*, 428(6980):287–292, MAR 18 2004.

[72] R. Standfuss, A.C.T. van Scheltinga, M. Lamborghini, and W. Kuhlbrandt. Mechanisms of photoprotection and nonphotochemical quenching in pea light-harvesting complex at 2.5A resolution. *EMBO Journal*, 24(5):919–928, MAR 9 2005.

[73] A. Sukenik, A. Livne, A. Neori, Y.Z. Yacobi, and D. Katcoff. Purification and characterization of a light-harvesting chlorophyll-protein complex from the marine Eustigmatophyte Nannochloropsis sp. *Plant and Cell Physiology*, 33(8):1041–1048, DEC 1992.

[74] J.S. Brown. Functional-organization of Chlorophyll a and Carotenoids In the Alga, Nannochloropsis salina. *Plant Physiology*, 83(2):434–437, FEB 1987.

[75] L. Bogorad. Phycobiliproteins and complementary chromatic adaptation. *Annulal review of Plant Physiology and Plant Molecular Biology*, 26:369–401, 1975.

[76] K.S. Kan and J.P. Thornber. Light-harvesting chlorophyll a-b-protein complex of Chlamydomonas-reinhardii. *Plant Physiology*, 57(1):47–52, 1976.

[77] A. Pandit, T. Morosinotto, M. Reus, A.R. Holzwarth, R. Bassi, and H.J.M. de Groot. First solid-state NMR analysis of uniformly 13C-enriched major light-harvesting complexes from Chlamydomonas reinhardtii and identification of protein and cofactor spin clusters. *Biochimica et Biophysica Acta (BBA) - Bioenergetics*, 1807(4):437 – 443, 2011.

[78] A. Sukenik, A. Livne, K.E. Apt, and A.R. Grossman. Characterization of a gene encoding the light-harvesting violaxanthin-chlorophyll protein of Nannochloropsis sp (Eustigmatophyceae). *Journal of Phycology*, 36(3):563–570, JUN 2000.

[79] E. Pfundel and W. Bilger. Regulation and possible function of the violaxanthin cycle. *Photosynthesis Research*, 42(2):89–109, NOV 1994.

[80] W.M. Manning and H.H. Strain. Chlorophyll d, a green pigment of red algae. *Journal of Biological Chemistry*, 151(1):1–19, NOV 1943.

[81] S.W. Jeffrey. Profiles of photosynthetic pigments in ocean using thin-layer chromatography. *Marine Biology*, 26(2):101–110, 1974.

[82] G. Bonente, S. Pippa, S. Castellano, R. Bassi, and M. Ballottari. Acclimation of Chlamydomonas reinhardtii to Different Growth Irradiances. *Journal of Biological Chemistry*, 287(8):5833–5847, FEB 17 2012.

[83] H.H. Strain, W.M. Manning, and G. Hardin. Chlorophyll c (chlorofucine) of diatoms and dinoflagellates. *Journal of Biological Chemistry*, 148(3):655–668, JUN 1943.

[84] J.E.W. Polle, K.K. Niyogi, and A. Melis. Absence of Lutein, Violaxanthin and Neoxanthin Affects the Functional Chlorophyll Antenna Size of Photosystem-II but not that of Photosystem-I in the Green Alga Chlamydomonas reinhardtii. *Plant and Cell Physiology*, 42(5):482–491, 2001.

[85] M. Koller, A. Salerno, P. Tuffner, M. Koinigg, H. Böchzelt, S. Schober, S. Pieber, H. Schnitzer, M. Mittelbach, and G. Braunegg. Characteristics and potential of micro algal cultivation strategies: a review. *Journal of Cleaner Production*, 37(0):377 – 388, 2012.

[86] B. Karlson, D. Potter, M. Kuylenstierna, and R.A. Andersen. Ultrastructure, pigment composition, and 18S rRNA gene sequence for Nannochloropsis granulata sp nov (Monodopsidaceae, Eustigmatophyceae), a marine ultraplankter isolated from the Skagerrak, northeast Atlantic Ocean. *Phycologia*, 35(3):253–260, MAY 1996.

[87] J. Fabregas, A. Maseda, A. Dominguez, M. Ferreira, and A. Otero. Changes in the cell composition of the marine microalga, Nannochloropsis gaditana, during a light : dark cycle. *Biotechnology Letters*, 24(20):1699–1703, OCT 2002.

[88] N.J. Antia and J.Y. Cheng. The keto-carotenoids of two marine coccoid members of the Eustigmatophyceae. *British Phycological Journal*, 17:39–50, 1982.

[89] P. Müller, X.P. Li, and K.K. Niyogi. Non-photochemical quenching. A response to excess light energy. *Plant Physiology*, 125(4):1558–1566, APR 2001.

[90] I. Baroli and K.K. Niyogi. Molecular genetics of xanthophyll-dependent photoprotection in green algae and plants. *Philosophical Transactions of the Royal Society of London Series B-biological Sciences*, 355(1402):1385–1393, OCT 2000.

[91] K.K. Niyogi. Safety valves for photosynthesis. *Current Opinion in Plant Biology*, 3:455–460, 2000.

[92] P. Horton and A. Hague. Studies on the induction of chlorophyll fluorescence in isolated barley protoplasts. IV. Resolution of non-photochemical quenching. *Biochimica et Biophysica Acta (BBA) - Bioenergetics*, 932:107–115, 1988.

[93] K.K. Niyogi, A.R. Grossman, and O. Bjorkman. Arabidopsis mutants define a central role for the xanthophyll cycle in the regulation of photosynthetic energy conversion. *Plant Cell*, 10(7):1121–1134, JUL 1998.

[94] X.P. Li, O. Bjorkman, C. Shih, A.R. Grossman, M. Rosenquist, S. Jansson, and K.K. Niyogi. A pigment-binding protein essential for regulation of photosynthetic light harvesting. *Nature*, 403(6768):391–395, JAN 27 2000.

[95] C. Formighieri, F. Franck, and R. Bassi. Regulation of the pigment optical density of an algal cell: Filling the gap between photosynthetic productivity

in the laboratory and in mass culture. *Journal of Biotechnology*, 162:115–123, 2012.

[96] G. Bonente, F. Passarini, S. Cazzaniga, C. Mancone, M.C. Buia, M. Tripodi, R. Bassi, and S. Caffarri. The Occurrence of the PsbS Gene Product in Chlamydomonas reinhardtii and in Other Photosynthetic Organisms and Its Correlation with Energy Quenching. *Photochemistry and Photobiology*, 84(6):1359–1370, NOV-DEC 2008.

[97] G. Bonente, M. Ballottari, T.B. Truong, T. Morosinotto, T.K. Ahn, G.R. Fleming, K.K. Niyogi, and R. Bassi. Analysis of LhcSR3, a Protein Essential for Feedback De-Excitation in the Green Alga Chlamydomonas reinhardtii. *Plos Biology*, 9(1), JAN 2011.

[98] N.R. Baker. *Chlorophyll fluorescence: A probe of photosynthesis in vivo in Annual Review of Plant Biology*, volume 59 of *Annual Review of Plant Biology*. 2008.

[99] H.Y. Yamamoto, R.C. Bugos, and A. David H. *Biochemistry and Molecular Biology of the Xanthophyll Cycle in The Photochemistry of Carotenoids*, volume 8 of *Advances in Photosynthesis and Respiration*. Springer Netherlands, 2004.

[100] R. Goss and T. Jakob. Regulation and function of xanthophyll cycle-dependent photoprotection in algae. *Photosynthesis Research*, 106(1-2, SI):103–122, NOV 2010.

[101] K.K. Niyogi, O. Bjorkman, and A.R. Grossman. Chlamydomonas xanthophyll cycle mutants identified by video imaging of chlorophyll fluorescence quenching. *Plant Cell*, 9:1369–1380, AUG 1997.

[102] M. Eskling, P.O. Arvidsson, and H.E. Akerlund. The xanthophyll cycle, its regulation and components. *Physiologia Plantarum*, 100:806–816, AUG 1997.

[103] A.M. Gilmore and H.Y. Yamamoto. Time-resolution of the antheraxanthin- and Delta pH-dependent chlorophyll a fluorescence components associated with photosystem II energy dissipation in Mantoniella squamata. *Photochemistry and Photobiology*, 74(2):291–302, AUG 2001.

[104] F.A. Depauw, A. Rogato, M.R. d'Alcala, and A. Falciatore. Exploring the molecular basis of responses to light in marine diatoms. *Journal of Experimental Botany*, 63(4, SI):1575–1591, FEB 2012.

[105] M. Lohr and C. Wilhelm. Algae displaying the diadinoxanthin cycle also possess the violaxanthin cycle. *Proceedings of the National Academy of Sciences of the United States of America*, 96(15):8784–8789, JUL 20 1999.

[106] D. Kirilovsky and A. Wilson. A new photoactive protein acting as a sensor of light intensity: the Orange Carotenoid Protein (OCP). *Photosynthesis Research*, 91(2-3):291–292, FEB 2007.

[107] R. Kana, E. Kotabova, R. Sobotka, and O. Prasil. Non-Photochemical Quenching in Cryptophyte Alga Rhodomonas salina is Located in Chlorophyll a/c Antennae. *Plos One*, 7(1), JAN 3 2012.

[108] B. Wang, Y.Q. Li, N. Wu, and C.Q. Lan. CO_2 bio-mitigation using microalgae. *Applied Microbiology and Biotechnology*, 79(5):707–718, JUL 2008.

[109] J.B.K. Park, R.J. Craggs, and A.N. Shilton. Wastewater treatment high rate algal ponds for biofuel production. *Bioresource Technology*, 102(1):35–42, JAN 2011.

[110] A. Richmond. Efficient utilization of high irradiance for production of photoautotropic cell mass: A survey. *Journal of Applied Phycology*, 8(4-5):381–387, 1996.

[111] F. Lehr and C. Posten. Closed photo-bioreactors as tools for biofuel production. *Current Opinion in Biotechnology*, 20(3):280–285, JUN 2009.

[112] I. Di Termini, A. Prassone, C. Cattaneo, and M. Rovatti. On the nitrogen and phosphorus removal in algal photobioreactors. *Ecological Engineering*, 37(6):976–980, JUN 2011.

[113] A.M. Jawarneh and A.S. Al-Shyyab. Potential of solar energy in zarqa region. *World Academy of Science, Engineering & Technology*, pages 107 – 111, 2011.

[114] W. Duff. Advanced Solar Domestic Hot Water systems: A Report of the Task 14 Advanced Solar Domestic Hot Water Systems Working Group (International Energy Agency (IEA): Solar Heating and Cooling Program), OCT 1996.

[115] http://www.3tier.com/en/support/resource maps/, Mar. 26th 2013.

[116] R.E. Blankenship, D.M. Tiede, J. Barber, G.W. Brudvig, G. Fleming, M. Ghirardi, M.R. Gunner, W. Junge, D.M. Kramer, A. Melis, T.A. Moore, C.C. Moser, D.G. Nocera, A.J. Nozik, D.R. Ort, W.W. Parson, R.C. Prince, and R.T. Sayre. Comparing photosynthetic and photovoltaic efficiencies and recognizing the potential for improvement. *Science*, 332(6031):805–809, MAY 2011.

[117] R.H. Wijffels and M.J. Barbosa. An outlook on microalgal biofuels. *Science*, 329(6006):769–799, NOV 2010.

[118] http://www.climate charts.com/images/, Mar. 26th 2013.

[119] A. Vonshak, A. Abeliovich, S. Boussiba, S. Arad, and A. Richmond. Production of Spirulina biomass - effects of environmental-factors and population-density. *Biomass*, 2(3):175–185, 1982.

[120] X. Li, H.Y. Hu, K. Gan, and Y.X. Sun. Effects of different nitrogen and phosphorus concentrations on the growth, nutrient uptake, and lipid accumulation of a freshwater microalga Scenedesmus sp. *Bioresource Technology*, 101(14):5494–5500, JUL 2010.

[121] H. Hu and K. Gao. Response of growth and fatty acid compositions of Nannochloropsis sp to environmental factors under elevated CO_2 concentration. *Biotechnology Letters*, 28(13):987–992, JUL 2006.

[122] E. Jacob-Lopes, C.H.G. Scoparo, L.M.C.F. Lacerda, and T.T. Franco. Effect of light cycles (night/day) on CO_2 fixation and biomass production by microalgae in photobioreactors. *Chemical Engineering and Processing*, 48(1):306–310, JAN 2009.

[123] A. Richmond and Z. Cheng-Wu. Optimization of a flat plate glass reactor for mass production of Nannochloropsis sp outdoors. *Journal of Biotechnology*, 85(3):259–269, FEB 2001.

[124] P. Carlozzi. Dilution of solar radiation through "culture" lamination in photobioreactor rows facing south-north: A way to improve the efficiency of light utilization by cyanobacteria (Arthrospira platensis). *Biotechnology and Bioengineering*, 81(3):305–315, FEB 2003.

[125] C.U. Ugwu, J.C. Ogbonna, and H. Tanaka. Light/dark cyclic movement of algal culture (Synechocystis aquatilis) in outdoor inclined tubular photobioreactor equipped with static mixers for efficient production of biomass. *Biotechnology Letters*, 27(2):75–78, JAN 2005.

[126] J. Doucha and K. Livansky. Outdoor open thin-layer microalgal photobioreactor: potential productivity. *Journal of Applied Phycology*, 21(1):111–117, FEB 2009.

[127] G.C. Zittelli, F. Lavista, A. Bastianini, L. Rodolfi, M. Vincenzini, and M.R. Tredici. Production of eicosapentaenoic acid by Nannochloropsis sp cultures in outdoor tubular photobioreactors. *Journal of Biotechnology*, 70(1-3):299–312, APR 1999.

[128] D.O. Hall, F.G.A. Fernandez, E.C. Guerrero, K.K. Rao, and E.M. Grima. Outdoor helical tubular photobioreactors for microalgal production: Modeling of fluid-dynamics and mass transfer and assessment of biomass productivity. *Biotechnology and Bioengineering*, 82(1):62–73, APR 2003.

[129] T. Sato, S. Usui, Y. Tsuchiya, and Y. Kondo. Invention of outdoor closed type photobioreactor for microalgae. *Energy Conversion and Management*, 47(6):791–799, APR 2006.

[130] M.E. Huntley and D.G. Redalje. CO_2 mitigation and renewable oil from photosynthetic microbes: A new appraisal. *Mitigation and Adaptation Strategies for Global Change*, 12(4):573–608, DEC 2007.

[131] Y.C. Li, Y.F. Chen, P. Chen, M. Min, W.G. Zhou, B. Martinez, J. Zhu, and R. Ruan. Characterization of a microalga Chlorella sp well adapted to highly concentrated municipal wastewater for nutrient removal and biodiesel production. *Bioresource Technology*, 102(8):5138–5144, APR 2011.

[132] Y.S. Yun, S.B. Lee, J.M. Park, C.I. Lee, and J.W. Yang. Carbon dioxide fixation by algal cultivation using wastewater nutrients. *Journal of Chemical Technology and Biotechnology*, 69(4):451–455, AUG 1997.

[133] E.B. Sydney, W. Sturm, J.C. de Carvalho, V. Thomaz-Soccol, C. Larroche, A. Pandey, and C.R. Soccol. Potential carbon dioxide fixation by industrially important microalgae. *Bioresource Technology*, 101(15):5892–5896, AUG 2010.

[134] J. Yang, M. Xu, X.Z. Zhang, Q.A. Hu, M. Sommerfeld, and Y.S. Chen. Life-cycle analysis on biodiesel production from microalgae: Water footprint and nutrients balance. *Bioresource Technology*, 102(1):159–165, JAN 2011.

[135] A.F. Clarens, E.P. Resurreccion, M.A. White, and L.M. Colosi. Environmental life cycle comparison of algae to other bioenergy feedstocks. *Environmental Science & Technology*, 44(5):1813–1819, MAR 2010.

[136] W. Gerbens-Leenes, A.Y. Hoekstra, and T.H. van der Meer. The water footprint of bioenergy. *Proceedings of the National Academy of Sciences of the United States of America*, 106(25):10219–10223, JUN 23 2009.

[137] N.J. Schmidt. Isolation and characterization of mutants impaired in excess energy dissipation in the Eustigmatophyceae alga Nannochloropsis gaditana. Master's thesis, Rheinische Friedrich-Wilhelms-University of Bonn, July 2012.

[138] S. Berteotti. Domestication of algae to obtain bio-fuel: mutagenesis of Nannochloropsis gaditana and construction of new expression vector. Master's thesis, University of Verona, Italy, 2011.

[139] R.R.L. Guillard. Culture of phytoplankton for feeding marine invertebrates. *In Smith WL, Chanle MH (eds), Culture of Marine Invertebrate Animals, plenum Press, New York*, pages 26–60, 1975.

[140] J. Cerveny, I. Setlik, M. Trtilek, and L. Nedbal. Photobioreactor for cultivation and real-time, in-situ measurement of O_2 and CO_2 exchange rates, growth dynamics, and of chlorophyll fluorescence emission of photoautotrophic microorganisms. *Engineering in Life Sciences*, 9(3):247–253, JUN 2009.

[141] A.M. Gilmore and H.Y. Yamamoto. Resolution of lutein and zeaxanthin using a non-endcapped, lightly carbon-loaded C18 high-performance liquid chromatographic column. *Journal of Chromatography A*, 543(0):137 – 145, 1991.

[142] R.J. Porra, W.A. Thompson, and P.E. Kriedemann. Determination of accurate extinction coefficients and simultaneous-equations for assaying chlorophyll-a and chlorophyll-b extracted with 4 different solvents - verification of the concentration of chlorophyll standards by atomic-absorption spectroscopy. *Biochimica Et Biophysica Acta*, 975(3):384–394, AUG 1989.

[143] A. Knaps. Sunrise and sunset data in Jülich (Germany) from Forschungszentrum Jülich GmbH, Sicherheit und Strahlenschutz (S-UM). MAY 2013.

[144] J.M. Sandnes, T. Ringstad, D. Wenner, P.H. Heyerdahl, I. Kallqvist, and H.R. Gislerod. Real-time monitoring and automatic density control of large-scale microalgal cultures using near infrared (NIR) optical density sensors. *Journal of Biotechnology*, 122(2):209–215, MAR 23 2006.

[145] A.N. Dodd, N. Salathia, A. Hall, E. Kevei, R. Toth, F. Nagy, J.M. Hibberd, A.J. Millar, and A.A.R. Webb. Plant circadian clocks increase photosynthesis, growth, survival, and competitive advantage. *Science*, 309(5734):630–633, JUL 22 2005.

[146] E.A. Titlyanov, T.V. Titlyanova, and K. Luning. Diurnal and circadian periodicity of mitosis and growth in marine macroalgae. II. The green alga Ulva pseudocurvata. *European Journal of Phycology*, 31(2):181–188, MAY 1996.

[147] J. Beator and K. Kloppstech. The circadian oscillator coordinates the synthesis of apoproteins and their pigments during chloroplast development. *Plant Physiology*, 103(1):191–196, SEP 1993.

[148] E. Kruse, B. Grimm, J. Beator, and K. Kloppstech. Developmental and circadian control of the capacity for delta-aminolevulinic acid synthesis in green barley. *Planta*, 202(2):235–241, JUN 1997.

[149] K. Kloppstech. Diurnal and circadian rhythmicity in the expression of light-induced plant nuclear messenger-RNAs. *Planta*, 165(4):502–506, 1985.

[150] A.J. Millar and S.A. Kay. Circadian control of cab gene-transcription and messenger-RNA accumulation in Arabidopsis. *Plant Cell*, 3(5):541–550, MAY 1991.

[151] Y. Fujita. Protochlorophyllide reduction: A key step in the greening of plants. *Plant and Cell Physiology*, 37(4):411–421, JUN 1996.

[152] S.B. Hwang and D.L. Herrin. Control of lhc gene-transcription by the circadian clock in Chlamydomonas-reinhardtii. *Plant Molecular Biology*, 26(2):557–569, OCT 1994.

[153] S. Jacobshagen and C.H. Johnson. Circadian-rhythms of gene-expression in Chlamydomonas-reinhardtii - circadian cycling of messenger-RNA abundances of cab-II, and possibly of -tubulin and cytochrome-c. *European Journal of Cell Biology*, 64(1):142–152, JUN 1994.

[154] C.S. Yentsch and J.H. Ryther. Short-term variations in phytoplankton chlorophyll and their significance. *Limnology and Oceanography*, 2(2):140–142, 1957.

[155] K. Ostgaard and A. Jensen. Diurnal and circadian-rhythms in the turbidity of growing Skeletonema costatum cultures. *Marine Biology*, 66(3):261–268, 1982.

[156] K. Lüning, E.A. Titlyanov, and T.V. Titlyanova. Diurnal and circadian periodicity of mitosis and growth in marine macroalgae .3. The red alga Porphyra umbilicalis. *European Journal of Phycology*, 32(2):167–173, MAY 1997.

[157] K. Nozue and J.N. Maloof. Diurnal regulation of plant growth. *Plant Cell and Environment*, 29(3):396–408, MAR 2006.

[158] T. Ruts, S. Matsubara, A. Wiese-Klinkenberg, and A. Walter. Aberrant temporal growth pattern and morphology of root and shoot caused by a defective circadian clock in Arabidopsis thaliana. *Plant Journal*, 72(1):154–161, OCT 2012.

[159] A. Walter, W.K. Silk, and U. Schurr. Environmental Effects on Spatial and Temporal Patterns of Leaf and Root Growth. *Annual Review of Plant Biology*, 60:279–304, 2009.

[160] T. Ruts, S. Matsubara, A. Wiese-Klinkenberg, and A. Walter. Diel patterns of leaf and root growth: endogenous rhythmicity or environmental response? *Journal of Experimental Botany*, 63(9, SI):3339–3351, MAY 2012.

[161] S. Hagiwara, A. Bolige, Y.L. Zhang, M. Takahashi, A. Yamagishi, and K. Goto. Circadian gating of photoinduction of commitment to cell-cycle transitions in relation to photoperiodic control of cell reproduction in Euglena. *Photochemistry and Photobiology*, 76(1):105–115, JUL 2002.

[162] M.H.F. Henriques and J.M.S. Rocha. Influence of light: dark cycle in the cellular composition of Nannochloropsis gaditana. *Current Research Topics In Applied Microbiology and Microbial Biotechnology*, pages 273–277, 2009.

[163] C.H. Johnson, T. Kondo, and J.W. Hastings. Action spectrum for resetting the circadian phototaxis rhythm in the CW15 strain of Chlamydomonas. *Plant Physiology*, 97(3):1122–1129, NOV 1991.

[164] T. Kondo, C.H. Johnson, and J.W. Hastings. Action spectrum for resetting the circadian phototaxis rhythm in the CW15 strain of Chlamydomonas. 1. cells in darkness. *Plant Physiology*, 95(1):197–205, JAN 1991.

[165] D. Briassoulis, P. Panagakis, M. Chionidis, D. Tzenos, A. Lalos, C. Tsinos, K. Berberidis, and A. Jacobsen. An experimental helical-tubular photobioreactor for continuous production of Nannochloropsis sp. *Bioresource Technology*, 101(17):6768–6777, SEP 2010.

[166] P. Albertano. Effects of monochromatic lights on 4 species of Leptolyngbya. *Archiv Fur Hydrobiologie*, pages 199–214, DEC 1991.

[167] B.S. Costa, A. Jungandreas, T. Jakob, W. Weisheit, M. Mittag, and C. Wilhelm. Blue light is essential for high light acclimation and photoprotection in the diatom Phaeodactylum tricornutum. *Journal of Experimental Botany*, 64(2):483–493, JAN 2013.

[168] F. Bohne and H. Linden. Regulation of carotenoid biosynthesis genes in response to light in Chlamydomonas reinhardtii. *Biochemica et Biophysica ACTA-Gene Structure and Expression*, 1579(1):26–34, NOV 13 2002.

[169] M. Janssen, M. Janssen, M. de Winter, J. Tramper, L.R. Mur, J. Snel, and R.H. Wijffels. Efficiency of light utilization of Chlamydomonas reinhardtii under medium-duration light/dark cycles. *Journal of Biotechnology*, 78(2):123–137, MAR 10 2000.

[170] L. Dall'Osto, S. Caffarri, and R. Bassi. A mechanism of nonphotochemical energy dissipation, independent from PsbS, revealed by a conformational change in the antenna protein CP26. *Plant cell*, 17(4):1217–1232, APR 2005.

[171] L.M. Lubián and O. Montero. Excess light-induced violaxalathin cycle activity in Nannochloropsis gaditana (Eustigmatophyceae): effects of exposure time and temperature. *Phycologia*, 37(1):16–23, JAN 1998.

[172] N.J. Antia, T. Bisalputra, J.Y. Cheng, and J.P. Kalley. Pigment and cytological evidence for reclassification of Nannochloris oculata and Monallantus-salina in Eustigmatophyceae. *Journal of Phycology*, 11(3):339–343, 1975.

[173] T.G. Owens, J.C. Gallagher, and R.S. Alberte. Photosynthetic light-harvesting function of violaxanthin in Nannochloropsis spp (Eustigmatophyceae). *Journal of Phycology*, 23(1):79–85, MAR 1987.

[174] S.J. Whittle and P.J. Casselton. The Chloroplast Pigments of the Algal Classes Eustigmatophyceae and Xanthophyceae Part 1 Eustigmatophyceae. *British Phycological Journal*, 10(2):179–191, 1975.

[175] A.E. Solovchenko, O.B. Chivkunova, and I.P. Maslova. Pigment composition, optical properties, and resistance to photodamage of the microalga Haematococcus pluvialis cultivated under high light. *Russian Journal of Plant Physiology*, 58(1):9–17, 2011.

[176] I. Baroli, A.D. Do, T. Yamane, and K.K. Niyogi. Zeaxanthin accumulation in the absence of a functional xanthophyll cycle protects Chlamydomonas reinhardtii from photooxidative stress. *Plant Cell*, 15(4):992–1008, APR 2003.

[177] S.O. Lourenco, E. Barbarino, M.D.S. Bispo, D.A. Borges, C. Coelho-Gomes, P.L. Lavin, and F. Santos. Effects of Light Intensity On Growth, Inorganic Nitrogen Storage, and Gross Chemical Composition of Four Marine Microalgae In Batch Cultures, 2008.

[178] R.W. Eppley. Temperature and phytoplankton growth in sea. *Foishery Bulletin*, 70(4):1063–1085, 1972.

[179] P.A. Thompson, M.X. Guo, and P.J. Harrison. Effects of Variation In Temperature. 1. On the Biochemical-composition of 8 Species of Marine-phytoplankton. *Journal of Phycology*, 28(4):481–488, AUG 1992.

[180] J. Van Wagenen, T.W. Miller, S. Hobbs, P. Hook, B. Crowe, and M. Huesemann. Effects of Light and Temperature on Fatty Acid Production in Nannochloropsis salina. *Energies*, 5(3):731–740, MAR 2012.

[181] N.K. Vidyarathna and E. Graneli. Physiological responses of Ostreopsis ovata to changes in N and P availability and temperature increase. *Harmful Algae*, 21-22:54–63, JAN 2013.

[182] S.Y. Chen, L.Y. Pan, M.J. Hong, and A.C. Lee. The effects of temperature on the growth of and ammonia uptake by marine microalgae. *Botanical Studies*, 53(1):125–133, JAN 2012.

[183] F.L. Figueroa, C. Jimenez, L.M. Lubián, O. Montero, M. Lebert, and D.P. Hader. Effects of high irradiance and temperature on photosynthesis and photoinhibition in Nannochloropsis gaditana Lubián (Eustigmatophyceae). *Journal of Plant Physiology*, 151(1):6–15, JUL 1997.

[184] M.W. Fawley. Effects of light-intensity and temperature interactions on growth-characteristics of Phaeodactylum tricornutum (Bacillariophyceae). *Journal of Phycology*, 20(1):67–72, 1984.

[185] N.H. Norsker, M.J. Barbosa, M.H. Vermue, and R.H. Wijffels. Microalgal production - A close look at the economics. *Biotechnology Advances*, 29(1):24–27, JAN 2011.

Abbreviations

A	absorbance
A	antheraxanthin
A.U.	arbitrary units
ADP	adenosine diphosphate
ATP	adenosin triphosphate
bHLH-PAS	basic-helix-loop-helix - Per Arnt Sim
β-car	β-carotene
δ-ALA	δ-aminolevulinic acid
C	constant
Car	carotenoid
CCT	CONSTANS, CO-like, and TOC1
Chl	chlorophyll
CO_2	carbon dioxide
DDE	diadinoxanthin de-epoxidase
DEP	diatoxanthin epoxidase
DHA	docosahexaenic acid
e.g.	exempli gratia
EMS	ethyl methanesulfonate
EPA	eicosapentaenic acid
F	fluctuating
Fig.	figure
Fm	maximum fluorescence in dark-adapted state
Fm'	maximum fluorescence in light-adapted state
Fo	minimal fluorescence in dark-adapted state
Fs	minimal fluorescence in light-adapted state
H_2	hydrogen

HCl	hydrogen chloride
H_2O	water
HPLC	high performance liquid chromatography
i.e.	id est
LD	light-dark
LED	light-emitting diode
LHC	light harvesting complex
LL	continuous light
MeOH	methanol
N	nitrogen
N/A	not available
NADPH	nicotinamide adenine dinucleotide phosphate
NaH_2NO_3	monosodium nitrate
NaH_2PO_4	monosodium phosphate
NO_3	nitrate
NPQ	non-photochemical quenching
O_2	oxygen
OCP	orange carotenoid protein
OD	optical density
OD_{540}	optical density measured at 540 nm
OD_{680}	optical density measured at 680 nm
OD_{735}	optical density measured at 735 nm
P	phosphorus
PAR	photosynthetic active radiation
PBR	photobioreactor
POR	NADPH:protoChlide oxydoreductase
PS	photosystem
Q_A	primary quinone acceptor
qE	energy dependent quenching
qI	photoinhibitory quenching
qT	state-transition quenching
R^2	coefficient of determination
ROS	reactive oxygen species
rpm	rounds per minute

SD	standard deviation
sp.	species
TAG	triacylglyceride
temp.	temperature
UV	ultraviolet
V	violaxanthin
Vau	vaucheriaxanthin
VDE	violaxanthin de-epoxidase
v/v	volume/volume
wt.	weight
WT	wild type
x g	times gravity
ZEP	zeaxanthin epoxidase
ZT	Zeitgeber time

List of Figures

List of Tables

Publications and Posters

Publications during PhD

Regina Braun, Eva M. Farré, Ulrich Schurr, Shizue Matsubara (submitted).
"Effects of light and circadian clock on growth and chlorophyll accumulation of *Nannochloropsis gaditana* (Eustigmatophyte)"

Posters

Energy Hills, Netherlands
Regina Braun, Thorsten Brehm, Andreas Müller, Ulrich Schurr, Shizue Matsubara, Silvia Berteotti, Alessandro Alboresi, Roberto Bassi (2011)
"Strategies to Improve Biomass and Biofuel Production with Microalgae"

Cold Spring Harbor Laboratory, USA
Regina Braun, Eva M. Farré, Ulrich Schurr, Shizue Matsubara (2012)
"Are Growth and Photosynthesis of green microalga *Nannochloropsis gaditana* controlled by the circadian clock?"

2nd International Conference on Algal Biomass, Biofuels and Bioproducts, USA
Regina Braun, Ulrich Schurr, Shizue Matsubara (2012)
"Is there a circadian regulation of growth in the green microalga *Nannochloropsis gaditana*?"

Acknowledgements

I would like to thank Prof. Ulrich Schurr for giving me the opportunity to work at the IBG-2: Plant Sciences in the Forschungszentrum Jülich GmbH and appreciate his support during the last three years. I am also thankful to Prof. Georg Groth at the Heinrich Heine University of Düsseldorf, who kindly agreed to act as referee and commentator of my work.

Special thanks go to Dr. Shizue Matsubara who supported me with valuable advice, good discussions and patience during my PhD. I am very grateful for all the effort she put into me and my PhD project, which would have not been possible without her.

Thanks to Prof. Roberto Bassi for providing NPQ mutants and giving helpful advice.

I would like to thank the students who helped me with the setup and performance of experiments.

I am grateful for the help of many colleagues in the Forschungszentrum Jülich GmbH, for their support, ideas and time listening to problems and suggesting solutions. I am thankful for the friendly working atmosphere and the nice breaks.

Finally, I would like to thank Marc and my family, especially my parents, for their support.

Band / Volume 208
SGSreco - Radiologische Charakterisierung von Abfallfässern durch Segmentierte γ-Scan Messungen
T. H. Krings (2014), ix, 181, XI
ISBN: 978-3-89336-945-4

Band / Volume 209
Kühlkonzepte für Hochtemperatur-Polymerelektrolyt-Brennstoffzellen-Stacks
J. Supra (2014), III, 191 pp
ISBN: 978-3-89336-946-1

Band / Volume 210
Eigenschaften des Phosphorsäure-Polybenzimidazol-Systems in Hochtemperatur-Polymerelektrolyt-Brennstoffzellen
A. Majerus (2014), viii, 141 pp
ISBN: 978-3-89336-947-8

Band / Volume 211
Study on the Complex Li-N-H Hydrogen Storage System
L. Du (2014), I, 132 pp
ISBN: 978-3-89336-952-2

Band / Volume 212
Transport and Retention of Stabilized Silver Nanoparticles in Porous Media
Y. Liang (2014), IV, 109 pp
ISBN: 978-3-89336-957-7

Band / Volume 213
Effizienzoptimierte CO_2-Abtrennung in IGCC-Kraftwerken mittels Wassergas-Shift-Membranreaktoren
S. T. Schiebahn (2014), XXII, 203 pp
ISBN: 978-3-89336-958-4

Band / Volume 214
Lebensdauer und Schädigungsentwicklung martensitischer Stähle für Niederdruck-Dampfturbinenschaufeln bei Ermüdungsbeanspruchung im VHCF-Bereich
S. Kovacs (2014), IV, 140 pp
ISBN: 978-3-89336-959-1

Band / Volume 215
Micro- and Macro- Mechanical Testing of Transparent $MgAl_2O_4$ Spinel
O. Tokariev (2014), X, 99 pp
ISBN: 978-3-89336-960-7

Band / Volume 216
Potentiale des Strommanagements zur Reduzierung des spezifischen Energiebedarfs von Pkw
T. Grube (2014), IX, 255 pp
ISBN: 978-3-89336-961-4

Band / Volume 217
Transmutation von Transuranen in einem gasgekühlten beschleunigergetriebenen System
K. H. Biß (2014), IV, 157 pp
ISBN: 978-3-89336-964-5

Band / Volume 218
Untersuchung des photochemischen Terpenoidabbaus in der Atmosphärensimulationskammer SAPHIR
M. Kaminski (2014), 148, VI pp
ISBN: 978-3-89336-967-6

Band / Volume 219
Interaction of Phosphoric Acid with Cell Components in High Temperature Polymer Electrolyte Fuel Cells
F. Liu (2014), i, 147 pp
ISBN: 978-3-89336-972-0

Band / Volume 220
Machbarkeitsstudie zum Aufbau und Betrieb eines Prüfstandes für Antriebsstränge von Windenergieanlagen mit Getriebe im Leistungsbereich bis 15 MW am Standort Forschungszentrum Jülich
(2014), 72 pp
ISBN: 978-3-89336-973-7

Band / Volume 221
Phenotyping Nannochloropsis gaditana under different conditions in controlled photobioreactors in laboratory and upscaled photobioreactors in greenhouse
R. Braun (2014), III, 177 pp
ISBN: 978-3-89336-975-1

Energie & Umwelt / Energy & Environment
Band / Volume 221
ISBN 978-3-89336-975-1

JÜLICH
FORSCHUNGSZENTRUM